

E151 (*sym15*), a low nodulating mutant of *Pisum sativum* L.:  
a study of  
its nodulation phenotype, nodule functioning,  
and nodule development

by

Emily S. Macdonald

Honours Bachelor of Science, Wilfrid Laurier University, 2009

A

THESIS

submitted to the Department of Biology, Faculty of Science

in partial fulfilment of the requirements for the

Master of Science in Integrative Biology

Wilfrid Laurier University

2011

© Emily S. Macdonald 2011



Library and Archives  
Canada

Published Heritage  
Branch

395 Wellington Street  
Ottawa ON K1A 0N4  
Canada

Bibliothèque et  
Archives Canada

Direction du  
Patrimoine de l'édition

395, rue Wellington  
Ottawa ON K1A 0N4  
Canada

*Your file* *Votre référence*  
ISBN: 978-0-494-81511-3  
*Our file* *Notre référence*  
ISBN: 978-0-494-81511-3

#### NOTICE:

The author has granted a non-exclusive license allowing Library and Archives Canada to reproduce, publish, archive, preserve, conserve, communicate to the public by telecommunication or on the Internet, loan, distribute and sell theses worldwide, for commercial or non-commercial purposes, in microform, paper, electronic and/or any other formats.

The author retains copyright ownership and moral rights in this thesis. Neither the thesis nor substantial extracts from it may be printed or otherwise reproduced without the author's permission.

---

In compliance with the Canadian Privacy Act some supporting forms may have been removed from this thesis.

While these forms may be included in the document page count, their removal does not represent any loss of content from the thesis.

#### AVIS:

L'auteur a accordé une licence non exclusive permettant à la Bibliothèque et Archives Canada de reproduire, publier, archiver, sauvegarder, conserver, transmettre au public par télécommunication ou par l'Internet, prêter, distribuer et vendre des thèses partout dans le monde, à des fins commerciales ou autres, sur support microforme, papier, électronique et/ou autres formats.

L'auteur conserve la propriété du droit d'auteur et des droits moraux qui protègent cette thèse. Ni la thèse ni des extraits substantiels de celle-ci ne doivent être imprimés ou autrement reproduits sans son autorisation.

---

Conformément à la loi canadienne sur la protection de la vie privée, quelques formulaires secondaires ont été enlevés de cette thèse.

Bien que ces formulaires aient inclus dans la pagination, il n'y aura aucun contenu manquant.

  
**Canada**

I hereby declare that I am the sole author of this thesis.

I authorize Wilfrid Laurier University to lend this thesis to other institutions or individuals for the purpose of scholarly research.

I further authorize Wilfrid Laurier University to reproduce this thesis by photocopying or by other means, in total or in part, at the request of other institutions or individuals for the purpose of scholarly research.

## Abstract

Root nodules form when a symbiotic relationship is established between plants of the legume family and rhizobia. While the former receives assimilated nitrogen, the latter gains carbohydrates. Throughout this thesis, I have taken an integrative approach to understand both members of the relationship. The pea mutant E151 (*sym15*) was previously described as a low nodulator when compared to the wild-type Sparkle. In this study, I broaden the characterization of the E151 nodule phenotype and its nodule organogenesis; studies were conducted to get a full view of E151 nodulation over the plant's lifetime. To accomplish this, nodule distribution was observed through the use of nodulation maps and nodule organogenesis stages were observed on flood- and spot-inoculated plants grown in pouches. It was observed that the nodules covered a more extensive zone of the root system than Sparkle. E151 nodule organogenesis was blocked at two stages. The first block was in the epidermal program when the infection thread (IT) had entered the epidermis but could not breach into the cortex, and the second in the cortical program when the IT was present in the inner cortex but the inner cortical cells which had begun to divide did not lead to the formation of a nodule primordium. A plant mechanism, known as autoregulation of nodulation (AON), is used to monitor the number of nodules produced on a root system because the formation of these new structures is costly to the plant. The nodules which first emerge elicit a signal which travels to a receptor in the shoot; upon perception of this root-signal, a shoot-signal is produced and translocated to the root where it inhibits further nodule emergence. I have studied E151 nodule development to assess whether the nodules arrested early in growth abort or are merely dormant. It was found that E151 early-formed nodules are in fact aborted and are never re-triggered to emerge. For a majority of this thesis, R50 (*sym16*) was used as a control to determine whether the findings were characteristic of E151 or of mutants in general. This was especially critical when observing the response of the pea to different rhizobial strains. For years, four bacterial strains had been used in our lab to study the symbiotic relationship between pea and rhizobia. The legume-side of the association had been well documented; however, the lab had never investigated its rhizobial-side to know the efficiency of each strain. For this component, my objective was to compare the efficiency of these four strains at forming nodules with the three pea lines. It was determined that E151 did have a differential response to the strains compared to Sparkle and R50. The efficiency of the association was also analyzed and the definition of efficiency was brought into the spotlight.



These results allowed me to not only visualize the individual partners, but get a glimpse into the interaction between the two partners, both of which ultimately affect the success of the symbiosis. The research has put together pieces of the puzzle but has also opened many new doors into the investigation of the nodulation phenotype and nodule development of mutants.

## **Acknowledgements**

I would like to thank Dr. Frédérique Guinel for the opportunity to work in her lab and for the support she has provided in my completion of this project. I am especially grateful for the encouragement and the opportunities that she has given me. I would also like to thank my committee members Dr. Mihai Costea (Biology, Wilfrid Laurier University) and Dr. Trevor Charles (Biology, University of Waterloo), and my external examiner Dr. John Markham (Biology, University of Manitoba) for contributing to the success of this project.

I would like to give a special thanks to Dr. Mihai Costea and Stephanie Riviere for allowing me into their lab to use their microscope. They were both always willing to help when needed.

I thank Gena Braun and Jiangxiao Sun for their technical support with the Qubit System. They were always approachable and supportive during the many months of understanding and troubleshooting the system.

I extend my gratitude to my fellow lab-mates Christian Huynh, Lindsey Clairmont, and Peter De Carvalho. A special thanks to Scott Clemow and Chengli Long for always being willing to help and for their mentorship.

Special thanks to my friends that I have made in the Masters program. Specifically, I would like to thank Nish Pais for always being supportive, encouraging, and overall a great friend.

Finally, I would like to thank my family and Sean McConnell for their unconditional love and encouragement that they have provided me; they have contributed to a larger part of me completing this thesis.

## Table of Contents

Abstract.....	iii
Acknowledgements.....	v
List of Tables .....	ix
List of Figures .....	x
Chapter I: Introduction .....	1
1.1 The association .....	1
1.2 The organogenesis of the nodule .....	2
1.3 Autoregulation of nodulation .....	3
1.4 Model legumes and mutants as a tool .....	5
1.5 E151 ( <i>sym15</i> ).....	6
1.6 Objectives .....	7
Chapter II: Nodulation Distribution .....	8
2.1 Introduction .....	8
2.1.1 Objectives.....	10
2.2 Materials and methods.....	10
2.2.1 Plant growth conditions .....	10
2.2.2 Bacterial growth conditions.....	11
2.2.3 Counting of nodules.....	11
2.2.4 Microsoft Excel 2007.....	13
2.2.5 Quantitative analysis.....	13
2.2.6 Statistical analysis .....	13
2.3 Results.....	15
2.3.1 Nodulation maps.....	15
2.3.2 Distribution of Sparkle nodules .....	15
2.3.3 Distribution of E151 nodules .....	20
2.3.4 Distribution of R50 nodules .....	22
2.4 Discussion.....	22
2.4.1 The E151 nodulation phenotype.....	22
2.4.2 The usefulness of the nodulation maps.....	24
Chapter III: Impact of Bacterial Strain on Nodulation Efficiency .....	27
3.1 Introduction .....	27
3.1.1 Rhizobial strains .....	27
3.1.2 Nitrogenase.....	29
3.1.3 Measuring efficiency.....	30

3.1.4 Objectives.....	31
3.2 Materials and methods.....	32
3.2.1 Assessment of four bacterial strains.....	32
3.2.2 Nitrogenase activity .....	33
3.3 Results.....	39
3.3.1 Bacterial strain effect on Sparkle .....	39
3.3.2 Bacterial strain effect on E151.....	46
3.3.3 Bacterial strain effect on R50.....	46
3.3.4 Comparison of the three pea lines.....	47
3.4 Discussion.....	50
3.4.1 Pea lines and bacterial strains .....	50
3.4.2 Nitrogenase activity and HUP <sup>-</sup> .....	53
3.4.3 Assessment of efficiency.....	54
Chapter IV: E151 Early-formed Nodules .....	56
4.1 Introduction .....	56
4.1.1 Objectives.....	58
4.2 Materials and methods.....	58
4.2.1 Flood-inoculation and macro-observations.....	58
4.2.2 Spot-inoculation and micro-observations .....	61
4.3 Results.....	63
4.3.1 Nodule organogenesis of Sparkle .....	63
4.3.2 Nodule organogenesis of E151 .....	67
4.3.3 Nodule excision.....	73
4.4 Discussion.....	73
4.4.1 Organogenesis – E151 phenotype .....	73
4.4.2 The placement of E151 according to other pea mutants .....	77
Chapter V: Concluding Remarks .....	83
5.1 The E151 nodulation phenotype and its efficiency .....	83
5.1.1 Characterize E151 nodule distribution. (Chapter II) .....	83
5.1.2 Determine if E151 has a differential response to rhizobial strains. (Chapter III) .....	83
5.1.3 Determine the efficiency of the E151- <i>Rhizobium</i> association. (Chapter III).....	83
5.1.4 Confirm the location of the block in E151 nodule organogenesis. (Chapter IV) .....	84
5.1.5 Determine whether E151 early-formed nodules are aborted or arrested. (Chapter IV) .....	84
5.2 Classifying low nodulators .....	84
5.3 E151 in the context of AON .....	88

References .....	89
Appendices.....	99
Appendix A.....	99
Appendix B.....	100
Appendix C.....	101

## List of Tables

<b>Table 2-1. Nodule number and DW for each pea line over time. ....</b>	<b>21</b>
<b>Table 2-2. Nodulation zone ratios for each pea line over time.....</b>	<b>21</b>
<b>Table 3-1. Equations used to determine nitrogen fixation .....</b>	<b>38</b>
<b>Table 3-2. Plant return on nodule construction cost for the three pea lines inoculated with HUP<sup>+</sup> (as in Oono and Denison, 2010). ....</b>	<b>45</b>
<b>Table 3-3. Specific nodulation of the three pea lines inoculated with HUP<sup>+</sup> (as in Fei and Vessey, 2009).....</b>	<b>48</b>
<b>Table 3-4. Specific nodule DW of the three pea lines inoculated with HUP<sup>+</sup> (Gulden and Vessey, 1998).....</b>	<b>48</b>
<b>Table 3-5. Nodule construction cost, specific nodulation, and specific nodule DW of the three pea lines inoculated with HUP<sup>+</sup> at 42 DAI.....</b>	<b>49</b>
<b>Table 3-6. Electron allocation coefficient (EAC) values for the three pea lines when inoculated with HUP<sup>+</sup> and measured using the Qubit system.....</b>	<b>51</b>
<b>Table 4-1. Percentage of infection events at each stage for Sparkle and E151. ....</b>	<b>68</b>
<b>Table 5-1. Nodulation phenotypes of super-, hyper-, and enhanced nodulators compared to WT.....</b>	<b>85</b>
<b>Table 5-2. Nodulation phenotype of the low nodulators E151 and R50 compared to WT Sparkle. ....</b>	<b>87</b>

## List of Figures

Figure 2-1. A nodulated root system on a grid.....	12
Figure 2-2. Diagrams illustrating how nodulation zone ratios were calculated.....	14
Figure 2-3. Nodulation maps of Sparkle over time.....	16
Figure 2-4. Nodulation maps of E151 over time.....	17
Figure 2-5. Nodulation maps of R50 over time. ....	18
Figure 2-6. Nodulated root system of Sparkle, E151, R50. ....	19
Figure 3-1. Flow diagram of the Qubit apparatus.....	34
Figure 3-2. Photograph of a plant attached to the Qubit system.....	36
Figure 3-3. Nodule number on roots of Sparkle, E151, and R50 when inoculated with four bacterial strains.....	40
Figure 3-4. Individual nodule DW of Sparkle, E151, and R50 when inoculated with four bacterial strains.....	41
Figure 3-5. Nodule morphology of the 3 pea lines inoculated with each bacterial strain. ...	42
Figure 3-6. Nitrogen fixation of three pea lines Sparkle, E151, R50.....	43
Figure 3-7. Average nitrogen fixation for three pea lines. ....	44
Figure 4-1. The growth of plants in pouches.....	59
Figure 4-2. Sparkle grown in a pouch at 11 DAI and 21 DAI. ....	64
Figure 4-3. Observations of the root system and nodules of Sparkle.....	65
Figure 4-4. Total number of infection events for each stage of Sparkle and E151 root segments.....	66
Figure 4-5. Sparkle nodule organogenesis.....	69
Figure 4-6. Observations of the root system and nodules of E151. ....	70
Figure 4-7. E151 in stage E of nodule organogenesis, where the infection thread has penetrated the inner cortex and there are inner cortical cell divisions. ....	72
Figure 4-8. Sparkle plant which had its nodules excised.....	74
Figure 4-9. The location of <i>sym15</i> on the modified schematic of Guinel and Geil (2002). ...	79
Figure 4-10. Placement of <i>sym15</i> on the modified schematic of Tsyganov et al. (2002). ....	80
Figure 4-11. The placement of E151 on the model by Shtark et al. (2010).....	82

## Chapter I: Introduction

### 1.1 The association

Fossil evidence suggests that the first legumes appeared about 56 Ma (Lavin *et al.*, 2005). They were domesticated over 3000 years ago, for example for *Phaseolus vulgaris* L. (bean) and *Glycine max* L. Merr. (soybean), and since this time legumes have been heavily relied on as essential crops (Graham and Vance, 2003). A mutualistic relationship can occur between species from the Fabaceae family and bacteria of the Rhizobiaceae family. Through this association, a new structure known as a nodule is formed. Sprent (2007) states that nodulated legumes evolved during a period of environmental change where the conditions may have led to nitrogen limitations for the plants, favouring the evolution of symbioses. Approximately 85% of legume species are capable of forming a symbiotic relationship with bacteria of the family Rhizobiaceae (Kneen *et al.*, 1994). The bacteria provide the plant with a usable form of nitrogen while the plant offers the bacteria protection and an energy source. This association has continued to evolve over time; Sprent (2007) hypothesized that the earliest nodules were formed from direct infection through the epidermis and that infection threads developed later, with legumes having their origin later than 40 Ma undergoing a root-hair based infection (Sprent, 2009). Caetano-Anollés (1997) state that nitrogen fixation is second only to photosynthesis based on its importance in the growth and development of plants.

Since the beginning of the 1960s, the increase in the world's population has led to a large increase in food demand which has been made possible by agricultural improvements, with fertilizers playing an important role (FAO, 2006). The world fertilizer use has increased almost fivefold since 1960 (FAO, 2006). Caetano-Anollés (1997) state there is a greater than 20% loss of fertilizers to nitrification in the soil and leaching into groundwater. Biological nitrogen fixation offers a sustainable agricultural solution to meeting agricultural demands. It is estimated that from 70 to 80 percent of future crop increases in developing countries will have to come from higher crop yields due to the lack of arable land (FAO, 2006). We must rethink strategies on how to increase crop yield without polluting our environment. Bhatia *et al.* (2001) state that several alterations to the process of nitrogen fixation may lead to a more sustainable agriculture:



1. promoting early nodulation, 2. optimizing nodule number and weight, 3. ensuring nodulation by the most efficient bacterial strain, and 4. lengthening the duration of nitrogen fixation activity.

## 1.2 The organogenesis of the nodule

To initiate symbiosis, the rhizobia and plant must recognize one another through the use of chemical signals. Host-specificity is determined by the flavonoids that the plant secretes in the rhizosphere and the ability of the rhizobia to recognize that signal (Brelles-Mariño and Ané, 2008). The flavonoids induce the expression of the *nodD* gene; the product of this gene acts as an inducer for the expression of the common *nod* (*nodulation*) genes *ABC* (Brelles-Mariño and Ané, 2008). These bacterial genes code for the enzymes responsible for the synthesis of Nod factors (Brelles-Mariño and Ané, 2008), upon which the commencement of nodule organogenesis relies (Gage and Margolin, 2000).

In short, the rhizobia associate with one root hair and become trapped by the root hair curling around the colony. Soon after, the root cell wall invaginates to form an infection thread (IT) which houses the rhizobia; as these divide, the IT progresses to the inner cortex of the root (Gage and Margolin, 2000). Meanwhile, the cortical cells divide and a nodule primordium forms and becomes a nodule meristem (Guinel and Geil, 2002). In the cells behind the nodule meristem, the IT undergoes an exocytotic process where a vesicle with one or a few bacteria surrounded by a membrane pinches off; this organelle-like structure is a symbiosome (Oldroyd and Downie, 2008). Within the symbiosome, the rhizobia differentiate into bacteroids, which are capable of fixing nitrogen (Oke and Long, 1999). Guinel and Geil (2002) suggested that the different steps described above could be considered as part of two programs, an epidermal and a cortical program. The progression through these stages and the emergence of a successful nodule require strict coordination between the two programs. Ding and Oldroyd (2009) suggested that the hormone abscisic acid is the coordinator. Nodule development in pea has been dissected crudely by Guinel and LaRue (1991) into six stages: A) IT in root hair or epidermis, B) IT in cortex with no divisions, C) IT in cortex associated with divisions, D) nodule primordium, E) nodule meristem, and F) mature emerged nodule. Since then, with the study of more *Pisum sativum* L. (pea) mutants, others have refined the different stages (Guinel and Geil, 2002; Tsyganov *et al.*, 2002; Voroshilova *et al.*, 2009).

Some legumes such as *Medicago sativa* L. (alfalfa) and pea form indeterminate nodules, the initial cell divisions of which occur in the inner cortex, while others such as soybean and bean form determinate nodules which initiate from cell divisions in the outer cortex (Hirsch, 1992). The two types of nodules have different growth patterns. Indeterminate nodules have a persistent nodule meristem, while determinate nodules lack this feature (Hirsch, 1992). Indeterminate nodules are oblong and contain distinguishable histological zones: Zone I: meristematic zone; Zone II: early symbiotic zone where the rhizobia invade the host cells; Interzone II-III: area where bacteria differentiate into bacteroids; Zone III: late symbiotic zone or fixation zone where nitrogen is being fixed; Zone IV: senescent zone where both bacteroids and plant cells degrade; and Zone V: saprophytic zone where some rhizobia that did not differentiate into bacteroids are capable of division (Guinel, 2009). Determinate nodules are spherical and do not have distinct zones. While indeterminate nodules have a peripheral zone containing the vasculature on the outside of the infected zones, determinate nodules have their vasculature throughout the structure with a scleroid layer surrounding infected tissues (Guinel, 2009).

### **1.3 Autoregulation of nodulation**

The process of nitrogen fixation is costly to the plant and requires 16 ATP to convert atmospheric nitrogen to ammonium (Layzell and Atkins, 1997). Because of this large investment, the organism has evolved a mechanism known as autoregulation of nodulation (AON) to control the number of nodules it produces (Caetano-Anollés and Gresshoff, 1991a). AON has been of continued interest to researchers but much of the mechanism is still hypothesized. It involves long-distance signalling between the shoot and the root (Kinkema *et al.*, 2006). A root-derived signal is transported to the shoot where it is perceived, triggering the assembly of a shoot-derived signal; this signal is then translocated to the root where upon being sensed it inhibits nodulation (Okamoto *et al.*, 2009). Through this systemic mechanism, nodules formed on older roots suppress the emergence of those on younger roots.

Although little is known about the specifics of the steps involved in this mechanism, pieces of information are starting to come together and researchers are just beginning to uncover the big picture, at least in *Lotus japonicus* (Regel) K. Larson. The initial trigger of AON is unknown, although it is proposed to be either the formation of the nodule primordium (Li *et al.*, 2009) or the Nod factors (Lin *et al.*, 2010). The root signal is thought to be the product of a short

peptide-coding gene, the *CLE* gene; among 39 *LjCLE* genes identified, two, *CLE-Root Signal 1* (*LjCLE-RS1*) and *LjCLE-RS2*, were upregulated 24 hours after rhizobial inoculation (Okamoto *et al.*, 2009). The products of these genes are indeed ligands of the known shoot receptors which are known to be receptor-like kinases (Krusell *et al.*, 2002), specifically LjHAR1 in *L. japonicus* (Magori *et al.*, 2009). This receptor is orthologous to the *Arabidopsis thaliana* (L.) Heynh. receptor kinase CLAVATA1 and is thus described as clavata-like (Kinkema *et al.*, 2006). Another member in the mechanism, the product of the gene *LjTML* (*TOO MUCH LOVE*), has been identified as a possible receptor or mediator of the shoot-signal (Magori *et al.*, 2009). As for the shoot-derived inhibitor, it is a small compound with a molecular mass of less than 1000 Da; it is expected to be neither a protein nor an RNA molecule (Lin *et al.*, 2010). In *L. japonicus*, the signal of AON takes three days to take effect within the plant (Suzuki *et al.*, 2008). In pea, little has been discovered about the components of AON. The only parts of the mechanism known are PsSYM29, a receptor found to be orthologous to LjHAR1 (Krusell *et al.*, 2002) and PsSYM28 which encodes a protein similar to the AtCLV2 protein (Krusell *et al.*, 2011).

Scientists have been using mutants, specifically supernodulators, to study AON. There are many such supernodulating mutants across many different legume genera. These mutants do not control correctly their nodule number, resulting in the production of an increased number of nodules compared to wild-type (WT) on their root systems; often their nodule numbers are 5 to 20 percent larger than those of the WT (Novák, 2010a). Gresshoff *et al.* (2005) identified five common characteristics of mutants with an absence of AON: when compared to the WT, 1. their nodule number is larger, 2. their nodulation interval (i.e. the space that the nodules occupy) is increased, 3. their nodule mass per plant is increased, 4. their nodule number is increased in the presence of nitrate, an inhibitor of nodulation in the WT; and 5. their root system is less developed. Furthermore, scientists have performed reciprocal grafting experiments with these mutants to assess whether their nodulation phenotype is root- or shoot-controlled. For example, *Ljhar1* is shoot-controlled (Jiang and Gresshoff, 2002) while *nts382* and *nts1116* of soybean are root controlled (Delves *et al.*, 1986). With the description of newer mutants, Gresshoff's classification needs to be re-evaluated. For example, what has been missing from this classification is the distinction between super- and hyper-nodulators (Novák, 2010a). Supernodulators are mutants which form an excessive amount of nodules which emerge outside

the initial zone of nodulation, whereas hypernodulators form many more nodules but the distribution of these is the same as that of the wild-type (Novák, 2010a). Another difference is that supernodulators are nitrate-insensitive and ethylene-sensitive while hypernodulators are nitrate-sensitive and ethylene-insensitive (Novák, 2010a). An example of a determinate supernodulator is *Gmnts382* (Carroll *et al.*, 1985), while some indeterminate supernodulators are *Mtlss* (Schnabel *et al.*, 2010) and *PsRisfixC* (Novák, 2010b). Determinate hypernodulators are *Gmnark* (Okamoto *et al.*, 2009), *Ljhar1* (Krusell *et al.*, 2002), while some indeterminate hypernodulators include *Mtsickle* (Penmetsa *et al.*, 2003), *Mtsunn* (Penmetsa *et al.*, 2003), *Psnod3* (Li *et al.*, 2009), *Pssym28* (Sagan and Duc, 1996; Krusell *et al.*, 2011), and *Pssym29* (Krusell *et al.*, 2002).

#### **1.4 Model legumes and mutants as a tool**

Legumes have a large impact on agriculture worldwide, as they can be found on all continents except Antarctica and represent a large number of crop species (Sprent, 2001). Genetic and nodulation research initiated with the study of legumes such as pea, soybean, and alfalfa as these were important crops. Lately, however, there has been a rise in molecular studies which has put in the spot-light two model legumes, *L. japonicus* as the model legume forming determinate nodules and *Medicago truncatula* Gaertn. (barrel medic) as the model forming indeterminate nodules (Zhu *et al.*, 2005). These model legumes have allowed the signal transduction pathway leading to nodulation to be mostly deciphered, permitting scientists to turn to mutants with physiological problems such as an abnormal AON. Interesting to the agricultural community is the recent turn of the scientists to crops with larger genomes such as soybean (Kereszt *et al.*, 2007), bean (Estrada-Navarrete *et al.*, 2007), and pea (Clemow, 2010).

In this thesis, the symbiotic relationship between pea and *Rhizobium leguminosarum* will be studied. From a combined effort by labs in the United States, Russia, France, and Australia, more than 200 symbiotic pea mutant lines are known and from these mutants, over forty pea symbiotic genes have been identified (Borisov *et al.*, 2000). These labs have studied many different aspects of the pea/*Rhizobium* association: nodule organogenesis (Tsyganov *et al.*, 1998; Tsyganov *et al.*, 2003; Voroshilova *et al.*, 2009); symbiotic genes (Kneen *et al.*, 1994; Krusell *et al.*, 2002, Sagan and Duc, 1996); or hormone control (Ferguson *et al.*, 2005a; Held *et al.*, 2008;

Lorteau *et al.*, 2001).

In our lab, we study the nodule organogenesis of pea through multiple approaches such as exogenous hormone application, grafting, microscopy, and molecular techniques. As an example, let me introduce the pea mutant R50 (*sym16*) which has been studied in our lab. The pale leaves and the stunted height of R50 pointed towards cytokinin (CK) as the hormone involved, and it was further determined that CK levels were higher in R50 than in WT (Ferguson *et al.*, 2005b). Exogenous treatment of this hormone to WT led it to phenocopy R50 low nodulation phenotype (Lorteau *et al.*, 2001); however, exogenous treatments of CK-receptor antagonist did not affect nodulation (Long, 2010). Held *et al.* (2008) have shown that the high levels of CK in R50 were due to a defective CK oxidase, an enzyme which degrades the active forms of CK. Clemow (2010) has fine-tuned the techniques of spot-inoculation and transformation to begin molecular work on R50. From the work of these students, R50 has been better understood, especially its nodulation phenotype and nodule organogenesis.

### **1.5 E151 (*sym15*)**

E151 was generated by ethyl-methane sulfonate mutagenesis of Sparkle (WT) seeds (Kneen *et al.*, 1994). The gene involved is *sym15*, a symbiotic gene presumably placed on chromosome 7 (Kneen *et al.*, 1994). The mutation caused multiple phenotypic effects such as a shorter third internode length, a shorter primary root length, and a lighter root dry weight (DW), and therefore we can label the mutant as pleiotropic. At this point in time, I would like to focus on the nodulation traits of E151. At 21 days after inoculation (DAI), E151 has very few emerged nodules compared to WT and is considered to be a low nodulator (Kneen *et al.*, 1994). It was discovered that a block occurs in the cortical program, preventing the nodule primordium from maturing to a nodule meristem (Chlup, 2007; Delanghe, 2007). However, it was noted that mature nodules were present on the mutant's roots at a later time than that which had previously been observed (Macdonald, 2009). E151 was also determined to be a delayed nodulator as it takes about a week longer than WT to produce emerged nodules; it also has an extended nodulated zone (Macdonald, 2009). Although few E151 nodules do emerge, those that are mature are unique as they have a multi-lobed morphology and consequently weigh more than those of WT, a trait linking E151 to an abnormal AON (Gresshoff *et al.*, 2005). The results of these studies led the lab to suggest that E151 may be deficient in sending or receiving a signal to

accomplish AON control. Since E151 is root-controlled (Chlup, 2007), the source of the AON deficiency must be in the root but could be in two different locations, either at the source of the root-signal or in the reception of the shoot-signal.

## **1.6 Objectives**

This thesis focuses on the nodulation phenotype of the pea mutant E151 (*sym15*). Another pea mutant well-studied in our lab, R50 (*sym16*), was used as a control along with the wild-type Sparkle. I hypothesize that E151 early-formed nodules are aborted because they are blocked in nodule organogenesis leading to no nodule emergence. I also hypothesize that E151 is deficient in sending the AON signal and that the multi-lobed nodules surface further down on the root system as a form of compensation. Specifically, my objectives were as follows:

1. Characterize E151 nodule distribution. (Chapter II)
2. Determine if E151 has a differential response to rhizobial strains. (Chapter III)
3. Determine the efficiency of the E151-*Rhizobium* association. (Chapter III)
4. Confirm the location of the block in E151 nodule organogenesis. (Chapter IV)
5. Determine whether E151 early-formed nodules are aborted or arrested. (Chapter IV)

## Chapter II: Nodulation Distribution

### 2.1 Introduction

Nodule distribution can affect shoot development and seed yield because the nitrogen fixed in the nodules must ultimately be transferred to the shoot. For example, Burias *et al.* (1990) indicate that nodules closer to the soil surface are more sensitive to environmental changes than those further from the surface; thus, in drought conditions, nodules lower down on the root system are preferred for optimal plant growth. Nodule distribution has been sporadically documented, likely because of the tedious work required and the lack of standardization.

Where nodules form on a root has been well studied. Bhuvaneswari *et al.* (1980) identified a most susceptible zone where soybean lateral roots were more vulnerable to rhizobial infection, and consequently most of the nodules were found there. The most susceptible zone has been described as a small restricted location just above the root tip where the epidermal cells have elongated but have not yet differentiated in mature root hairs. Anatomically, nodules have been noted to emerge opposite xylem poles, and thus were not considered to be random in their emergence from the root (Bond, 1948).

Because of the timing of inoculation in a lab setting, the roots susceptible to infection are near the top of the root system and nodules form at the crown. This nodulation pattern is said to be noticed because of the limited migration capabilities of rhizobia (Wadisirisuk *et al.*, 1989). Also of interest is that different bacteria associate with different root types in *Vicia faba* L. (faba bean; Ofek *et al.*, 2007). These authors suggested that the reason for this bacterial root preference is the different exudate profiles of the roots as exemplified by Ofek *et al.* (2007) who demonstrated that roots subjected to high salinity conditions bore different bacterial communities than roots under controlled conditions. It has already been demonstrated that primary and lateral roots may be different in their anatomy, for example, Pepper *et al.* (2007) showed that the primary root of pea had a triarch vascular pole pattern while its lateral roots had a tetrarch pattern. Thus, bacteria may be capable of sensing anatomical and physiological differences. These results show how important the timing of inoculation, the root anatomy, and the environment are when observing the association. Perhaps these differences could explain the

disparity seen in nodule distribution among species, e.g. on lateral roots for pea but on primary roots for *L. japonicus*.

The emergence and distribution of nodules are highly regulated by both hormonal and environmental cues (Ferguson *et al.*, 2010). For example, exogenous ethylene was found to inhibit nodule formation and this inhibition was overcome by treating plants with silver (1 or 5 $\mu$ M), an inhibitor of ethylene action (Lee and LaRue, 1992). In fact ACC oxidase, the ultimate enzyme catalyzing the production of ethylene, has been localized opposite phloem poles; this may explain why nodules form in the cortex facing the xylem (Heidstra *et al.*, 1997). Environmental cues may be exemplified by nitrate and light. In soybean, nitrate (15mM) inhibits infection events within 18 hours of inoculation (Malik *et al.*, 1987), whereas in pea, light suppresses nodulation (Lee and LaRue, 1992). Genotype can control also nodule distribution, as was observed by Burias *et al.* (1990). In this study, the authors categorized nodule distribution on multiple soybean genotypes according to nodule presence in either the upper, median or lower part of the root system; they also identified preferential zones and occasional zones of nodulation. Only two of the five genotypes had nodules covering the whole root system, with preferential zones into the lower part of the root system. The authors suggested that host genotypes can be characterized by their nodule profile. If a standardization of nodule profiling or mapping were developed, we could better compare mutants and other legume species.

Pueppke (1986) stated that distribution could be a useful quantitative indicator of nodulation rate and efficiency; it could be used as the basis for mutant characterization, and inferences to other legumes could be made. The author observed nodule distribution on the primary roots of *Macroptilium atropurpuratum* (DC.) Urb. (siratro) and *Vigna unguiculata* (L.) Walp. (cowpea) seedlings, each species having been inoculated with two different types of bacteria; differences were seen in the distribution between the two legumes but also between the bacteria used on a single species. As for Nishimura *et al.* (2002), they proposed that nodule distribution could be assessed by a ratio of nodule zone length to root length. Doing so, they determined that the nodules of a mutant of *L. japonicus* covered a larger space on the root than the WT.



### **2.1.1 Objectives**

From the above findings, one realizes that legume species and mutants of species can be distinguished by the distribution of their nodules. However, few studies have yet been performed to assess this important parameter, likely because of the difficulty to study large root systems. Macdonald (2009) proposed the use of nodulation maps to compare nodulation distribution in pea mutants. From preliminary data using nodulation maps, E151 was portrayed as a low and a delayed nodulator, in both time and space. The goal of this study was to confirm these results by observing more plants to determine the distribution in both time and space of E151 nodules compared to those of Sparkle. Here, R50 was compared to Sparkle as a control to determine whether the trends seen for E151 were characteristic of pea mutants in general.

## **2.2 Materials and methods**

### **2.2.1 Plant growth conditions**

Thirty seeds of each Sparkle and E151 were surface-sterilized with an 8% bleach (store-bought, 5.5% sodium hypochlorite) solution treatment (5 mins) followed by four 1 min-rinses of sterile water. The seeds were then left in the dark to imbibe for approximately eighteen hours (Guinel and Sloetjes, 2000). Cylindrical black Conetainers® (6.4 cm in diameter, 656 mL in volume, Stuewe & Sons, Inc., Tangent, OR, USA), the bottoms of which were lined with a mesh, were prepared with a 50:50 mixture of autoclaved vermiculite and turface (both soil components were purchased from Plant Products Company Ltd., Brampton, ON, Canada) which was wetted the night before planting. One seed was planted per pot, approximately 1 cm below the surface. The tray with the pots was filled with water and kept in the growth room under 8 hours of dark at 18°C and 16 hours of light at 23°C (light intensity of 120 to 150  $\mu\text{E m}^{-2} \text{s}^{-1}$ ). The pots were covered with wet paper towel and plastic to maintain moisture for germination; those covers were removed once the shoots had emerged from the soil. The plants were inoculated 5 days after planting (DAP) with 2mL of a 5% rhizobial solution (see below) using a sterile serological pipette. Low nutrient solution (Appendix A) was added 5 DAI followed by a regime of water, low nutrient solution, water, etc. until appropriate harvest. The experiment was replicated 4 times. These exact same steps were repeated in a separate experiment with Sparkle and R50 as a

mutant control to compare against E151; the only difference was the time of inoculation of 3 DAP, because contrary to typical pea studies, 5 DAP for E151 was deemed the best by Chlup (2007).

### **2.2.2 Bacterial growth conditions**

Each culture was prepared from a stab of *Rhizobium leguminosarum* bv. *viciae* 128C53K (generous gift of Dr. Stewart Smith, EMD Crop BioScience, Milwaukee, WI, USA) stored at -20°C on yeast mannitol agar (Appendix B). Two loopfuls were added to a flask of 20 mL of yeast mannitol broth (Appendix C) which was placed in an orbital shaking water-bath (New Brunswick Model C-76; Fisher-Scientific) at 100 rpm and 25°C, for 48 hours. Cultures were grown until they reached the stationary growth phase and had an absorbance reading between 0.8 and 1.1 at 600 nm on a spectrophotometer (Cary-Win UV), at which time a 5% bacterial solution was made in sterile water.

### **2.2.3 Counting of nodules**

Six plants of each line were randomly removed on harvest days (14, 21, 28, 35, and 42 DAI). The shoot was separated from the root using a sharp blade. The cotyledons were removed and the root system was placed on a grid (printed on a sheet of paper and placed in a plastic sheet) made of 2 cm x 1 cm rectangles (Fig. 2-1). The top of the root was positioned at the top left-hand corner of the grid, in the upper left corner of the first rectangle. The primary root was placed along the left-hand side of the grid with all lateral roots pulled towards the right-hand side. Individual nodules located in each rectangle were counted and their number recorded; each emerged nodule was considered whether it was white, pink, or green in colour. The nodules of each plant were removed as they were counted and placed in a pre-weighed microcentrifuge tube. These tubes were then set in a 60°C oven for 3 days, at which time they were weighed on a balance (Mettler Toledo, Zurich, Switzerland) once the tubes had cooled down. The mass of the empty tube was subtracted from the mass of the tube containing the nodules to get their DW. This number was then divided by the number of nodules on each plant to get an average of the individual DW of a nodule.



**Figure 2-1. A nodulated root system on a grid.**

The primary root was aligned to the left-hand side with each of the lateral roots spread towards the right-hand side. The nodules found in each box (2 cm by 1 cm) were tallied to map the distribution of the nodules on the root system.

#### **2.2.4 Microsoft Excel 2007**

The numbers of nodules were entered into a Microsoft Excel 2007 spreadsheet in a template similar to that of the grid. Data were pooled for each pea line at each harvest time to get an average, i.e., the values in each grid for each plant were added to get an average number of nodules for that location on the root system. A surface graph was made to show the location of the nodules on a 2D-representation of the root system, referred from now on as nodulation map with different colours indicating different ranges of nodule numbers.

#### **2.2.5 Quantitative analysis**

Three calculations (Fig. 2-2) were performed following the production of the nodulation maps. The spread of the nodules on the root system in a vertical direction was represented by the nodulation zone ratio based on the primary root (Fig. 2-2A). This ratio was calculated by subtracting the location of the nodule the closest to the cotyledons from the location of the nodule the furthest from the cotyledons and dividing this by the length of the primary root (as per Nishimura *et al.*, 2002). The spread of the nodules on the root system in a horizontal direction was achieved by the nodulation zone ratio based on the longest lateral root (Fig. 2-2B). This ratio was calculated by subtracting the location of the nodule the closest to the primary root from the location of the nodule the furthest from the primary root and dividing this by the length of the longest lateral root. The third calculation was performed to obtain the nodulation zone ratio based on the surface area covered by the root system (Fig. 2-2C). This surface area was assumed to be that of a triangle; thus it was calculated as the length of the primary root multiplied by the length of the longest lateral root, divided by two. The surface area that the nodules occupied (number of rectangles on the grid bearing any nodule multiplied by the rectangle surface area) was divided by the root surface area. The three extrapolated values were then multiplied by 100 to get a percentage.

#### **2.2.6 Statistical analysis**

Two-way ANOVAs were performed using Sigma Plot 11.0 (Systat Software, Inc., San Jose, CA, USA) on nodule number and individual nodule DW data. Comparisons were made between pea lines as well as between consecutive time points within a pea line.



**Figure 2-2. Diagrams illustrating how nodulation zone ratios were calculated.**

The nodulated surface area based on the primary root (A) was calculated by the formula  $(LNP - HNP) \div PR$ . The nodulated surface area based on the longest lateral root (B) was calculated by the formula  $(FNP - CNP) \div LLR$ . The nodulated surface area based on the root surface area (C) was calculated by the formula  $NSA \div RSA$ . To obtain percentages, each of the values were multiplied by 100. CNP (closest nodule position), FNP (furthest nodule position), HNP (highest nodule position), LNP (lowest nodule position), NSA (nodulated surface area), RSA (root surface area).

## **2.3 Results**

### **2.3.1 Nodulation maps**

A classification for pea root systems has been established based on length of lateral roots and their position on the primary root (McPhee, 2005). According to this classification, Sparkle had a triangular, distal, long lateral root length root system. MCPhee (2005) stated that using a uniform classification system would strengthen the understanding of data collection. With this in mind, my hope was that the nodulation maps would offer a standardized method of observing nodule distribution so that once multiple mutants and legumes are observed, a classification system may be developed.

The nodulation maps (Figs. 2-3 to 2-5) should be read as if the primary root was on the left-hand side and each of the lateral roots was spread towards the right-hand side. The cotyledons should be imagined to be in the top left corner of the map. The nodulation maps do not show the whole root system but rather focus on where the nodules are located. Therefore, from the maps one could see in a 2D representation where the nodules were observed on the root system. Nodule formation was restricted to lateral roots with the occasional nodules appearing on the primary root as in Bond (1948). These primary root nodules were larger than those found on the lateral roots which was also noted by Guinel and LaRue (1991). However, primary root nodules did not appear more often on a single pea line than on another (data not shown).

### **2.3.2 Distribution of Sparkle nodules**

The nodules of Sparkle were mostly located in close proximity to the cotyledons and the primary root (Figs. 2-3 and 2-6A); most nodules were centered about 1 cm from the primary root and 2 cm down from the cotyledons (Fig. 2-3), which fits with the results of Guinel and LaRue (1991). The nodules were restricted in their position covering one single area over time; this restricted zone was considered as one population of nodules. This population generally covered a vertical range of 5cm, with no nodules present past 12.5 cm from the cotyledons and 13 cm from the primary root (Fig. 2-3), even though the length of the primary root was generally around 18 cm in length and the longest lateral root was about 27 cm long. By 21 DAI, the nodule number of Sparkle had reached a plateau as the plant had grown all the nodules that it

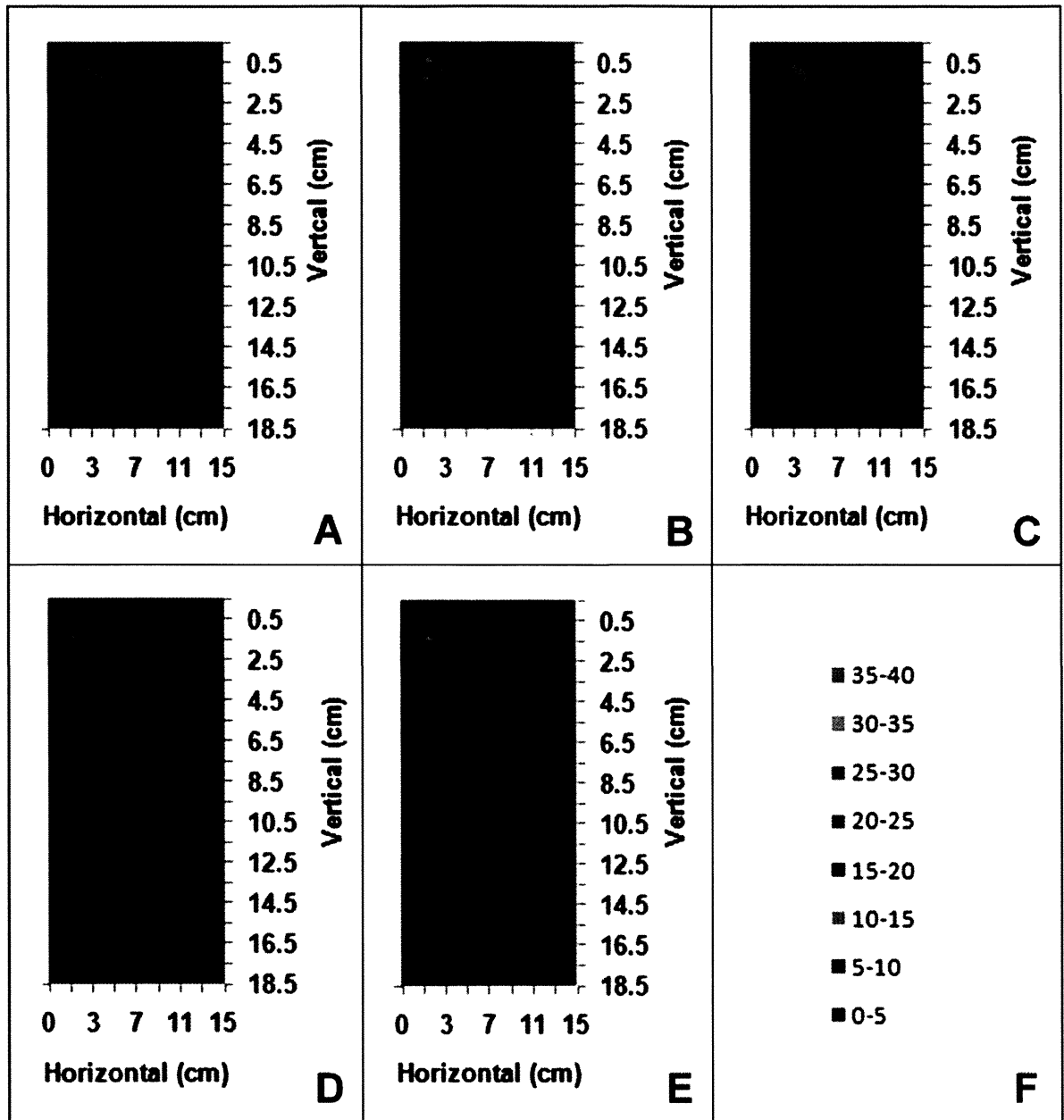


**Figure 2-3. Nodulation maps of Sparkle over time.**

Nodules were counted and the data were entered into Microsoft Excel 2007 where surface graphs were made. The maps are made to represent the root system, as if the cotyledons were in the top left-hand corner, with the primary root running down the left-hand side, and each of the lateral roots spread towards the right. The maps do not show the whole root system but rather focus on the most-nodulated area. (A) 14 DAI. (B) 21 DAI. (C) 28 DAI. (D) 35 DAI. (E) 42 DAI. (F) Legend depicting the average number of nodules each colour represents in the nodulation maps. (n = 24)

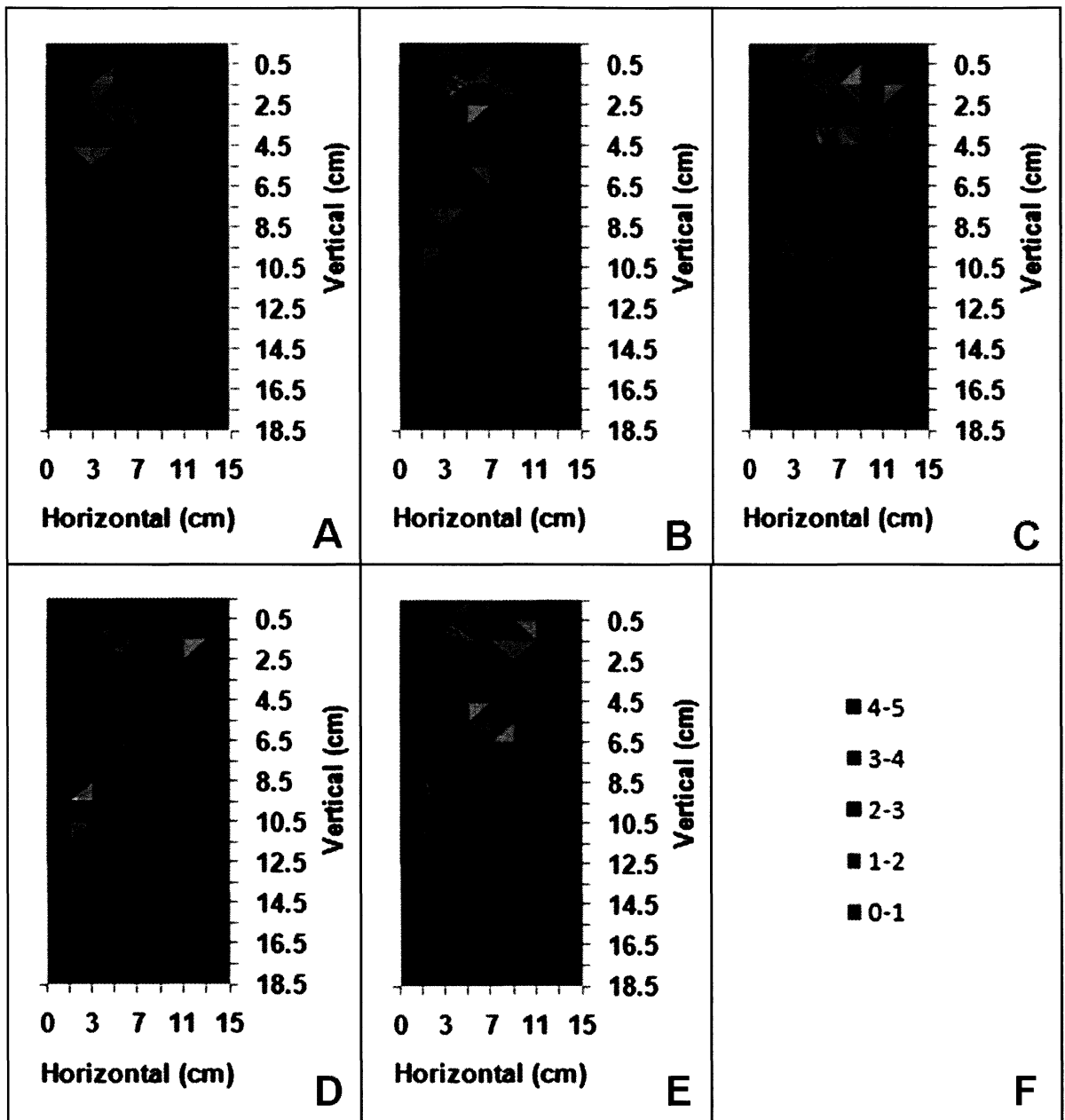


**Figure 2-4. Nodulation maps of E151 over time.**

Nodules were counted and the data were entered into Microsoft Excel 2007 where surface graphs were made. The maps are made to represent the root system, as if the cotyledons were in the top left-hand corner, with the primary root running down the left-hand side, and each of the lateral roots spread towards the right. The maps do not show the whole root system but rather focus on the most-nodulated area. (A) 14 DAI. (B) 21 DAI. (C) 28 DAI. (D) 35 DAI. (E) 42 DAI. (F) Legend depicting the average number of nodules each colour represents in the nodulation maps. (n = 24)



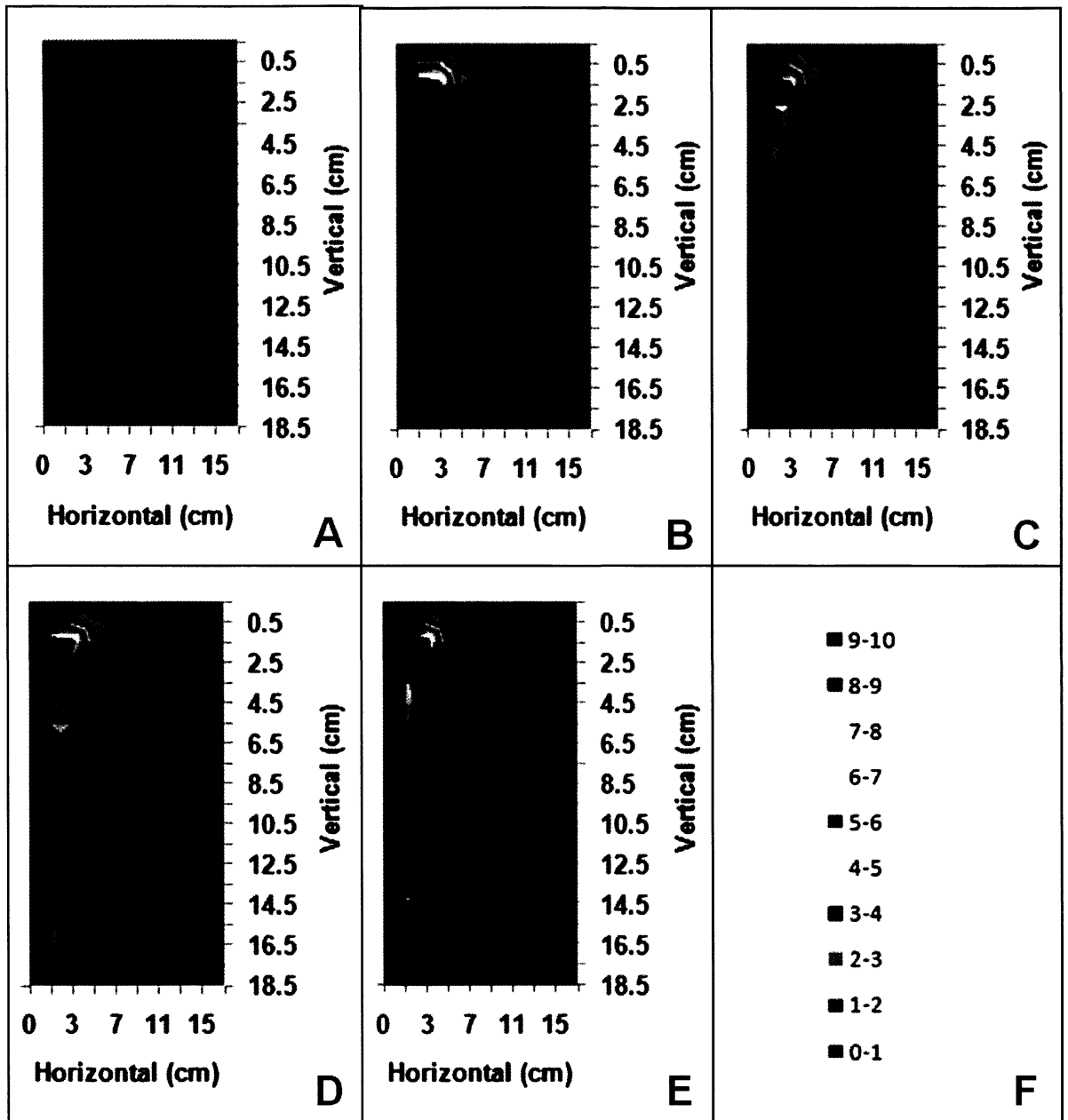


**Figure 2-5. Nodulation maps of R50 over time.**

Nodules were counted and the data were entered into Microsoft Excel 2007 where surface graphs were made. The maps are made to represent the root system, as if the cotyledons were in the top left-hand corner, with the primary root running down the left-hand side, and each of the lateral roots spread towards the right. The maps do not show the whole root system but rather focus on the most-nodulated area. (A) 14 DAI. (B) 21 DAI. (C) 28 DAI. (D) 35 DAI. (E) 42 DAI. (F) Legend depicting the average number of nodules each colour represents in the nodulation maps. (n = 24)

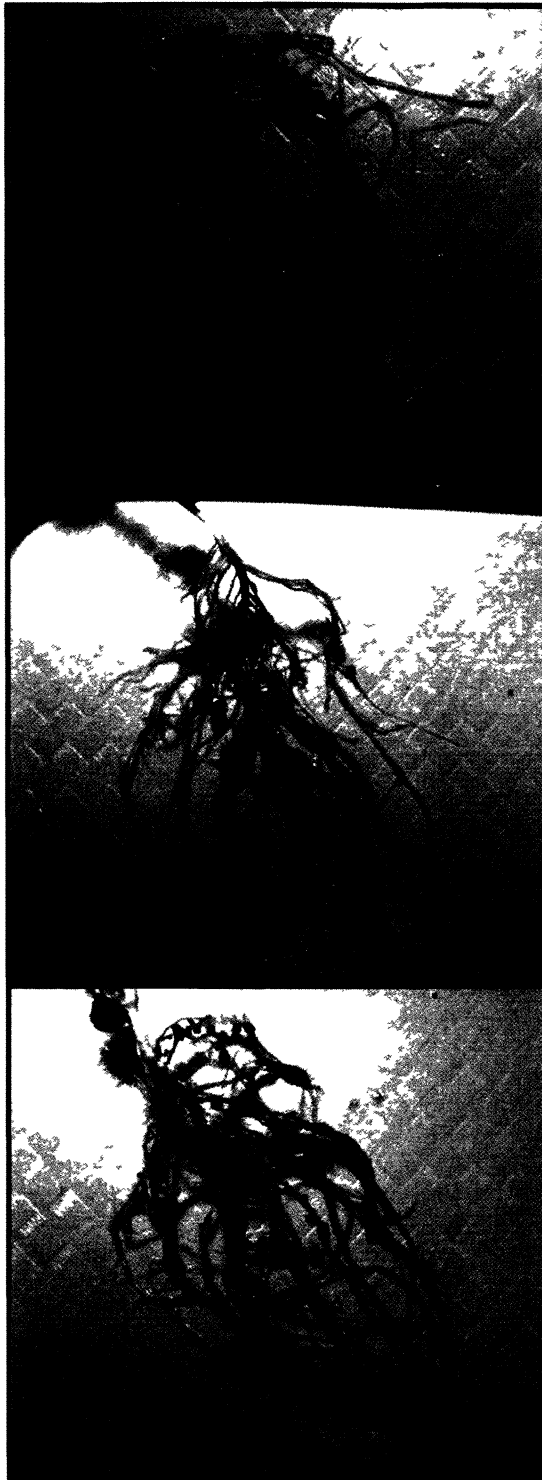


**Figure 2-6. Nodulated root system of Sparkle (A), E151 (B), R50 (C).** Each photograph was taken at 28 DAI and each of the plants was inoculated with *R. leguminosarum* bv. *viciae* 128C53K.

would grow (Table 2-1). However, the total DW of the nodules reached a plateau at 35 DAI, resulting in these nodules increasing in individual weight up until 35 DAI (Table 2-1). The nodule DW per plant was the highest of the three pea lines; however the individual DW was the least heavy because of the high nodule number. Therefore, nodules of Sparkle are in great abundance but are rather small compared to other pea lines. Interestingly, the nodules did not cover a significant amount of the root system, only 8.6% of the entire root system, with a larger spread noted in the horizontal direction than in the vertical direction (Table 2-2).

### **2.3.3 Distribution of E151 nodules**

From the scale on the nodulation maps, it was clearly seen that E151 was a low nodulator (Fig. 2-4F); in fact this was noted as a four-fold difference at 28 DAI in nodule number compared to Sparkle (Table 2-1). At that time, all the nodules were formed and a plateau was reached (Table 2-1). The nodules grew in size over time as the individual nodule DW increased until 35 DAI (Table 2-1). Although the total nodule DW per plant was the least heavy of the three pea lines, the individual nodule DW was the heaviest. Therefore, E151 produced very few nodules but these nodules grew quite large over time, perhaps as a form of compensation.

E151 nodules spread further down the root system and covered a larger amount of the root system than those of Sparkle. From this spread, three populations of nodules were detected with their highest nodule densities at 2.5, 5, and 11 cm down from the cotyledons and each of these 3cm away from the primary root which was further away than for Sparkle (Fig. 2-4). The nodules covered a total of 10.6% of the root system, an increase of 2% from the surface area covered by the nodules on Sparkle (NSA ratio, Table 2-2). By 28 DAI, E151 nodules had spread as far as they would and because nodule number had stopped to increase by this point, the nodules were only growing in size. Roughly in E151 the same amount of root as in Sparkle was covered by nodules in a horizontal direction by 21 DAI (LLR ratio, Table 2-2).

A drastic increase, not seen in Sparkle, in nodule number, nodule DW, and nodulation zone ratios from 14 to 21 DAI was observed, indicating that there was a temporal delay by about a week in E151 nodule development (Tables 2-1 and 2-2). This delay was accompanied by the spatial distribution delay already mentioned above (Figs. 2-4 and 2-6B).

**Table 2-1. Nodule number and DW for each pea line over time.**

		14 DAI	21 DAI	28 DAI	35 DAI	42 DAI
nodule number	SPK	190.04 ± 10.75 <sup>AB</sup>	213.58 ± 11.97 <sup>AB</sup>	209.71 ± 11.63 <sup>AB</sup>	209.42 ± 11.52 <sup>AB</sup>	210.29 ± 10.33 <sup>AB</sup>
	E151	6.79 ± 1.54 <sup>Aa</sup>	29.08 ± 3.74 <sup>ACab</sup>	53.50 ± 4.96 <sup>ACb</sup>	49.04 ± 3.77 <sup>AC</sup>	44.58 ± 2.45 <sup>AC</sup>
	R50	6.33 ± 3.56 <sup>Ba</sup>	68.17 ± 13.88 <sup>BCab</sup>	98.88 ± 8.40 <sup>BCb</sup>	118.75 ± 7.34 <sup>BC</sup>	106.50 ± 8.68 <sup>BC</sup>
nodule dry weight per plant (in mg)	SPK	22.3 ± 1.17 <sup>ABa</sup>	54.1 ± 5.48 <sup>ABa</sup>	69.8 ± 9.44 <sup>ABb</sup>	106.0 ± 13.3 <sup>ABb</sup>	104.0 ± 12.6 <sup>AB</sup>
	E151	0.38 ± 0.11 <sup>A</sup>	10.3 ± 1.60 <sup>Aa</sup>	27.6 ± 2.38 <sup>Aa</sup>	35.4 ± 2.27 <sup>A</sup>	36.9 ± 3.48 <sup>AC</sup>
	R50	0.31 ± 0.19 <sup>B</sup>	10.1 ± 2.82 <sup>Ba</sup>	30.0 ± 3.42 <sup>Bab</sup>	50.2 ± 4.10 <sup>Bb</sup>	62.7 ± 4.76 <sup>BC</sup>
individual nodule dry weight (in mg)	SPK	0.121 ± 0.006	0.258 ± 0.022	0.329 ± 0.037 <sup>Aa</sup>	0.542 ± 0.082 <sup>Aa</sup>	0.538 ± 0.086 <sup>A</sup>
	E151	0.0349 ± 0.007 <sup>a</sup>	0.377 ± 0.066 <sup>Ab</sup>	0.573 ± 0.06 <sup>ABbc</sup>	0.855 ± 0.103 <sup>ABc</sup>	0.871 ± 0.087 <sup>AB</sup>
	R50	0.018 ± 0.008	0.116 ± 0.024 <sup>Aa</sup>	0.297 ± 0.021 <sup>Ba</sup>	0.446 ± 0.037 <sup>Bb</sup>	0.629 ± 0.045 <sup>Bb</sup>

Values are means ± standard error (n=24 for each line, for each time). Same letters indicate significance. Significance between pea lines within a time point is denoted by capital letters. Significance between time points within a pea line is denoted by lower case letters. Two way ANOVAs were performed (p=0.001). DAI = Days after inoculation. SPK = Sparkle.

**Table 2-2. Nodulation zone ratios for each pea line over time.**

		14 DAI	21 DAI	28 DAI	35 DAI	42 DAI
PR nodulation zone ratio	SPK	19.2 ± 1.2 <sup>AB</sup>	18.7 ± 1.3 <sup>A</sup>	22.3 ± 1.7 <sup>AB</sup>	24.6 ± 2.4 <sup>A</sup>	22.8 ± 1.5 <sup>AB</sup>
	E151	9.8 ± 1.9 <sup>ACa</sup>	24.1 ± 1.7 <sup>ab</sup>	34.0 ± 1.6 <sup>ACb</sup>	31.2 ± 2.0 <sup>B</sup>	36.2 ± 1.7 <sup>A</sup>
	R50	7.3 ± 3.3 <sup>BCa</sup>	33.2 ± 3.3 <sup>Aab</sup>	48.0 ± 4.0 <sup>BCb</sup>	53.0 ± 3.1 <sup>AB</sup>	45.9 ± 3.4 <sup>B</sup>
LLR nodulation zone ratio	SPK	27.6 ± 1.5 <sup>AB</sup>	29.3 ± 1.7 <sup>A</sup>	29.2 ± 1.9	36.2 ± 1.7 <sup>A</sup>	38.3 ± 1.3
	E151	14.0 ± 2.6 <sup>ACa</sup>	30.1 ± 2.1 <sup>Ba</sup>	35.2 ± 2.9	33.1 ± 2.3	33.9 ± 1.5
	R50	5.0 ± 1.8 <sup>BCa</sup>	19.3 ± 2.0 <sup>ABab</sup>	32.3 ± 2.4 <sup>b</sup>	37.0 ± 2.7 <sup>A</sup>	36.0 ± 2.7
NSA nodulation zone ratio	SPK	7.7 ± 0.6 <sup>AB</sup>	7.2 ± 0.6	8.6 ± 0.8 <sup>A</sup>	8.2 ± 0.7 <sup>A</sup>	8.0 ± 0.5 <sup>A</sup>
	E151	2.3 ± 0.4 <sup>ACa</sup>	7.2 ± 0.6 <sup>ab</sup>	10.6 ± 0.6 <sup>Bb</sup>	8.7 ± 0.7 <sup>B</sup>	9.5 ± 0.4 <sup>B</sup>
	R50	1.6 ± 0.6 <sup>BCa</sup>	9.2 ± 1.1 <sup>ab</sup>	14.4 ± 1.3 <sup>ABbc</sup>	17.6 ± 1.1 <sup>ABcd</sup>	13.9 ± 1.3 <sup>ABd</sup>

Values are percentage means ± standard error (n=24 for each line, for each time). Same letters indicate significance. Significance between pea lines within a time point is denoted by capital letters. Significance between time points within a pea line is denoted by lower case letters. Two way ANOVAs were performed (p=0.001). DAI = Days after inoculation. LLR = Longest lateral root. NSA = Nodulated surface area. PR = Primary root. SPK = Sparkle.

### **2.3.4 Distribution of R50 nodules**

As E151, R50 was characterized as a low nodulator (Kneen *et al.*, 1994). This was confirmed by the nodulation maps (Fig. 2-5F); R50 produced about half the number of Sparkle nodules (Table 2-1). R50 nodules continued to form until 28 DAI, when the nodule number reached a plateau (Table 2-1). A drastic increase in nodule number, nodule DW, and nodulation zone ratios from 14 to 21 DAI was also seen in R50, showing that it too is a delayed nodulator by about a week (Tables 2-1 and 2-2). R50 nodules were much smaller than those of Sparkle and E151, but they continued to grow in size as they increased in individual DW until 42 DAI. Of the three pea lines, for both nodule DW per plant and individual nodule dry weight, R50 produced the median nodule weight (Table 2-1).

The nodules of R50 were at first restricted in their location on the root system and at 21 DAI, their pattern highly resembled that of Sparkle nodules (Figs. 2-5A and 2-5B). However, from 28-42 DAI the nodule distribution became stretched, with the nodules covering a larger vertical range of the root (Figs. 2-5C to 2-5E, 2-6C). There appeared to be four populations of nodules, centered at 1.5, 6.5, 12, and 16.5 cm down from the cotyledons with each population located 2 cm from the primary root (Fig. 2-5). The lower populations appeared when the plant was older as they were not present before 21 DAI. From the nodulation zone ratio according to the primary root, R50 had a larger vertical percentage of the root covered by nodules compared to the other pea lines (Table 2-2), as already seen in the nodulation maps. The nodules covered at most 17.6% of the root system, an increase by 7 and 6% of Sparkle and E151 root systems, respectively (Table 2-2). Once the plants were older, i.e. past 21 DAI, roughly the same amount of root was covered by nodules horizontally, according to the nodulation zone ratio based on the longest lateral root (Table 2-2).

## **2.4 Discussion**

### **2.4.1 The E151 nodulation phenotype**

Kneen *et al.* (1994) first characterized the mutants E151 and R50; at 21 DAI, low nodulating and non-nodulating mutants were studied for characteristics such as nodule number,

plant height, third internode length, primary root length, and root DW. It was determined that E151 and R50 were both low nodulators with pleiotropic traits distinguishing them from the wild-type Sparkle. These observations which were taken at one time point only gave us a snapshot of information about that plant at that specific time. The authors did not notice a delay in nodulation because both earlier and later time points were not considered.

Both E151 and R50 were later confirmed to be low nodulators (Chlup, 2007 and Guinel and Sloetjes, 2000, respectively). In this study, I compared E151 nodulation distribution to that of its WT and to that of another mutant R50. I found that delayed nodulation must be added to the phenotype of both mutants. Both a temporal and a spatial delay were seen for the two pea mutants. The temporal delay was noted as a shift in nodule appearance by about a week, whereas the spatial delay was seen as a shift in nodule distribution on the root system. As a result, E151 and R50 both had extended zones of nodulation compared to Sparkle; however, the two mutants differed in their nodule distribution as shown by the nodulation maps. E151 produced approximately a quarter of the number of nodules that Sparkle produced, and R50 produced about half of that number. Compared to R50, E151 produced significantly less nodules, indicating that perhaps different categories should be recognized in the label of low nodulation phenotype. The nodules of E151 were found to weigh the heaviest of the three pea lines; because the E151 nodule number was lower, a lighter weight of nodules on the plant overall was observed compared to the other pea lines. This is another indication that E151 and R50 may belong to different categories of mutants.

Sparkle, like any other pea grown in a lab setting, had nodules concentrated at the top of the root system. Nodules do not appear lower down on the root because the plant restricts the number of its nodules through the mechanism of AON. From Kneen *et al.* (1994) who described E151 as having a less developed root system, one may have thought that E151 did not have nodules further up on the root system because there were no laterals; however this was not the case as there were an equivalent amount of lateral roots in the mutant as in Sparkle. As well, as seen with a microscope, root hairs were present on the lateral roots at the top of the root system, therefore there should not have been any problem with infection. Likely, the reason why no nodules were present at the top of the root was because either the root hairs were not at a proper developmental stage to allow infection to occur or infection occurred but a block in nodule development resulted. We know the latter is correct as Chlup (2007) found a block at the nodule

primordium formation stage. The question arises now about the fate of the nodules. Are the nodules aborted or in a dormant phase? This problem will be considered in Chapter IV.

From the differences in nodule distribution between E151 and R50, the two mutants likely do not possess the same ability to autoregulate because they exhibit dispersive and inconsistent patterns of nodule distribution. Burias *et al.* (1990) suggest that nodule distribution is a genotypic constant, even though nitrogen fixation and nodule mass are phenotypic variations; the authors demonstrated that the soybean cultivars they studied did not possess all the same ability to autoregulate. In the lab, we are now undertaking a comparative AON study for pea mutants by using a technique known as approach-grafting (Li *et al.*, 2009).

#### **2.4.2 The usefulness of the nodulation maps**

The nodulation maps confirmed that the approach taken by Guinel and LaRue (1991) was valid. Guinel and LaRue (1991) examined the 3<sup>rd</sup> lateral root of pea at a section 1 to 1.5 cm away from the primary root, which they determined by visual observations alone to be a zone representative of nodulation. The authors wanted a standard method to study nodule organogenesis in pea mutants. We now know this was an accurate location to take root samples as this is where the most populated area of nodules is located. Guinel has now used this method on four different mutants (E2, Guinel and LaRue, 1991; E107, Guinel and LaRue, 1992; R50, Guinel and Sloetjes, 2000; and E151, Delanghe, 2007). I would suggest that the nodulation maps be now added as a tool to study pea nodulation mutants because they offer qualitative data from which many quantitative data can be extrapolated (see below). One of the above mutants, E2, had much less nodules than Sparkle, resembling more E151 than R50, and these nodules were found within 2.5 cm of the primary root. It would be interesting to map the nodule distribution of this mutant to see if it exhibits a delayed nodulation phenotype as well.

The nodulation zone ratio of Nishimura *et al.* (2002) allowed for a quantification of the amount of root system covered by nodules, which had not previously been calculated. It gave me the idea to do similar calculations in the hope of refining further the nodulation phenotype of E151. At 28 DAI, E151 was found to have nodules which covered 34% of the root system in a vertical direction while those of R50 covered 48% of the root; both mutants had larger ranges than that of Sparkle which was 22% (Table 2-2). Surprisingly, the nodules cover a relatively

small area of the root surface area, i.e. about 10% (Table 2-2). These quantitative data could be used to compare pea mutants with mutants from other species. It was found that the *L. japonicus* mutant *astray* had a larger nodulation zone ratio than the wild-type, and this ratio reached 31% (Nishimura *et al.*, 2002). This large ratio was not seen in the pea mutants studied here; however, the roots of *L. japonicus* are much shorter than those of pea. The nodulation maps (Macdonald, 2009) proved to be an asset to the lab as they have allowed for easy comparisons to be made between mutants and WT but also between different hormone treatments. Thus, nodulation maps have been used to analyze the effects of cytokinin derivatives on nodule distribution on a mutant (Long, 2010). These nodulation maps would likely be valuable for the visualization of nodule distribution for legume species which bear numerous nodules. I collaborated with two computer scientists, John Zupancic and Dr. Nora Znotinas (Wilfrid Laurier University, Waterloo, ON, Canada) in the hopes of making a program to expedite the time it takes to locate and count the nodules. We thought that a picture would be taken of the root system, this would be uploaded to the computer software, which would analyze the picture to produce a nodulation map. The program thus far can detect and trace the primary root and each of the lateral roots and can place a mark where a nodule is located (Zupancic *et al.*, 2010). The computer scientists have stopped with the project for now as they cannot figure out how to circumvent the difficulty of detecting nodules which may overlap or may not be large enough to be distinguished in size from an emerging lateral root. A new approach must be taken if we want to go further with the software and improve its accuracy. Further work on this software could potentially allow for a 3D modelling system to be developed to have a more accurate representation of the root system.

The representation of the root system and that of the nodule distribution of legumes have been attempted before. Thus, Caetano-Anollés and Gresshoff (1993) represented nodule distribution in soybean through 3D bar graphs. The authors considered the location of the nodules on 1cm segments of the lateral roots. Although the graph is presented in 3D, the representation of the root system is still in 2D. There were much less nodules in soybean than we have for pea, perhaps allowing for an easier representation of the root system. The nodulation maps presented in this thesis are similar to those of Caetano-Anollés and Gresshoff (1993) but I trust they offer more information and can be read more easily. With the nodulation maps, it is easier to visualize a root placed over the graph to know how the nodules appear on the root system. As well, instead of observing the plants at one time point, only giving a snap-shot



of the nodule distribution profile of the plant, one can conduct a full developmental study which is important if one wants to study AON for example.

More recently, Lira Jr. and Smith (2000), because observing nodule population dynamics is important although is a labour intensive task, developed a technique that involved growing legume seedlings in pouches, scanning the plants to achieve an image, locating each nodule on the image, and manually marking it with a black dot (Lira Jr. and Smith, 2000). A root system sketch with black dots was then produced by the software. Ultimately, they had to count the black dots, making the technique as tedious as the one I used. The authors determined that the most accuracy involved the hand separation of the roots before scanning, but the researchers admitted that this procedure is destructive and therefore not completely precise (Lira Jr. and Smith, 2000). I trust the nodulation maps in this thesis offer more information.

## Chapter III: Impact of Bacterial Strain on Nodulation Efficiency

### 3.1 Introduction

#### 3.1.1 Rhizobial strains

Specificity between the two partners of the symbiosis is one of the oldest studied areas in legume nodulation (Sprent, 2007). A large amount of host specificity exists concerning rhizobia. For example, *Sinorhizobium meliloti* induces nodules on only a few species of the genera *Medicago*, *Melilotus*, and *Trigonella* from the subfamily Papilionoideae, while *Bradyrhizobium* spp. has a broader host range and can nodulate legumes from Papilionoideae and Mimosoideae (Koch *et al.*, 2010). Certain rhizobial species nodulate only certain legumes, for example *R. leguminosarum* bv. *viciae* infects species of the genera *Lathyrus*, *Lens*, *Vicia* and *Pisum* (Sprent, 2009). However, pea is only nodulated by *R. leguminosarum* bv. *viciae*; within this bacterial biovar there are many different strains, one such example is 128C53 which is used often to challenge pea. These strains are distinct in that they have slightly different genomes and slightly different effects on the plant and its nodulation (Young *et al.*, 2006). Laguerre *et al.* (2007) mentioned that differences in nodule number on pea can be explained, most of the time, by the effect of the rhizobial strain, not by the plant cultivar.

When working in a lab, the outcome of the rhizobial strain infection on seed yield and plant growth is often not considered. In recent years, plant researchers have been biased towards the molecular functioning of the nodule; they have focused more on nodule organogenesis and signal transduction pathway than on crop yield. This has led to faulty findings. For example, for a decade, the *S. meliloti* and *M. truncatula* association had been studied as the model for indeterminate nodulation. Once the *S. meliloti* strain 1021 genome was sequenced (Galibert *et al.*, 2001), the next logical step was to sequence the host genome. *M. sativa* having a large genome, difficult to work with genetically, researchers turned to *M. truncatula* without ever questioning the efficiency of the association (Terpolilli *et al.*, 2008). Terpolilli *et al.* (2008) have found that the *S. meliloti* strain 1021 is actually ineffective in association with *M. truncatula*, while it is effective with *M. sativa*. It seems here that we have not followed a common saying, and in studying the forest, we have forgotten to clearly understand the trees. Therefore, when we

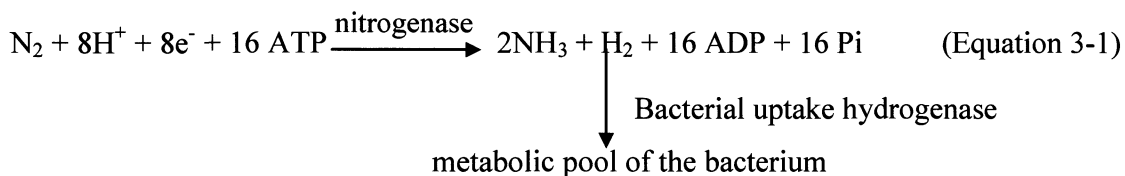
work in a lab setting, we must keep in mind the effect of the symbiosis on yield, and think of the field perspective as we strive to optimize shoot growth and seed yield for agricultural purposes. Indeed, among the many alterations to nitrogen fixation proposed by Bhatia *et al.* (2001), that of ensuring nodulation by the most efficient bacterial strain is of importance here. The strain which ultimately infects the plant has an effect on its growth and biomass because of the physiological functioning of the nodule. Thus, in an experiment involving multiple cultivars and strains, Skøt (1983) determined that the DW of three pea cultivars was dependent on the strain of *Rhizobium* used; he further noted that different combinations of pea line and *Rhizobium* produced varying amounts of nitrogen, even so large as a 200% difference. Of interest is Skøt's use of the rhizobial strain 128C53 (further denoted as HUP<sup>+</sup>), which we use most often in our lab; this rhizobial strain produced many large, red, healthy root nodules on each cultivar (Skøt, 1983). However, plants nodulated by HUP<sup>+</sup> experienced a decrease in shoot biomass relative to total biomass and had a lower nitrogen content than those plants of the same cultivar which were inoculated with the *R. leguminosarum* strain 1045 (Skøt, 1983). For a lab experiment, HUP<sup>+</sup> is sufficient to study but in an agricultural-context, the latter is likely better. Chen and Thornton (1940) stated that as early as the 1890's it was known that bacterial strains differed in their ability to benefit the host legume; it is surprising that today we are still trying to optimize the association.

Mutated bacterial strains are often used to understand strain efficiency in nodulation. Downie *et al.* (1985) created mutant strains of *Rhizobium leguminosarum* bv. *viciae* by inserting the transposon Tn5 into their nodulation genes; five classes of *nod* mutations were recognized based on the mutant strains' nodulation phenotypes on pea plants. Three classes (I, II, and III) were defective in the epidermal program of nodulation and two classes (IV and V) were delayed in their cortical program (Downie *et al.*, 1985). From this study, the authors were attempting to understand the active genes of the *Rhizobium* which allowed it to invade the host legume and initiate the formation of a nodule (Downie *et al.*, 1985). In this case, efficiency is classified as the ability to form an emerged nodule; the authors began with nodule organogenesis to see the outcome on nodule physiology.

### 3.1.2 Nitrogenase

When considering the plant-bacteria symbiosis, the bottom line is nitrogen fixation and it is therefore important to understand what is happening within the nodule. The bacteria which differentiate into bacteroids in the symbiosome are responsible for fixing nitrogen within the nodule (e.g., Oke and Long, 1999). The bacteroids express the enzyme nitrogenase that reduces atmospheric nitrogen to ammonia, as seen in Equation 3-1 (Downie, 2005). Nitrogenase is oxygen-sensitive but requires high levels of ATP to function; so it actually needs oxygen (Downie, 2005). To solve this paradox, the host plant has evolved multiple strategies. For example, an oxygen diffusion barrier located in the nodule cortex protects the enzyme from being in close proximity to oxygen (Schulze, 2004). Leghaemoglobin is also present in the cytoplasm of the host cells containing the symbiosomes; the protein forages the oxygen and regulates its entry to the bacteroids via the symbiosome membrane (Downie, 2005). The haemoglobin is a red-coloured protein which gives the nodules their pinkish colour when they are active (Sprent, 2008).

The amount of nitrogen that is fixed can be determined by measuring the activity of the nitrogenase (Equation 3-1). Previously, the acetylene reduction assay was used to measure this activity as the enzyme was found to act non-specifically on the acetylene, breaking its triple bond, and converting it to ethylene (Hardy *et al.*, 1968). More recently, a gas-flow through system (Qubit Systems, Kingston, ON, Canada) which measures hydrogen evolution, a by-product of the reaction (Equation 3-1), is being used to determine nitrogenase activity; it is a more accurate and less dangerous method (Layzell *et al.*, 1984; Hunt and Layzell, 1993). The only drawback to this technique is that a strain lacking the uptake hydrogenase enzyme must be used so the hydrogen remains within the soil to be measured (see arrow bringing back H<sub>2</sub> to bacteria in Equation 3-1).



### 3.1.3 Measuring efficiency

When reading the literature, it is difficult to understand exactly what is meant by efficiency as explained below. Some researchers consider efficiency as purely a function of the bacterial strain, i.e. of its ability to fix nitrogen, while others consider the effect of the bacteria on the plant and speak more about the nodule efficiency or the efficiency of the association.

It has been proposed that rhizobia lacking the hydrogenase enzymes (HUP<sup>-</sup>) are energetically inefficient in their symbiosis as more energy is put towards hydrogen evolution than towards nitrogen fixation (Schubert and Evans, 1976). More recently, view points are changing and researchers have argued that those rhizobia which release hydrogen into the soil are bringing an added benefit to the plant because this hydrogen is consumed by hydrogen-oxidizing bacteria which have plant growth-promoting properties (Golding and Dong, 2010). These soil microorganisms are found to multiply rapidly around HUP<sup>-</sup> root nodules (Stein *et al.*, 2005).

Some investigators have even developed equations to quantify how a symbiosis is more efficient than another (Gulden and Vessey, 1998; Fei and Vessey, 2009; Oono and Denison, 2010). For example, the return on nodule construction cost can be determined from the ratio of host biomass per nodule mass (Oono and Denison, 2010). This ratio affects the per-plant nodule construction cost and will increase for legumes which do not interact with effective strains (Oono and Denison, 2010). Legumes typically continue to form nodules until they sensed that a sufficient amount of nitrogen has been attained; consequently, those legumes associated with a less effective strain will form many more nodules than those with a more effective strain (Oono and Denison, 2010). That ineffective strains produce more numerous and smaller nodules has been known since 1940 (Chen and Thornton, 1940).

Another way to define efficiency is by considering the nitrogen fixed in relation to the carbon spent, i.e. carbon consumed or respired. Oono and Denison (2010) determined this value of nitrogen fixation efficiency using a gas flow-through system similar to the system mentioned earlier with an infrared gas analyzer for CO<sub>2</sub>; they were able to increase the external oxygen to increase nodule CO<sub>2</sub> production, which is measured with the analyzer. To make their point, the authors compared the fixation efficiency of the bacterial strains of the legumes which host swollen bacteroids (i.e. peas and *Arachis hypogea* L. [peanuts]) to that of those which host non-swollen bacteroids (i.e. beans and cowpeas). Swollen bacteroids are those which no longer

divide normally, while non-swollen bacteroids divide normally once they are outside of their nodules; these latter bacteroids are similar in shape and size to free-living bacteria (Oono and Denison, 2010). Oono and Denison (2010) suggested that swollen bacteroids may provide more of a benefit to legumes than non-swollen bacteroids; the former would have more of their energy contributing to nitrogen fixation, thus increasing nodule efficiency. When comparing peas to beans, the authors used two strains on each host, *R. leguminosarum* strain 4292 which nodulates only bean, a wild-type *R. leguminosarum* strain 3841 which only nodulates pea, and A34, a *R. leguminosarum* strain which nodulates beans and was genetically engineered to nodulate pea. In the case of A34 nodulating pea, 33% of the nitrogenase activity was used for H<sub>2</sub> production rather than for nitrogen fixation; typically this value must be at least 25%, therefore the fixation of the symbiosis A34-pea seems to be good (Oono and Denison, 2010). A higher fixation efficiency is often correlated with the production of more plant mass relative to nodule mass (Oono and Denison, 2010).

#### **3.1.4 Objectives**

From this short introduction to nodulation efficiency, one can see that this parameter depends on both organisms, and on the environmental conditions of the plant and of the bacteria within the nodule. Furthermore, it depends on the interest of the researcher. For this last reason, it is difficult to navigate in the literature. Of interest to me is whether the four lab strains associate equally well with the plant and result in the production of an efficient nodule. If so, these nodules would allow the plant to optimize the relationship between its nutritional allocation to nitrogen fixation and to growth. The four strains examined were 1. HUP<sup>+</sup> strain which is the wild-type strain we used most often in the lab, 2. HUP<sup>-</sup> which is a wild-type isolate lacking the uptake hydrogenase enzyme, 3. A34 which is the transgenic strain mentioned earlier, and 4. lacZ which is the A34 strain with a lacZ insertion. Typically, in the lab, we have looked at nodule number and nodule DW but perhaps these are not the best determinants of an efficient association. The objective of this chapter was to assess the efficiency of the association between the four bacterial strains we used in the lab and the three pea lines studied in Chapter II. Efficiency here was characterized based on nodule number, nodule DW, and nodule

morphology. Nitrogen fixation rate was also determined but only using the HUP<sup>+</sup> strain because of the system's limitations.

## 3.2 Materials and methods

### 3.2.1 Assessment of four bacterial strains

#### 3.2.1.1 Bacterial strain inoculation and plant growth

Seeds of the pea lines Sparkle, E151, and R50 were surface-sterilized, imbibed, planted, and grown as in Chapter II. Each bacterial culture was prepared from a stab of *R. leguminosarum* bv. *viciae* stored in a -20°C freezer on yeast-mannitol agar (Appendix B). Once each culture became slightly cloudy and had an absorbance reading between 0.8 and 1.1 at 600 nm on a spectrophotometer (Cary-Win UV), it was at the right growth stage (i.e. stationary phase) to prepare the inoculum. Seedlings were inoculated with 5mL of a 5% rhizobial solution using a sterile serological pipette. R50 plants were inoculated 3 DAP while Sparkle and E151 plants were inoculated 5 DAP. Planting was scheduled so inoculation occurred on the same day for all three pea lines. The plants were submitted to the watering regime stated in Chapter II.

Four different bacterial strains were compared. The strain 128C53K (HUP<sup>+</sup>) is WT strain, the strain 128C79 (HUP<sup>-</sup>) is WT isolate lacking the uptake hydrogenase enzyme (Nelson and Salminen, 1982); both are *Rhizobium leguminosarum* bv. *viciae* strains (generous gifts of Dr. Stewart Smith, EMD Crop BioScience, Milwaukee, WI, USA). The strain A34 is a transgenic strain, which is a derivative of 8401, a strep-resistant derivative of *R. leguminosarum* bv. *phaseoli*; its sym plasmid was cured and replaced by the sym plasmid pRL1JI (Downie, personal communication). Strain 8401, previously nodulating only bean, was thus engineered in A34 to nodulate pea (Oono and Denison, 2010). A34 was used in comparison to its mutant lacZ8401 (lacZ) which had a *hemA-lacZ* construct (from pGD499) inserted into a plasmid, i.e. pXLGD4, other than the sym plasmid. The *hemA* gene encodes the first enzyme of the common tetrapyrrole pathway, the  $\delta$ -aminolevulinic synthetase; the insertion of *lacZ* in the enzyme's promoter region deactivates the enzyme (Leong *et al.*, 1985). A34 and lacZ were both generous gifts of Dr. Allan Downie (John Innes Centre, Norwich, UK).

### **3.2.1.2 Counting of nodules**

Plants were harvested from their Conetainers<sup>®</sup> at 28 DAI and 35 DAI to count their nodules. Nodule morphology was first observed and photographs were taken of the nodules for each pea line and strain combination. Nodules were then excised while counted, and placed in labelled and pre-weighed centrifuge tubes which were later placed in an oven and weighed as in Chapter II. Four plants of each pea line were harvested each counting day. The experiment was repeated in three replications, resulting in a total of 12 plants for each pea line for each time and strain combination.

### **3.2.1.3 Analysis of results**

The averages (and standard errors) of nodule number, nodule DW per plant, and individual DW of a nodule on a per plant basis for each trial were calculated. Three-way ANOVAs were performed using Sigma Plot 11.0 (Systat Software, Inc., San Jose, CA, USA). Comparisons were made between HUP<sup>+</sup> and HUP<sup>-</sup>, between A34 and its transformant lacZ, and between HUP<sup>+</sup> and A34 because both strains had been used on peas as a wild-type (Lee and LaRue, 1992, and Schneider *et al.*, 1999, respectively). Plant return on nodule construction cost was calculated by adding the DWs of the shoots and roots and dividing this by the nodule DW as per Oono and Denison (2010). Specific nodulation was calculated by dividing the nodule number by the DW of the roots as per Fei and Vessey (2009). The specific nodule DW was calculated by dividing the nodule DW by the DW of the roots as per Gulden and Vessey (1998).

## **3.2.2 Nitrogenase activity**

### **3.2.2.1 Qubit system**

The function of each component of the Qubit system (Kingston, ON) is explained here in the order of the component's appearance from left to right in Figure 3-1; this order mirrors the flow of the gas through the system. Either the N<sub>2</sub>:O<sub>2</sub> or the Ar:O<sub>2</sub> carrier gas was allowed to pass through the system through the 3-way valve. The pressure regulator regulated and stabilized the gas flow while the mass flow controller measured and reported the chosen flow to the computer. The hydrogen flow from the H<sub>2</sub> standard gas tank was set via the Alicat mass flow monitor. The



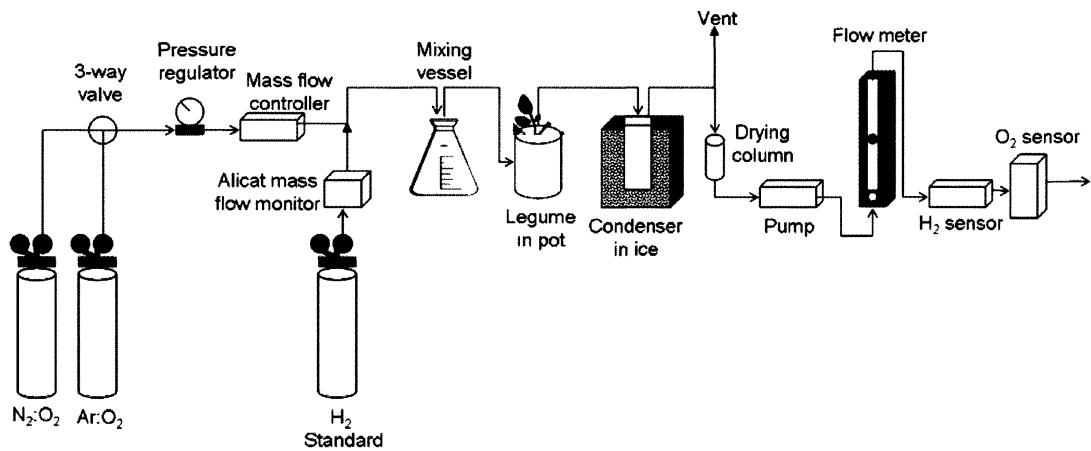


**Figure 3-1. Flow diagram of the Qubit apparatus (Qubit Systems Manual, 2005).**

Detailed explanations are given in the text. Here, as a plant is attached in the system between the mixing vessel and the condenser, plant measurements would be performed.

carrier gas and the standard gas were then combined in the mixing vessel. If the calibration was being performed, there was no plant attached and the mixing vessel was connected directly to the condenser in ice. If a plant was being measured, it was inserted between the mixing vessel and the condenser (Fig. 3-2); the gas entered the bottom of the pot and left through the top from the hole in the lid (Figs. 3-1 and 3-2). Regardless of a plant being connected or not, there is a vent (vent 1 in Fig. 3-2) in the tubing between the mixing vessel and the condenser to allow the proper flow to reach the sensors. The condenser partially removed moisture from the air; the drying column, containing magnesium perchlorate, further ensured that no moisture is left in the gas prior to it reaching the sensors. The pump provided gas to the sensors for analysis. The flow meter determined the portion of the gas flow that exited the system at the second vent (vent 2 in Fig. 3-2). The H<sub>2</sub> sensor detected the H<sub>2</sub> content in the gas while the O<sub>2</sub> sensor determined the partial pressure of oxygen and transmitted this to the computer where it was displayed as the percentage of oxygen.

### ***3.2.2.2 Plant growth conditions***

Seeds of Sparkle, E151, and R50 were surface-sterilized and imbibed as in Chapter II. Growth pots (9 cm diameter and 14.5 cm height; Qubit Systems, Kingston, ON, Canada) were filled with sterilized grade 16 silica sand (Bell and Mackenzie, Hamilton, ON, Canada) which was wetted the night before the seeds were planted. Sand was chosen as a substrate to allow easy gas flow from the roots to the surface. One seed was planted per pot, just beneath the surface so that it was covered by a thin layer of sand. This shallow planting was performed in order to place a lid onto the pot (Fig. 3-2) for measurements with the least amount of stress subjected to the leaves. Because the sand dried out quickly and the plants were not healthy in this medium, careful attention was given to keeping the sand moist, especially during germination and seedling development. The tray with the pots was filled with water and kept in the growth room under 8 hours of dark at 18°C and 16 hours of light at 23°C (light intensity of 120 to 150  $\mu\text{E m}^{-2} \text{s}^{-1}$ ). Seedlings were inoculated 3 DAP with 5 mL of a 5% HUP<sup>+</sup> bacterial solution using a sterile serological pipette. The plants were submitted to the watering regime stated in Chapter II. The experiment was performed in replication with plants totalling 16, 14, and 17 for Sparkle, E151, and R50, respectively.

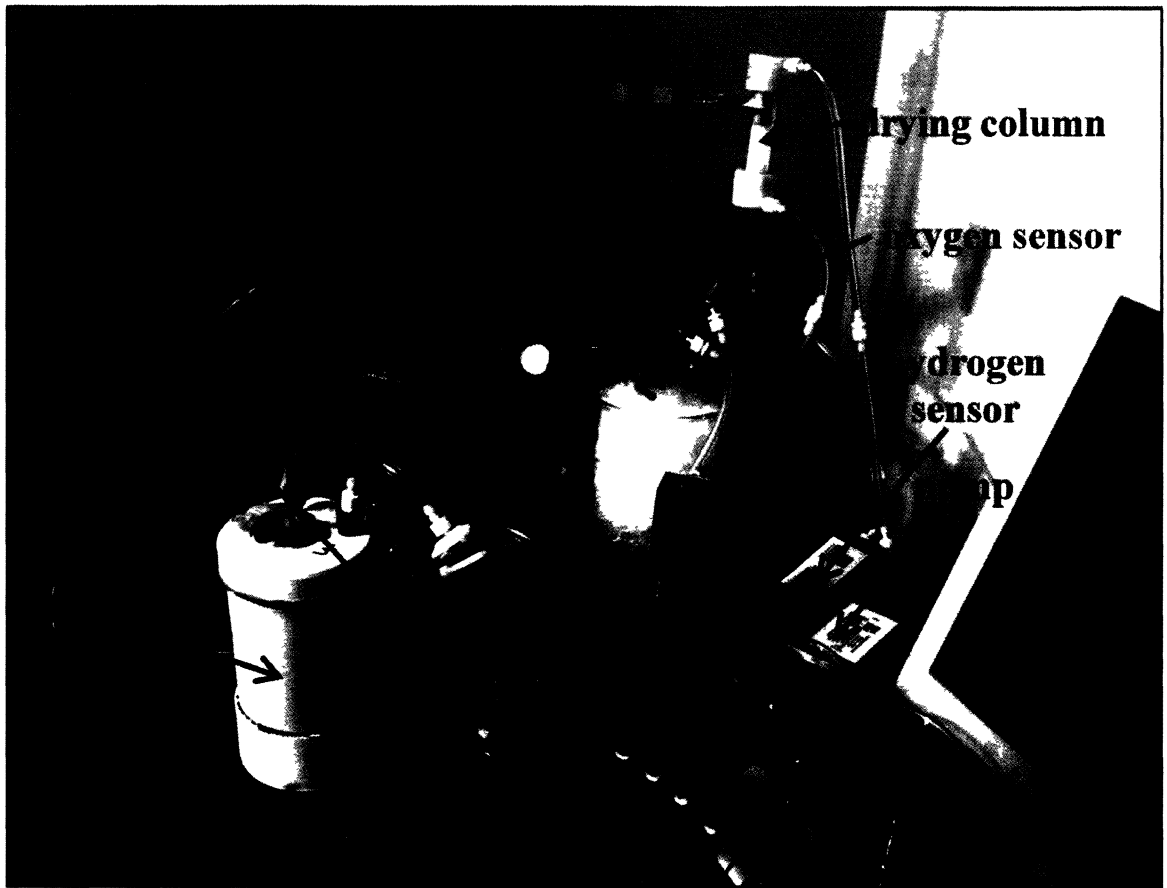


**Figure 3-2. A plant is attached to the Qubit system in this photograph.**  
The apparatus is located in the growth-room so the plant is the least stressed as possible before and during measurements.

### **3.2.2.3 Calibration of the system**

The protocol for calibration was followed for both the N<sub>2</sub>:O<sub>2</sub> and Ar:O<sub>2</sub> carrier gases as per the Qubit Systems Manual (2005). Through many trials, I determined that the following steps were beneficial. The pump was turned on the day before measurements were taken to allow gas to pass continually through the H<sub>2</sub> sensor to maintain high sensitivity. The sensor was left on throughout the experimental period. On the day of measurement, the magnesium perchlorate drying column was checked to ensure that no hard clump caused from absorbing moisture had formed. This column was changed often (about every other week) with new glass wool and well-packed magnesium perchlorate (Fisher Scientific) because a moist column could severely alter hydrogen evolution measurements. The Logger Pro 3 software (Qubit Systems, Kingston, ON, Canada) was used with the apparatus. The H<sub>2</sub> sensor was allowed to equilibrate until the hydrogen voltage stabilized.

### **3.2.2.4 Plant measurements**

The protocol for plant measurements was followed as per the Qubit Systems Manual (2005). The Qubit apparatus was kept in the growth room to minimize plant disturbance during measurements. Plants were not watered within two days of measurements because dry sand allows the gas to flow more easily through the pot and therefore measurements were taken more quickly. First, the stabilization voltage of the hydrogen evolved when using the N<sub>2</sub>:O<sub>2</sub> gas (Praxair Canada, Inc., Kitchener, ON, Canada) was recorded so that the apparent nitrogenase activity (ANA) could be determined (Equation 3-1). Second, the peak of hydrogen obtained when using the Ar:O<sub>2</sub> gas (Praxair Canada, Inc.) was assessed so that the total nitrogenase activity (TNA) was ascertained (Equation 3-2, Table 3-1).

### **3.2.2.5 Analysis of results**

The calibration points were used to generate calibration curves for each carrier gas that was used. The rates of H<sub>2</sub> [ppm] in ANA and TNA were determined using the equations acquired from the calibration curves and entering the hydrogen voltage measured for each plant. From these calculated rates, the ANA and TNA rates were obtained using Equation 3-3 and 3-4 (Table 3-1). The rate of nitrogen fixation was calculated from the ANA and TNA values (Equation 3-5, Table 3-1); a denominator of 3 was used because reducing N<sub>2</sub> to NH<sub>3</sub> requires 3

**Table 3-1. Equations used to determine nitrogen fixation**

Equation 3-2	$\text{Ar} + 8\text{H}^+ + 8\text{e}^- + 16 \text{ATP} \longrightarrow \text{H}_2 + 16 \text{ADP} + 16 \text{Pi}$
Equation 3-3	$\text{ANA} = \text{ANA flow (mL/min)}^* \times \text{P} \times \text{standard H}_2 \text{ concentration (ppm)}^{**} \times 60 \text{ mins/hr} / \text{R} \times \text{T}$
Equation 3-4	$\text{TNA} = \text{TNA flow (mL/min)}^* \times \text{P} \times \text{standard H}_2 \text{ concentration (ppm)}^{**} \times 60 \text{ mins/hr} / \text{R} \times \text{T}$
Equation 3-5	$\text{Nitrogen fixation rate } (\mu\text{mol N}_2/\text{hr}) = (\text{TNA}-\text{ANA})/3$
Equation 3-6	$\text{Electron allocation coefficient (EAC)} = 1 - (\text{ANA}/\text{TNA})$

ANA = apparent nitrogenase activity, TNA = total nitrogenase activity, EAC = electron allocation coefficient, P = atmospheric pressure, T = room temperature, R = 8314.5 mL kPa K<sup>-1</sup> mol<sup>-1</sup> constant

\* generally set to 1000 mL/min

\*\* value determined from H<sub>2</sub> flow (set by the operator) and the flow meter setting (which is usually 100 mL/min)

electron pairs, while the reduction of  $H^+$  to  $H_2$  only requires 1 electron pair. The relative allocation of electrons between  $H^+$  and  $N_2$  was calculated (Equation 3-6, Table 3-1). A higher electron allocation coefficient indicates that a greater proportion of nitrogenase activity is used for nitrogen fixation.

### 3.3 Results

#### 3.3.1 Bacterial strain effect on Sparkle

For Sparkle, the most nodules were formed with the wild-type  $HUP^+$  strain, and the least nodules were formed with  $lacZ$  (Fig. 3-3A). The heaviest nodules were also produced by  $HUP^+$  (Fig. 3-4A). The inoculation with the  $HUP^-$  strain resulted in an intermediate amount of nodules, which must be kept in mind when analyzing the nitrogen fixation results to estimate whether the results obtained are an under-estimation or an over-estimation for the other strains. There was no difference in Sparkle nodule number or DW from 28 to 35 DAI (Figs. 3-3A and 3-4A). Nodules were as expected; they had a standard oblong shape with a single indeterminate meristem (Guinel, 2009). Nodule morphology remained the same for all combinations with each strain (Fig. 3-5), apart for A34 and  $lacZ$  nodules which were smaller than those produced by the other two strains (Fig. 3-5). I followed over time the nitrogen fixation on an individual plant basis to extrapolate nitrogen fixation from hydrogen evolution. Little amounts of nitrogen were being fixed at 14 DAI (Fig. 3-6A), which was expected as nodules were fairly few and light pink at this time, as seen from results in Chapter II, indicating low activity. Peaks in nitrogen fixation around  $2.0 \mu\text{mol } H_2/\text{hr}$  were seen either at 21 or 28 DAI depending on the individual plant (Fig. 3-7). By 35 DAI, nitrogen fixation had decreased as both the nodules and the plant were senescing (Fig. 3-6A). Sparkle was more effective in nodule construction cost at 21 and 28 DAI than later on when the values were 11.8 and 16.7 g DW per g of nodule DW, respectively (Table 3-2).

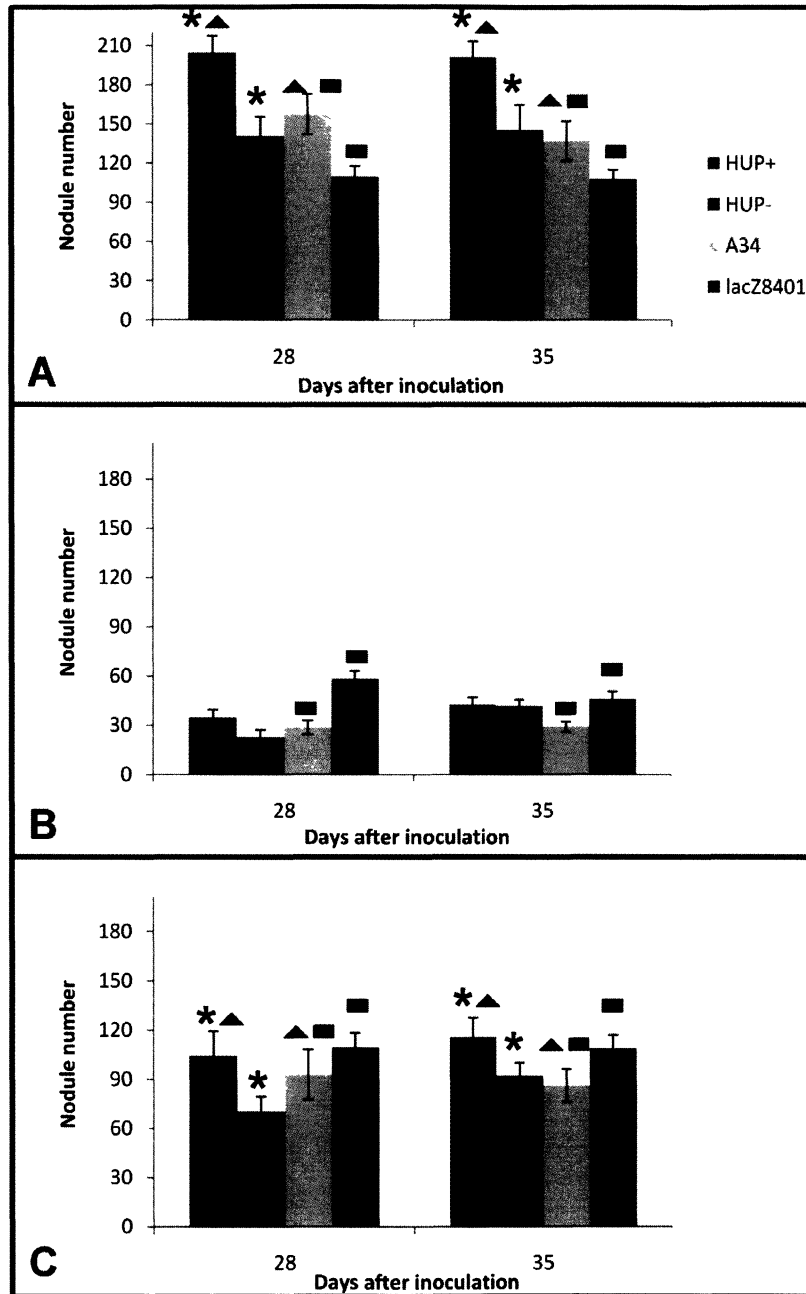
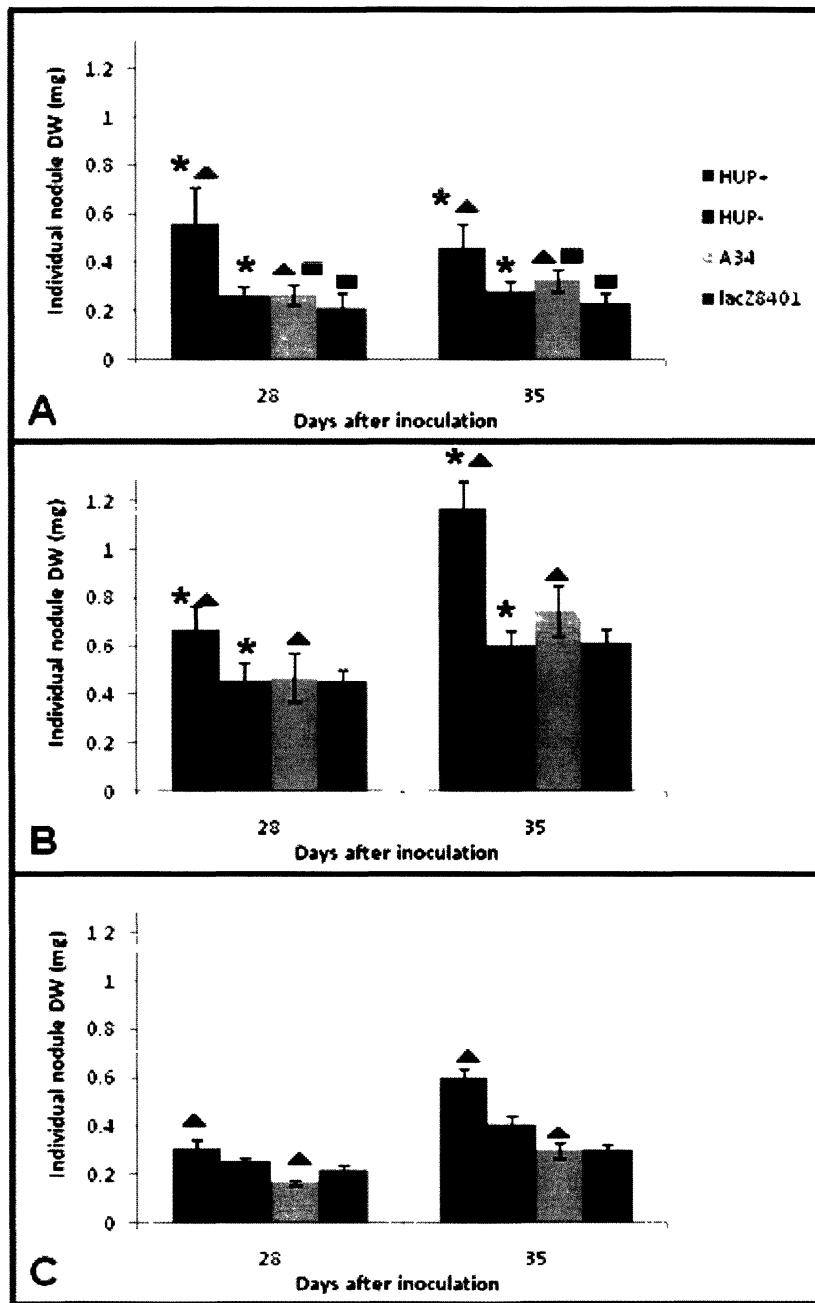


**Figure 3-3. Nodule number on roots of Sparkle (A), E151 (B), and R50 (C) when inoculated with four bacterial strains.**













The bars represent means  $\pm$  standard error. Blue bars represent HUP<sup>+</sup>, red bars represent HUP<sup>-</sup>, green bars represent A34, and purple bars represent lacZ. Three way ANOVAs were performed ( $p = 0.001$ ). Comparisons were made between HUP<sup>+</sup> and HUP<sup>-</sup> (asterisks), between HUP<sup>+</sup> and A34 (triangles), and between A34 and its transformant lacZ (squares). N = 12, in 3 replicates.



**Figure 3-4. Individual nodule DW of Sparkle (A), E151 (B), and R50 (C) when inoculated with four bacterial strains.**

The bars represent means  $\pm$  standard error. Blue bars represent HUP<sup>+</sup>, red bars represent HUP<sup>-</sup>, green bars represent A34, and purple bars represent lacZ. Three way ANOVAs were performed ( $p = 0.001$ ). Comparisons were made between HUP<sup>+</sup> and HUP<sup>-</sup> (asterisks), between HUP<sup>+</sup> and A34 (triangles), and between A34 and its transformant lacZ (squares). N = 12, in 3 replicates.



	SPK	E151	R50
HUP <sup>+</sup>			
HUP <sup>-</sup>			
A34			
lacZ			

**Figure 3-5. Nodule morphology of the 3 pea lines inoculated with each bacterial strain.**  
 Photographs were taken at 28 DAI.

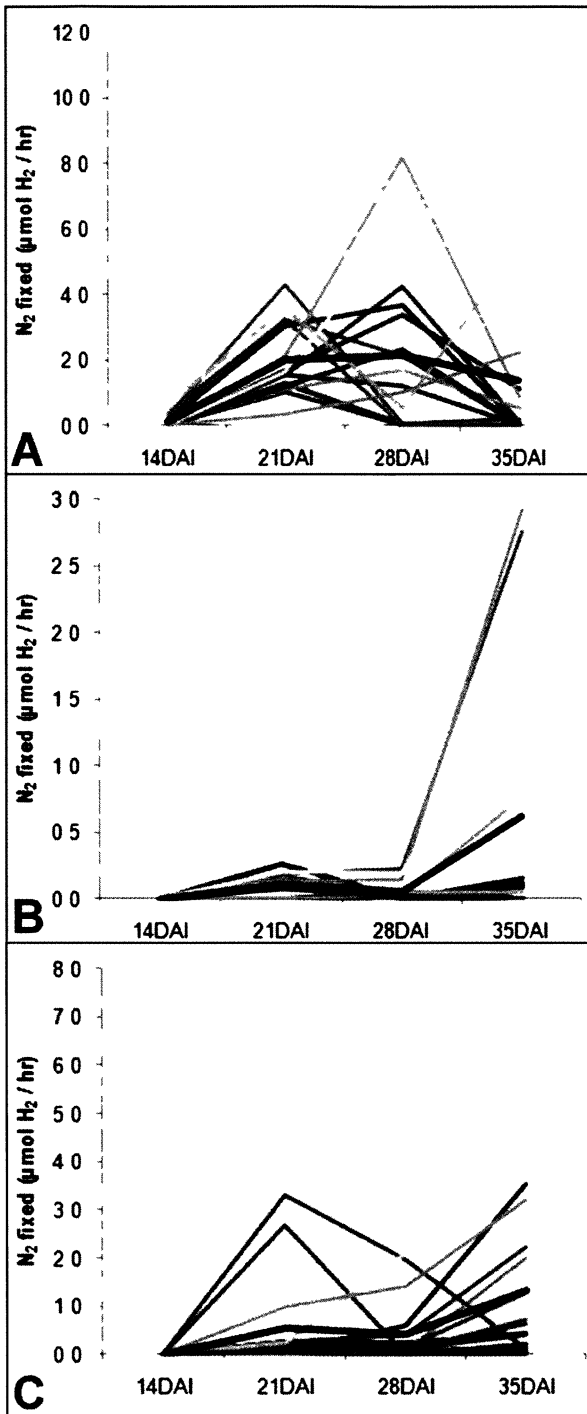


**Figure 3-6. Nitrogen fixation of three pea lines Sparkle (A), E151 (B), R50 (C).** Plants were inoculated with the HUP<sup>-</sup> strain. The Qubit apparatus was used for measurements of hydrogen evolution to extrapolate nitrogen fixation. Each coloured line represents the measurement of a single plant over time, i.e. from 14 to 35 DAI. The black line represents an average for all the plants measured of that pea line. Note the difference in scales of the y-axis.

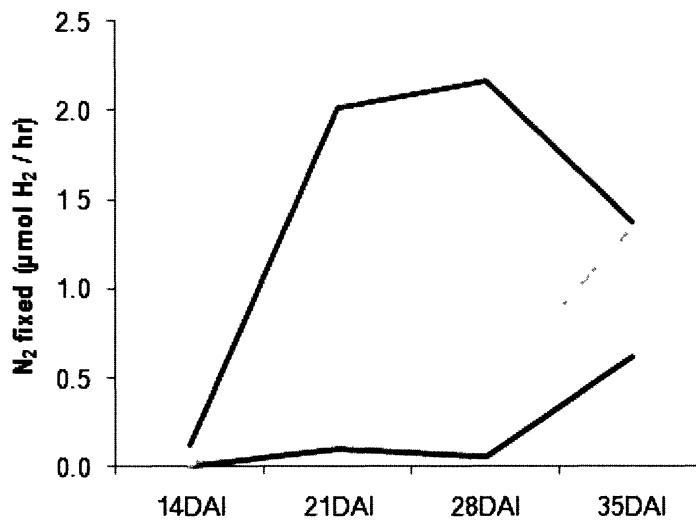


**Figure 3-7. Average nitrogen fixation for three pea lines.**  
 The black lines shown in the previous graphs are displayed here to compare the three pea lines (Sparkle: blue, E151: red, and R50: green). The experiment was performed in replication with plant totals reaching 16, 14, and 17 for Sparkle, E151, and R50, respectively.

**Table 3-2. Plant return on nodule construction cost for the three pea lines inoculated with HUP+ (as in Oono and Denison, 2010).**

	21 DAI	28 DAI	35 DAI	42 DAI
Sparkle	11.8	16.7	21.9	35.9
E151	197.0	38.8	35.4	43.8
R50	231.5	28.5	14.1	15.2

A lower nodule construction cost indicates the more efficient symbiosis. The data for 14 DAI are not shown because many E151 and R50 did not have any nodules at this time; therefore, they would not have any DW.

### 3.3.2 Bacterial strain effect on E151

E151 was confirmed to be a low nodulator with all strains (Fig. 3-3). With the bacterial strains, there was little difference between the number of nodules each bacterial strain produced on the root system, though lacZ produced the most nodules (Fig. 3-3B). There was an increase in nodule weight from 28 to 35 DAI, suggesting a continuation of growth and confirming the temporal delay (Fig. 3-4B) observed earlier (Chapter II). Each strain inoculated to E151 produced nodules which had a multi-lobed morphology (Fig. 3-5), indicating multiple meristems, an unusual characteristic for pea; however, the nodules of A34 and lacZ were smaller than those incurred by the other two strains. Nitrogen fixation was generally low until 28 DAI, at which time nitrogen fixation increased significantly, however, not as high as for Sparkle (Fig. 3-6). The increase mirrored the temporal delay mentioned above as little fixation occurred until 35 DAI (Figs. 3-6B and 3-7). At 35 DAI, nitrogen fixation was highest around 0.5  $\mu\text{mol H}_2/\text{hr}$ ; however, there were four plants that seemed to fix a greater amount at this time, averaging about 1.5  $\mu\text{mol H}_2/\text{hr}$  (Fig. 3-6B). E151 was more effective according to construction cost at 35 and 42 DAI than earlier when the values were 35.4 and 43.8 g DW per g of nodule DW, respectively (Table 3-2).

### 3.3.3 Bacterial strain effect on R50

R50 was confirmed to be a low nodulator (Fig. 3-3C). For R50, both HUP<sup>+</sup> and lacZ were equivalent in the number of nodules they promoted (Fig. 3-3C). R50 nodules were small and pale, independently of the bacterial strain, and the A34 and lacZ nodules appeared smaller than those of HUP<sup>+</sup> and HUP<sup>-</sup> (Fig. 3-5). As with E151, there was an increase in nodule weight for R50 from 28 to 35 DAI (Fig. 3-4C), indicating a temporal delay which was confirmed when nitrogen fixation was measured as little nitrogen fixation occurred until 35 DAI (Figs. 3-6C and 3-7). At 35 DAI, nitrogen fixation was greatest at about 1.0  $\mu\text{mol H}_2/\text{hr}$ , however, six plants did fix much more nitrogen at this time, averaging closer to 2.0  $\mu\text{mol H}_2/\text{hr}$  (Fig. 3-6C). R50 was more effective in nodule construction cost at 35 and 42 DAI when the values were 14.1 to 15.2 g DW per g of nodule DW, respectively (Table 3-2).

### 3.3.4 Comparison of the three pea lines

Of the three pea lines, Sparkle is the most efficient member for the pea-side of the relationship; this was to be expected since the two mutants have a gene important for nodulation mutated. E151 nodules weighed the most overall compared to the other two pea lines, independent of bacterial strain (Fig. 3-4B), likely because they were multi-lobed. R50 was an intermediate of the other two pea lines in terms of nodule number, but it bore small, light nodules (Figs. 3-5 and 3-4C). The most nodules on Sparkle were produced by HUP<sup>+</sup> (Fig. 3-3A), but for the two pea mutants, lacZ generated just as many nodules or exceeded the nodule number of HUP<sup>+</sup> (Figs. 3-3B and 3-3C). A34 was not the best, likely because it is a transgenic line. Although nodule size it was not measured, through observations, A34 and lacZ appeared to produce smaller nodules (Fig. 3-5), indicative of likely less ineffective strains (Oono and Denison, 2010). Overall, it may be said that nodule morphology is dependent on the host plant but nodule size is dependent on the rhizobial strain which challenges the plant. In general, the pea mutants responded to the rhizobial strains differentially from the wild-type.

I was able to perform temporal efficiency calculations only for HUP<sup>+</sup>, but this is sufficient because this strain is the wild-type and seems to be efficient. Sparkle had the highest specific nodulation at 14 and 21 DAI; this value was high for R50 at 35 and 42 DAI but was only about half of that of Sparkle (Table 3-3). E151 had a very low specific nodulation, about a quarter of the amount of Sparkle, which was at its highest at 28 and 35 DAI (Table 3-3). Sparkle had the largest specific nodule DW, and this value increased with time, while E151 had the lowest value which was about half of that of Sparkle (Table 3-4). As earlier, R50 exhibited median values which increased with time to reach a point at 42 DAI which was equal to that of Sparkle at 28 DAI, again suggesting a delay.

Comparisons of efficiency calculations were performed between those plants challenged with HUP<sup>+</sup> bacteria (Tables 3-2, 3-3, and 3-4) and those with HUP<sup>-</sup> bacteria (Table 3-5); however, only those obtained at 42 DAI values in the former could be considered as those with the HUP<sup>-</sup> bacteria were harvested at the end of the experiment (i.e. 42 DAI). The nodule construction costs of plants inoculated with HUP<sup>+</sup> (Table 3-2) were less than those challenged with HUP<sup>-</sup> (Table 3-5). Specific nodulation values were smaller when using HUP<sup>-</sup> (Table 3-5) than with HUP<sup>+</sup> (Table 3-3); however, the same trend was noted for the pea lines with Sparkle being the best, R50 the intermediate, and E151 the worst. Specific nodule DW values were

**Table 3-3. Specific nodulation of the three pea lines inoculated with HUP<sup>+</sup> (as in Fei and Vessey, 2009).**

	14 DAI	21 DAI	28 DAI	35 DAI	42 DAI
Sparkle	1933.9	2050.0	1830.6	1617.1	1527.4
E151	72.4	261.8	448.9	449.9	377.1
R50	74.3	733.2	779.2	1070.6	847.7

A higher specific nodulation indicates a more efficient symbiosis.

**Table 3-4. Specific nodule DW of the three pea lines inoculated with HUP<sup>+</sup> (Gulden and Vessey, 1998).**

	14 DAI	21 DAI	28 DAI	35 DAI	42 DAI
Sparkle	0.22	0.44	0.50	0.60	0.59
E151	0.003	0.08	0.22	0.27	0.30
R50	0.004	0.10	0.24	0.43	0.49

A higher specific nodule DW indicates a more efficient symbiosis.

**Table 3-5. Nodule construction cost, specific nodulation, and specific nodule DW of the three pea lines inoculated with HUP<sup>+</sup> at 42 DAI.**

	Nodule construction cost	Specific nodulation	Specific nodule DW
Sparkle	68.21	281.92	0.06
E151	352.34	71.22	0.05
R50	74.42	125.92	0.08



much less with HUP<sup>-</sup> (Table 3-5) than with HUP<sup>+</sup> (Table 3-4). Overall, it seems as though HUP<sup>-</sup> is much less efficient than HUP<sup>+</sup> but it also must be emphasized that Table 3-5 is representative of plants grown in sand. Sparkle fixed the most nitrogen while E151 fixed the least (Fig. 3-6).

The Qubit system allowed me to obtain another parameter of efficiency, the EAC. High EAC values indicate that a greater proportion of nitrogenase activity is used for nitrogen fixation than for hydrogen fixation. Sparkle had the highest amount of nitrogen fixation allocation at 21 DAI while for the two pea mutants, this occurred at 35 DAI; in particular, R50 had the median EAC values and E151 had the smallest EAC values (Table 3-6).

## 3.4 Discussion

### 3.4.1 Pea lines and bacterial strains

Here, the E151 and R50 nodulation phenotype of low and delayed nodulation has been confirmed. Overall, a temporal delay is seen for both E151 and R50 in nodule growth and in nitrogen fixation. Expectedly, the wild-type Sparkle is the most efficient member on the pea-side of the relationship based on efficiency calculations and EAC values. It is difficult, however, to identify which bacterial strain is the most efficient strain for each of the pea lines.

Let me focus on Sparkle first as it is the WT. Because of the large nodule numbers I obtained (Fig. 3-3), one would conclude based on the rationale of Oono and Denison (2010) that HUP<sup>+</sup> is the least efficient strain; however, if this were the case, one would think that these nodules would not weigh the most. Nodules occupied by more beneficial bacterial strains have been reported to be larger in size than those occupied by more detrimental strains (Simms *et al.*, 2006). As they produced the smallest nodules, A34 and lacZ should be considered less efficient strains. Furthermore, Terpolilli *et al.* (2008) suggested that a large nodule number and atypical nodule morphology are linked characteristics of ineffective nodulation. Large nodule numbers were seen in some cases here, i.e. HUP<sup>+</sup> had significantly more nodules with Sparkle, but atypical nodule morphology was not seen and morphology generally remained the same, independent of pea line. The two pea mutants did not perform as well, understandably because they have a mutation in one of their symbiosis genes, in particular E151 was the least efficient and R50 was the intermediate.

**Table 3-6. Electron allocation coefficient (EAC) values for the three pea lines when inoculated with HUP<sup>-</sup> and measured using the Qubit system.**

	14 DAI	21 DAI	28 DAI	35 DAI
Sparkle	0.542	0.584	0.532	0.486
E151	0.215	0.227	0.294	0.404
R50	0.233	0.338	0.436	0.568

Higher EAC values indicate that a greater proportion of nitrogenase activity is used for nitrogen fixation, therefore a greater efficiency.

Per plant construction cost of nodules is said to be greater for legumes when they do not associate with effective strains (Oono and Denison, 2010). Specific nodulation is another parameter, defined by Gulden and Vessey (1998), which represents the nodule production relative to root mass. Gulden and Vessey (1998) suggested that a decreased specific nodulation is indicative of a negative effect on nodule initiation and/or development rate. The authors stated that this parameter is more informative than whole plant nodulation in terms of understanding the effects of the symbiosis on the regulation of the nodulation process. They took this calculation one step further and determined specific nodule DW. Gulden and Vessey (1998) indicated that when the plants become solely dependent on nitrogen fixation as a nitrogen supply, they modify their growth rates of root and nodules to attain some optimal ratio of nodule DW to root DW. The authors used this ratio to calculate the specific nodule DW. Overall, these three calculations assess the optimization of the symbiosis. Measurements of each species separately only gives us an idea of one partner but the above calculations evaluate the relationship as a whole. All parameters reinforce that Sparkle is forming the best association with HUP<sup>+</sup>, E151 the least, and R50 the intermediate.

Another measure of nitrogenase activity is referred to as the potential nitrogenase activity; this is determined as the peak TNA obtained during an increase in partial pressure of O<sub>2</sub> (Hunt and Layzell, 1993). This calculation gives the O<sub>2</sub>-limitation coefficient of nitrogenase to estimate the O<sub>2</sub> limitation of nitrogenase within the nodule (Hunt and Layzell, 1993). Kiers *et al.* (2003) suggested that plants can control nodule size in part by altering oxygen supply. My data and previous information point to a role of the bacteria in nodule size. To distinguish the role(s) played by the two partners, we could use the technique used by Oono and Denison (2010) of determining nitrogen fixation rate in relation to carbon cost.

Shifting to think of the rhizobia in the association, Koch *et al.* (2010) suggested that certain features in the metabolic diversity of rhizobia are crucial for their adaptation and survival within a nodule and for their ability to infect multiple host legumes. Adaptation and survival are essential for the bacteria as crop legumes are known to enforce sanctions to the bacteria they host (Denison, 2000). In the field, researchers have known for a long time that a legume is challenged by many rhizobial strains. In fact, a nodule can be a mosaic of a number of bacteria (Wielbo *et al.*, 2010). Oono *et al.* (2011) stated that slight changes to rhizobial allocation of

resources between nitrogen fixation and bacterial reproduction can significantly increase rhizobial fitness with minimal risk of triggering sanctions.

Oono *et al.* (2011) suggested that plants are capable of shutting off resources to under-performing rhizobia, the outcome of which is seen in the differences in nodule size. For example, Gubry-Rangin *et al.* (2010) found that *M. truncatula* nodules containing fixing strains were larger and twice the weight than those formed by non-fixing strains. However, this size difference does not limit rhizobial reproduction (Oono *et al.*, 2011); in the experiment by Gubry-Rangin *et al.* (2010), a difference between non-fixing and fixing strains was not seen in plate counts of viable rhizobia per nodule. Oono *et al.* (2011) found that nodule weight and number of viable rhizobia per nodule were significantly greater for fixing than for non-fixing nodules. From these counts, it was also seen that pea and alfalfa can sanction their rhizobia more severely than soybeans (Oono *et al.*, 2011). Chen and Thornton (1940) stated that the volume of infected cells and the length of time before they disintegrate are both indicators of bacterial efficiency.

### 3.4.2 Nitrogenase activity and HUP<sup>-</sup>

Hydrogen is considered to be the regulator of the nitrogenase EAC (Golding and Dong, 2010), which is the ratio of electron flow through the nitrogenase enzyme that is put towards N<sub>2</sub> reduction compared to H<sub>2</sub> production (Eddie and Phillips, 1983). It has been said that for every molecule of N<sub>2</sub> reduced, at least one molecule of H<sub>2</sub> gas is produced; it is believed that at least 25% of the electron flow is directed to the latter, with the highest possible EAC being 0.75 (Hunt and Layzell, 1993). Legume symbiosis measured in the field generally results in an EAC in the range of 0.67 (e.g. Golding and Dong, 2010). In my study, the EAC was roughly 0.55, 0.3, and 0.45 for Sparkle, E151, and R50 respectively (Table 3-6). Therefore, Sparkle is quite efficient based on EAC; the nitrogenase is working more to reduce N<sub>2</sub> than to produce H<sub>2</sub>. In contrast, the two pea mutants, with their much lower EAC, likely use their nitrogenase to produce H<sub>2</sub>. It should be noted, however, that R50, close to senescence, becomes quite efficient; this reinforces the results obtained with the temporal study in R50 nodule functioning.

From my results of nodule number and nodule DW, it appears that HUP<sup>-</sup> is not as effective as HUP<sup>+</sup>; therefore, the nitrogen fixation data achieved from using HUP<sup>-</sup> can be viewed as an under-estimation for the rates that we would get with HUP<sup>+</sup>. It also must be noted that this

measure is an approximation because in the field the plant would be surrounded by a rich rhizosphere. With HUP<sup>-</sup> strains being less energetically efficient than HUP<sup>+</sup> strains (Schubert and Evans, 1976), one may wonder why both types of bacteria are present in the field, from an evolutionary point of view. It has been suggested that the benefits of plant growth with the HUP<sup>-</sup> association outweighs the energy efficiency of the HUP<sup>+</sup> symbioses, because other growth-promoting rhizobacteria are present around the nodule, and that these benefits may be advantageous for crop rotation and for decreasing the use of chemical fertilizers (Golding and Dong, 2010). Denison (2000) suggested that plant traits preferentially allocating resources to nodules housing cooperative strains could promote rhizobial cooperation, thereby monitoring bacterial strains within and outside of the nodule.

With the Qubit system and the bacterial strain HUP<sup>-</sup>, I was able to further separate the three pea lines in term of nodule function. However, one of the downfalls of that flow-through system is the need for bacterial strains without the uptake hydrogenase enzyme. I must recognize that I learned recently that A34 is actually a HUP<sup>-</sup> bacterial strain (Oono and Denison, 2010), and we could have actually measured its nitrogenase activity in association with the three pea lines using the Qubit system. This in turn indicates that the lacZ strain is also a HUP<sup>-</sup> strain. Future studies should include the measurements of these two strains on Sparkle using this system to compare fully the efficiency of nodulation between the three bacterial strains. Other downfalls are the sensitivity of the H<sub>2</sub> gas analyzer to water vapour, resulting in changes in pH<sub>2</sub> accompanying alterations in pO<sub>2</sub> (Hunt and Layzell, 1993), and the calibrations which are not simple as highlighted by Golding and Dong (2010). As well, although it could be considered as an advantage, is that one cannot obtain the number and DW of nodules at each age so one cannot extend the analysis to the calculations mentioned earlier. Finally, it is difficult to compare with other studies as this technique is not yet widely used.

### **3.4.3 Assessment of efficiency**

Understanding the rhizobial side of the mutualism is important for me. I realized early that we may be missing in the lab a large portion of the nodulation story by restricting the symbiosis to the plant partner. Overall, each experiment and calculation in this chapter has provided an insight into nodulation efficiency; however, to evaluate completely efficiency

multiple approaches should be taken. It seems more appropriate to measure efficiency based on components of both the members of the association rather than only considering the effect of either species on the overall symbiosis. As Bhatia *et al.* (2001) stated, agricultural methods could be improved if we ensure the most efficient rhizobial strains are those which are nodulating the plants.

## Chapter IV: E151 Early-formed Nodules

### 4.1 Introduction

Previous studies in the lab have been conducted to investigate E151 nodule organogenesis. Chlup (2007) performed optical sectioning on cleared whole root segments. He used lacZ bacteria so that the IT staining blue could easily be seen. He found that E151 nodule development was blocked at the stage where the IT is in the cortex but associated with inner cortical cell divisions (Chlup, 2007). However, it was unclear whether the IT was in the inner or outer cortex. Delanghe (2007) performed an experiment with the same rationale to that of Chlup, to confirm the location of the block in E151 nodule organogenesis. However, he used a different approach; he observed hand-sections of nodules, hosting HUP<sup>+</sup> bacteria, on segments of root which had been previously determined likely to bear nodules (Guinel and LaRue, 1991). The stage at which nodulation was blocked in E151 became then even more blurry because Delanghe (2007) found the block to occur at the nodule primordium stage. The difficulty of assessing the block may have been caused by the thickness of the pea root but also by the low number of events seen, and by the poor probability of finding with accuracy nodulation events in an entire pea root system which was allowed to grow into soil.

From the nodule distribution study (Chapter II), it was seen that a normal nodule distribution, which can be observed in Sparkle, involves nodules mainly emerging on lateral roots near the crown and close to the primary root. The oldest nodules, referred here as the early-formed nodules, are those which are on the lateral roots the closest to the crown as those are the roots which first emerged. On E151, however, nodules are more scattered in their location and have a distribution different from that of Sparkle. As well, it was noted in Chapter II that E151 nodulation is delayed, with nodules emerging later than those of Sparkle and with the space that the nodules cover shifted further down. The nodule distribution characteristic of the wild-type may be partly explained by a mechanism known as autoregulation of nodulation (AON) used to control the emergence of nodules as the cost of producing these structures is heavy on the plant (Caetano-Anollés and Gresshoff, 1991a); through AON, emerged nodules inhibit the formation of further nodules. In fact, I see AON as a regulation of multiple waves of

nodule formation, with the first wave inhibiting further nodules until more nitrogen is required by the plant, at which time a second wave will emerge.

E151 nodule organogenesis had to be re-visited to locate precisely the block as well as observe for any abnormalities in the E151 infection events. To have consistency and precision, growth pouches and spot-inoculation (Clemow, 2010) were considered essential for the study. The pouches allowed for the ease of visualizing the plant's root system, and therefore the nodules. Many researchers have used these pouches in nodulation experiments: for example, to focus more on the bacterial-side of the association and determine the amount of bacteria in the nodules (Weaver and Frederick, 1972); to test the susceptibility of different root cells on an array of legume species (Bhuvanewari *et al.*, 1981); or to observe the effects of hormones and their inhibitors on nodule formation (Peters and Crist-Estes, 1989). Whereas the earlier researchers flooded the pouches with inocula (a technique referred to as flood-inoculation), scientists after 1980 used a much more accurate technique to locate with ease the nodules (spot-inoculation), allowing more samples to be analyzed. Spot-inoculation is based on Bhuvanewari's finding that there is a most-susceptible zone of infection, and this is the location where the inoculum is placed. This technique was developed by Turgeon and Bauer (1983) for soybean roots where a droplet of *Rhizobium japonicum* was administered precisely to the root; the technique was apparently successful as there was an approximate 80% success rate of nodule formation. The authors indicate that this percentage is not higher because not all emerged root hairs may be susceptible to infection and not all bacterial cells may be capable of initiating infection. The refined technique for pea developed by Clemow (2010) was based on the work by Turgeon and Bauer (1983). Previous to Clemow's work, little success had been seen in spot-inoculating pea as it is a plant not amenable to many techniques.

Using flood- and spot-inoculation with pouches, I decided to study the fate of the nodulation events which were located in the usual place (Guinel and LaRue, 1991) to determine whether the E151 nodules formed further up on the root system are aborted or dormant and later re-triggered to continue through organogenesis. Indeed, Caetano-Anollés and Gresshoff (1991b) state that a plant mechanism of controlling nodulation is the arrest of previously-formed infections. To show this, the authors surgically excised emerged soybean nodules which led to the development of nodules from already initiated infections, in the same location as the initial



nodules (Caetano-Anollés and Gresshoff, 1991b). Thus, they concluded that nodules of soybean were arrested rather than aborted (Caetano-Anollés and Gresshoff, 1991b).

#### **4.1.1 Objectives**

Chlup (2007) who had previously worked with E151 suggested that nodule organogenesis was delayed in E151 but not arrested (Chlup, 2007). He had observed the plants until 21 DAI and hypothesized that later in time nodules would emerge, due to nodule organogenesis being reinitiated (Chlup, 2007). From Sparkle, we know that early-formed nodules appear close to the crown of the root system. However, in Chapter II, these nodules were not seen in E151; they were observed later on but shifted down. The question of whether the early-formed nodules are aborted or arrested now arises. In the former case, nodules would never emerge because its meristem never forms or is not functional; in the later case the nodule meristem would be re-triggered to grow. One of my objectives was to answer the question, and the second to pinpoint where the block was in E151 nodule organogenesis. Because I used spot-inoculation, I was able to increase the number of samples I observed and to improve the accuracy of the location of a nodule.

## **4.2 Materials and methods**

### **4.2.1 Flood-inoculation and macro-observations**

#### **4.2.1.1 Plant growth conditions**

Seeds of the pea lines Sparkle and E151 were surface-sterilized and imbibed as per Chapter II. Small square pots (8.5 cm in height and 9.5 cm in diameter) were prepared with a 50:50 mixture of autoclaved vermiculite and turface (both soil components were purchased from Plant Products Company Ltd., Brampton, ON, Canada) and wetted the night before planting. Five seeds were planted per pot, approximately 1 cm below the surface. The pots were placed in the growth room as per Chapter II. Three DAP, the seedlings were transferred to pouches (Fig. 4-1A, Mega International, West St. Paul, MN, USA) in a sterile flow hood as per Clemow

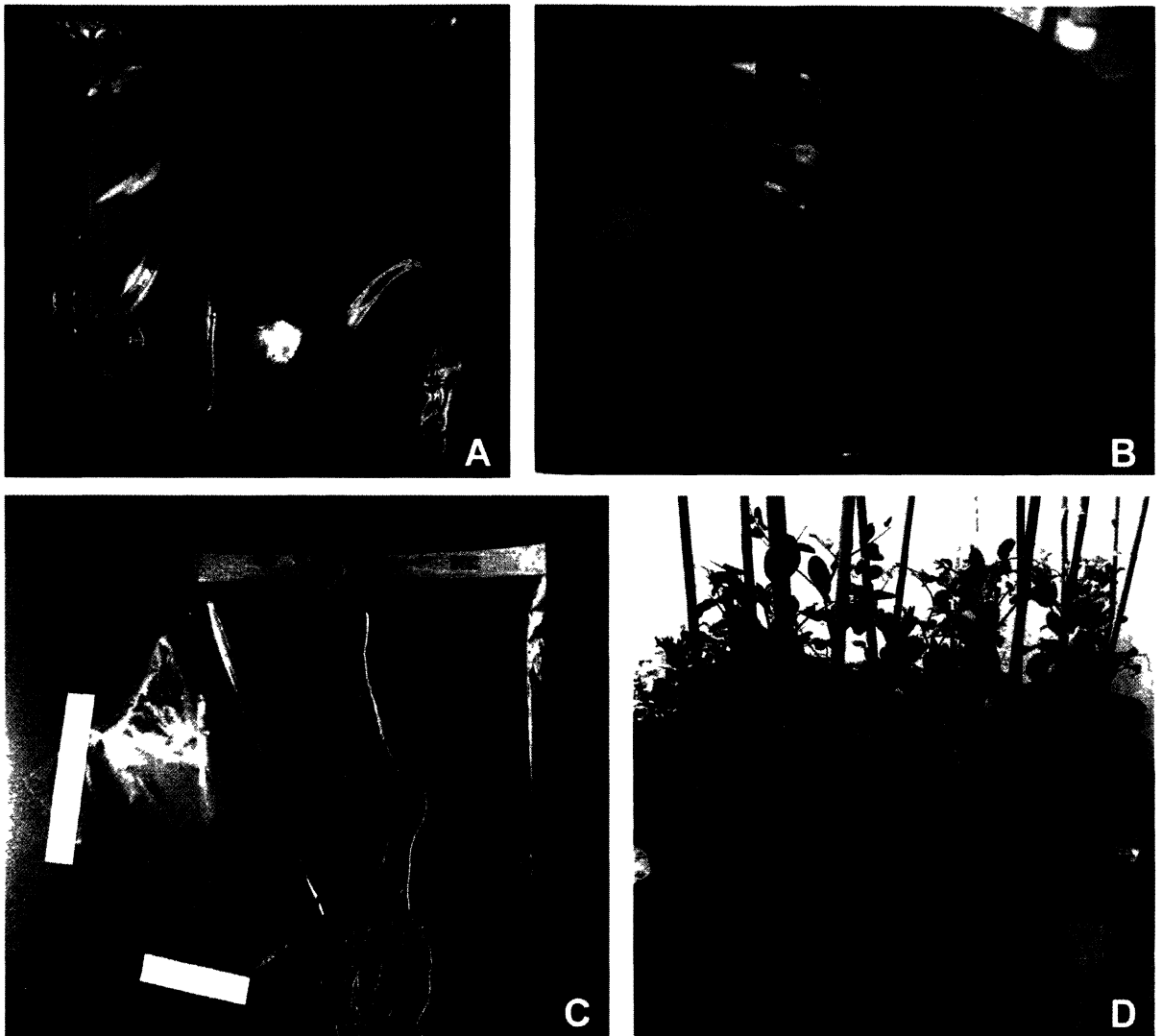


**Figure 4.1. The growth of plants in pouches.**

(A) The plants were grown in a clear plastic pouch so the whole root system could be seen. (B) Seedlings were transferred into the pouches 3 DAP. The brown paper was dampened with low nutrient solution, the bottom of the pouch was cut and its top taped closed to allow for moisture control. (C) A flap was cut open so a clear photograph could easily be taken of the nodulated root system. (D) The pouches were covered with a 50:50 vermiculite:soil mixture so that the roots were kept away from light. Plants were re-potted once pictures had been taken at each time point.

(2010). A small slit was made using a sharp blade in the trough of the filter paper located within the pouch. The paper wick in the pouch was dampened using sterile low-nitrogen nutrient solution (Appendix A). The seedling was placed in the pouch with the radicle going through the slit, and the cotyledons resting in the trough. The top of the pouch was taped closed except for a 1 cm segment where the shoot would emerge (Fig. 4-1B). The bottom of the pouch was cut to allow moisture to enter and leave the pouch, and its sides trimmed so that the pouch would fit in a large round pot (Fig. 4-1B; 15 cm in height and 11-15 cm in diameter). Four pouches were placed per pot, and the pots filled with a 50:50 mixture of autoclaved vermiculite and turface and placed in a metal tray. The pouches were flood-inoculated 5 DAP, i.e., 2 days after the transfer to the pouch, with 2 mL of a 5% rhizobial solution of 128C53K (gift of Dr. Stewart Smith) using a sterile serological pipette to release the rhizobial solution on the brown paper in the pouch, surrounding the root. Low nutrient solution (Appendix A) was added to the metal tray 10 DAI followed by a regime of water, low nutrient solution, water, etc. until harvest.

#### ***4.2.1.2 Macro-observations***

Two trials were performed where 24 plants of each line were observed, to gain a total of 48 plants. All the pouches were removed from the pots twice a week (7, 11, 14, 18, 21, 25, 28, 32, 35, and 42 DAI) and the root system observed for nodule development. On the first time of removal from the pot, the right-hand side of the pouch was cut open and a cut was made across the top of the pouch about 3cm down to create a flap (Fig. 4-1C). Pictures were taken using a digital camera (Olympus C-7070) on a stand (Kaiser Fototechnik repro kid 5360) which was set to 30, 25, 20, 15, and 10 cm away from the pouch. The camera was set to have the flash turned off. Once the flap was sealed using laboratory tape, the pouch was re-potted and left (Fig. 4-1D) until the next observation time-point. Images were up-loaded to the computer and the photographs of each root system were viewed so that each plant could be tracked over time. The nodules and roots were analyzed for time of senescence. Specifically, the zone where the early nodules formed was examined.

#### ***4.2.1.3 Nodule excision***

A similar experiment was performed where Sparkle and E151 plants (n=24) were grown in pouches and flood-inoculated following the same protocol as above but nodules were excised with a sharp razor blade at the root junction at 21 DAI. The plants within the pouches were re-

potted and their roots observed two weeks later at 35 DAI. Before re-potting, the location of the excised nodules was marked on the outer side of the pouch. Photographs were taken as above, before excision and on the day of observation.

#### **4.2.2 Spot-inoculation and micro-observations**

##### ***4.2.2.1 Plant growth conditions***

Seeds of the pea lines Sparkle and E151 were planted and transferred to pouches as above. The roots were spot-inoculated 8 DAP, i.e., 5 days after the transfer to the pouch to allow for the growth of some lateral roots, with 0.5  $\mu\text{L}$  (Eppendorf™ pipette with a range of 0.1-2.5  $\mu\text{L}$ ) of a 5% rhizobial solution of 128C53K. Although lacZ bacteria could have been used to indicate the stage of infection, they were not because the root had to be well cleared so inner cortical cells could easily be seen. Through preliminary experiments, I learned that the thorough clearing ended up removing the blue colouring. The drop of inoculum was placed directly onto a lateral root, approximately 0.5 to 1 cm from its tip, where root hairs were developing. Because plants were inoculated at 8 DAP, only a few lateral roots had emerged, close to the crown. Therefore, the nodulation events which were being observed were those in the upper part of the root system, i.e. those associated with the early-formed nodules. Five lateral roots were spot-inoculated on each plant and the location of the inoculation was marked on the outer side of the pouch. The pouch was left to lie flat for 10 minutes to ensure the bacteria remained localized in the area and did not spread extensively in the pouch. After that time, the pouches were replaced in the pots. The same watering regime as above was followed.

##### ***4.2.2.2 Micro-observations***

Three trials were performed where at 3, 7, 10, 14, 21, 28, and 35 DAI three plants of each line were randomly removed from different pots. On these plants, three of the five spot-inoculated lateral roots were cut 0.5 cm on either side of the mark of where the bacteria were placed. The lateral root segments were placed in small glass vials with caps (6.7 cm height and 12 mL capacity) and underwent a fixing and clearing regime adapted from Chlup (2007). The segments were fixed under vacuum for 1 h in a 1.25% (v/v) glutaraldehyde solution. The solution was composed of 1 mL 25% glutaraldehyde (Marivac, Canton de Gore, QC, Canada)

and 19 mL of 0.1 M phosphate buffer (5.3 g  $\text{KH}_2\text{PO}_4$ , 13.9 g  $\text{K}_2\text{HPO}_4$ , 1L deionised  $\text{H}_2\text{O}$ , pH 7.0). The segments were then rinsed two times in 0.1 M phosphate buffer (15 mins per rinse) and two times in deionised water (5 min per rinse). They were cleared under vacuum in 30% bleach (store-bought, 5.5% sodium hypochlorite) solution for 6 min and rinsed two times in deionised water for 5 min. The segments were then vacuum-infiltrated for 1h in a 30% glycerol solution and then for 1h in a 60% glycerol solution. The segments were left in the latter solution to preserve the roots for later use.

The root segments were observed with a Carl Zeiss Axiostar light microscope equipped with phase-contrast optics (objective 40X; Ph; NA = 0.65) for the presence of any one of eight nodulation events (adapted from Guinel and Sloetjes, 2000): (A) root hair curl with no infection thread, (B) root hair curl with an infection thread either in the epidermal cell or having progressed into the outer cortex; in either case, there were no divisions seen in the inner cortex, (C) infection thread present in the outer cortex with divisions in the inner cortical cells, (D) infection thread in the inner cortex with no inner cortical cell divisions associated, (E) infection thread present in the inner cortex with divisions in the inner cortical cells, (F) nodule primordium, (G) nodule meristem, (H) mature emerged nodule. Any sight of these nodulation events was scored on a tally sheet. The number of nodulation events per segment and accuracy of the spot-inoculation technique were determined.

The root segments were further observed with a Nikon Eclipse 50i compound microscope (objective 10X; NA = 0.25, objective 20X; NA = 0.40, and objective 40X; NA = 0.65) to see more clearly the infection thread and the inner cortex, and pictures were taken with a Pax-Cam Arc digital camera and Pax-it 7.0 imaging software ([www.paximaging.net](http://www.paximaging.net)).

Student's t-tests were performed to compare Sparkle and E151 using Sigma Plot 11.0 (Systat Software, Inc., San Jose, CA, USA) for the percentage of spot-inoculation accuracy and number of infections per 1 cm root segment data.

## 4.3 Results

### 4.3.1 Nodule organogenesis of Sparkle

The pouches proved to be useful as the same plant could be observed over time allowing me to track nodule development (Fig. 4-2). The plants did not appear to be stressed by their replanting throughout the experiment as the shoots were healthy and the root systems continued to grow (Fig. 4-2), leading to the primary root emerging out of the bottom of the pouch (Fig. 4-3). However, the plants appeared to senesce earlier than those grown in pots, by about a week.

Flood-inoculation allowed for the overall visualization of nodule emergence in pouches; it was confirmed that the same nodule distribution was noted as that in nodulation maps in Chapter II. At 21 DAI, numerous nodules had formed on the root system; these were pink (Fig. 4-3A), and therefore were assumed to fix actively nitrogen. The nodules grew in size but apparently not in number from 21 to 28 DAI (Figs. 4-3A and 4-3B). At 35 DAI, the nodules did not appear larger than those at 28 DAI but they were beginning to become green (Fig. 4-3C), indicating that senescence was occurring. By 42 DAI, all had turned green (Fig. 4-3D).

The spot-inoculation technique was essential as it gave a finite nodule location. Its success was rated as at least one nodulation event being present on the 1 cm root segment; there was an 81% spot-inoculation accuracy for Sparkle. It was observed that about 70% of the time there was more than one infection event on the root segment; there was an average of  $4.0 \pm 0.2$  infection events per cm of root segment. Graphs based on time and on stages of infection were both generated; however, only the latter are shown as they are visually more informative (Fig. 4-4). Sparkle had no stage A infections past 21 DAI, indicating that the roots were no longer susceptible to bacterial infection. It is interesting to compare stage B (Fig. 4-4B) where IT was either in the epidermis or outer cortex but without inner cortical cell division to stage D (Fig. 4-4D) which portrayed an IT having progressed to the inner cortex, still with no divisions. Apparently, if the cortical program had not been turned on, the epidermal program was arrested. On the same line of thought, it is worth to compare stages C and E (Figs. 4-4C and 4-4E). The former represents the IT in the outer cortex associated with inner cortical cell divisions, while the latter corresponds to the IT in the inner cortex which displays divisions. The comparison suggests that once the IT had progressed to the inner cortex, the cortical program had passed a key-step and was moving forward. Once the program was on, it moved to the primordium

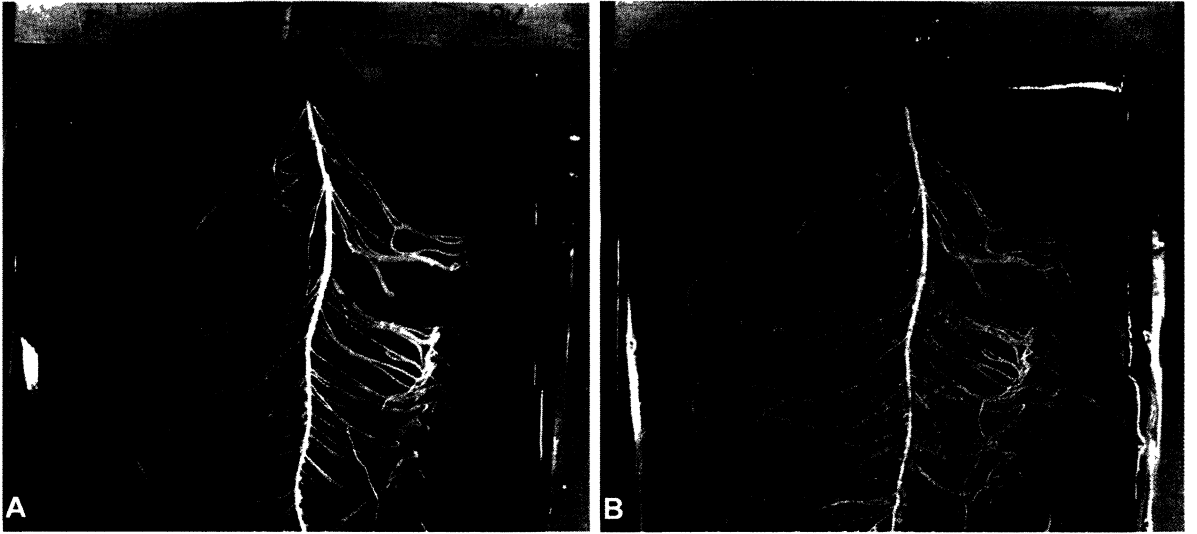


**Figure 4-2. Sparkle grown in a pouch at 11 DAI (A) and 21 DAI (B).**

The box acts as a reference point, demonstrating that the same plant can be observed over time. The plant is considered healthy as the roots continue to grow (box) and the nodules grow larger. Arrows indicate two nodules, the size of which can be seen to have grown over time.

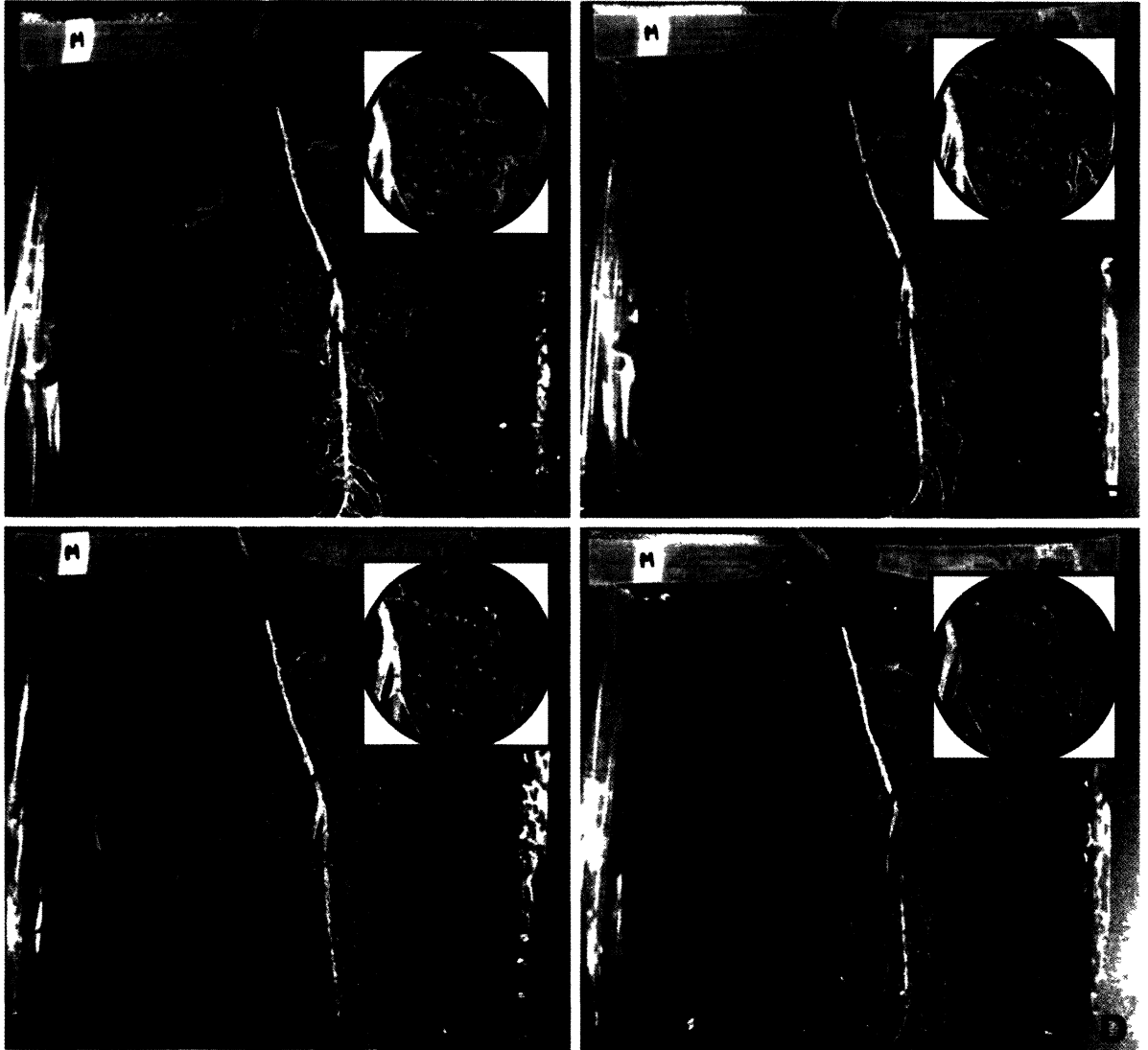


**Figure 4-3. Observations of the root system and nodules of Sparkle.**

The plants were grown in pouches and flood-inoculated. Plants were tracked over time at 21 DAI (A), 28 DAI (B), 35 DAI (C), and 42 DAI (D). Insets display a zoomed-in view of the nodules in that region of the root.



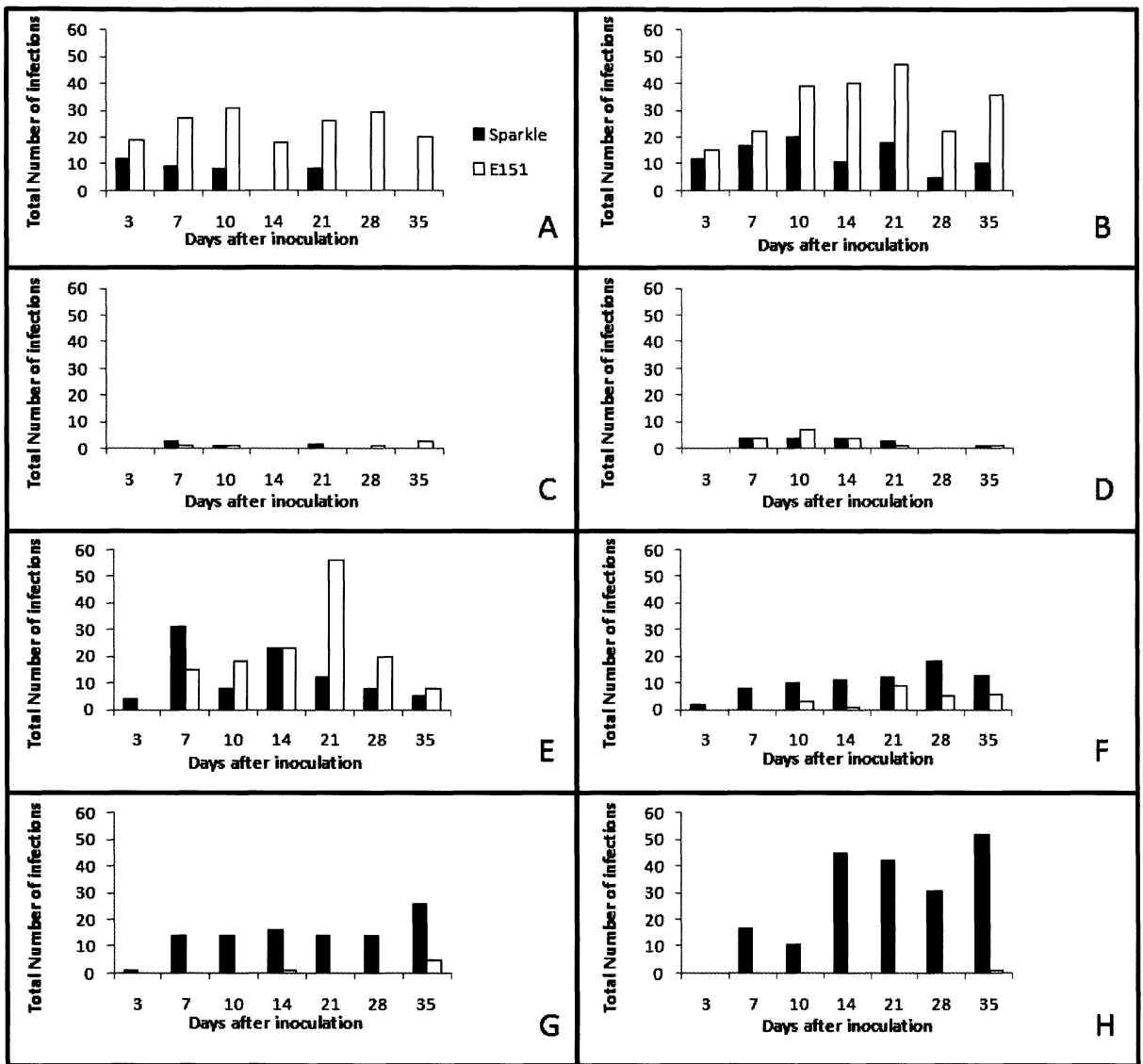


**Figure 4-4. Total number of infection events for each stage of Sparkle and E151 root segments.** Stage A is represented by a root hair curl (A). Stage B is represented by a root hair curl with an infection thread entering the epidermis and potentially progressing to the outer cortex but with no divisions deep in the cortex (B). Stage C is represented by the infection thread being present in the outer cortex with divisions in the inner cortical cells (C). Stage D is represented by the infection thread being present in the inner cortex with no associated divisions (D). Stage E is represented by the infection thread being present in the inner cortex with divisions in the inner cortical cells (E). Stage F is represented by a nodule primordium (F). Stage G is represented by a nodule meristem (G). Stage H is represented by an emerged nodule (H). The sum of infections was determined for each time. The total number of plants differed between pea lines and time; they are listed as follows for each time beginning with 3 days after inoculation for Sparkle/E151: 27/27, 26/24, 27/27, 27/25, 27/22, and 28/24.

formation (F; Fig. 4-4F), to the formation of a nodule meristem (G; Fig. 4-4G), and then to an emerged nodule (H; Fig. 4-4H). Since Sparkle had many events in E at the earlier times (Fig. 4-4E), these events of the cortical program had progressed through the timeline and therefore Sparkle displayed many events at the later times. Sparkle had most of its stage H event, an emerged nodule, by 35 DAI (Fig. 4-4H); therefore by this time, the nodules did not grow in number. From Table 4-1, it was seen that the highest percentage (33%) of infections were in stage H for all time points combined. It is of interest to note that it takes between three and seven DAI for a Sparkle nodule to emerge (Fig. 4-4G); this is not a long time.

The IT in Sparkle had a uniform diameter (Figs. 4-5A and 4-5B) throughout the cortex as was noted in Guinel and LaRue (1991). At times, more than one root hair would curl and more than one IT would be present (Fig. 4-5A). The IT had few branches as it progressed to the inner cortex (Fig. 4-5B). A clear link between the epidermal and cortical programs was often seen with the IT present in the nodule primordium (Fig. 4-5C). Once the meristem had reached the epidermal cells, the nodule cell mass would burst through the root and an emerged nodule would be seen (Fig. 4-5D). By 14 DAI for Sparkle, most of the nodules had emerged (as in Fig. 4-4G).

#### **4.3.2 Nodule organogenesis of E151**

There was a 78% accuracy with the spot-inoculation of E151, and this was not significantly different from that of Sparkle. It was also observed that about 70% of the time there was more than one infection event on the 1cm root segment. On average there were  $4.6 \pm 0.3$  infection events per cm of root segment; this was similar to what was seen in Sparkle.

In the pouches, E151 generally maintained its multi-lobed nodule morphology seen previously in other substrates. At 21 DAI, a few pink nodules had formed on the root system (Fig. 4-6A). The nodules continued to grow in size over time (Fig. 4-6), from 21 to 35 DAI. There were also more nodules at 35 DAI than at 21 DAI, indicative of a temporal delay. It was noticed that the nodules continued to enlarge for a longer period of time than those of Sparkle (Figs. 4-6A to 4-6C). The nodules were green by 42 DAI (Fig. 4-6D), which was a week later than in Sparkle. However, there were many less E151 nodules than in Sparkle, once again confirming the low nodulation phenotype of the mutant (compare Figs. 4-3 and 4-6).

**Table 4-1. Percentage of infection events at each stage for Sparkle and E151.**

	A	B	C	D	E	F	G	H
Sparkle	5.99	15.05	0.97	2.59	14.72	11.97	16.02	32.69
E151	29.09	38.33	0.91	2.58	24.24	3.64	1.06	0.15

The values represent an average of the total number of infections for that pea line with all time points combined.

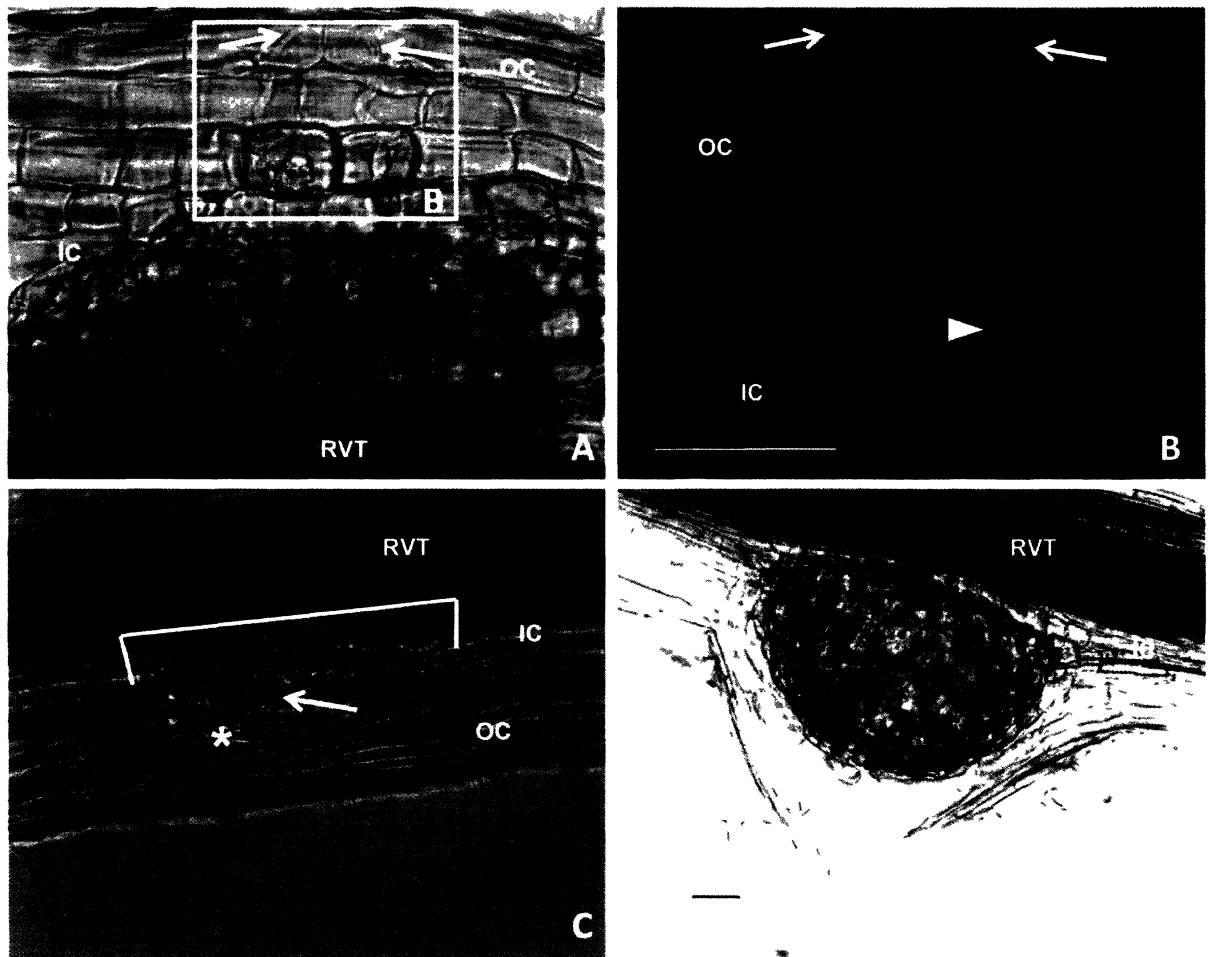


**Figure 4-5. Sparkle nodule organogenesis.**

In A a nodule meristem is displayed. It was triggered by two nodulation events since there were two infection threads (arrows) initiated in two different root hairs. The ITs are crossing the outer cortex (OC) and are associated with numerous divided cells in the inner cortex (IC). Note that the ITs progress perpendicularly to the surface and branch a few times. B is an inset of A where the ITs are seen to pass through OC without branching. Note how the IT apparently thickens when it encounters a periclinal cell wall (arrowhead). However, on either side of the wall, the IT is uniform in diameter. In C, a nodule meristem is seen forcing the OC. A layer of cortical cells (asterisk) is seen being pushed towards the surface. An IT likely resulting for the same nodulation event as the meristem is observed slightly off-center (arrow). It should be noted that the base of the nodule delineated by the white line is close to 450  $\mu\text{m}$ . In D. A nodule is seen just emerging. Numerous cortical cell layers have been breached. RVT = root vascular tissue. Bars represent 50 $\mu\text{m}$ . Samples were observed under a Nikon Eclipse 50i compound microscope (objective 10X; NA = 0.25 [C,D], objective 20X; NA = 0.40 [A], and objective 40X; NA = 0.65 [B]). The microscope was equipped with a PaxCam Arc digital camera. B is a composite image where many photographs were taken at different depths of field, and then stacked using a Pax-it imaging software ([www.paximaging.net](http://www.paximaging.net)) to give a sense of three-dimensionality.

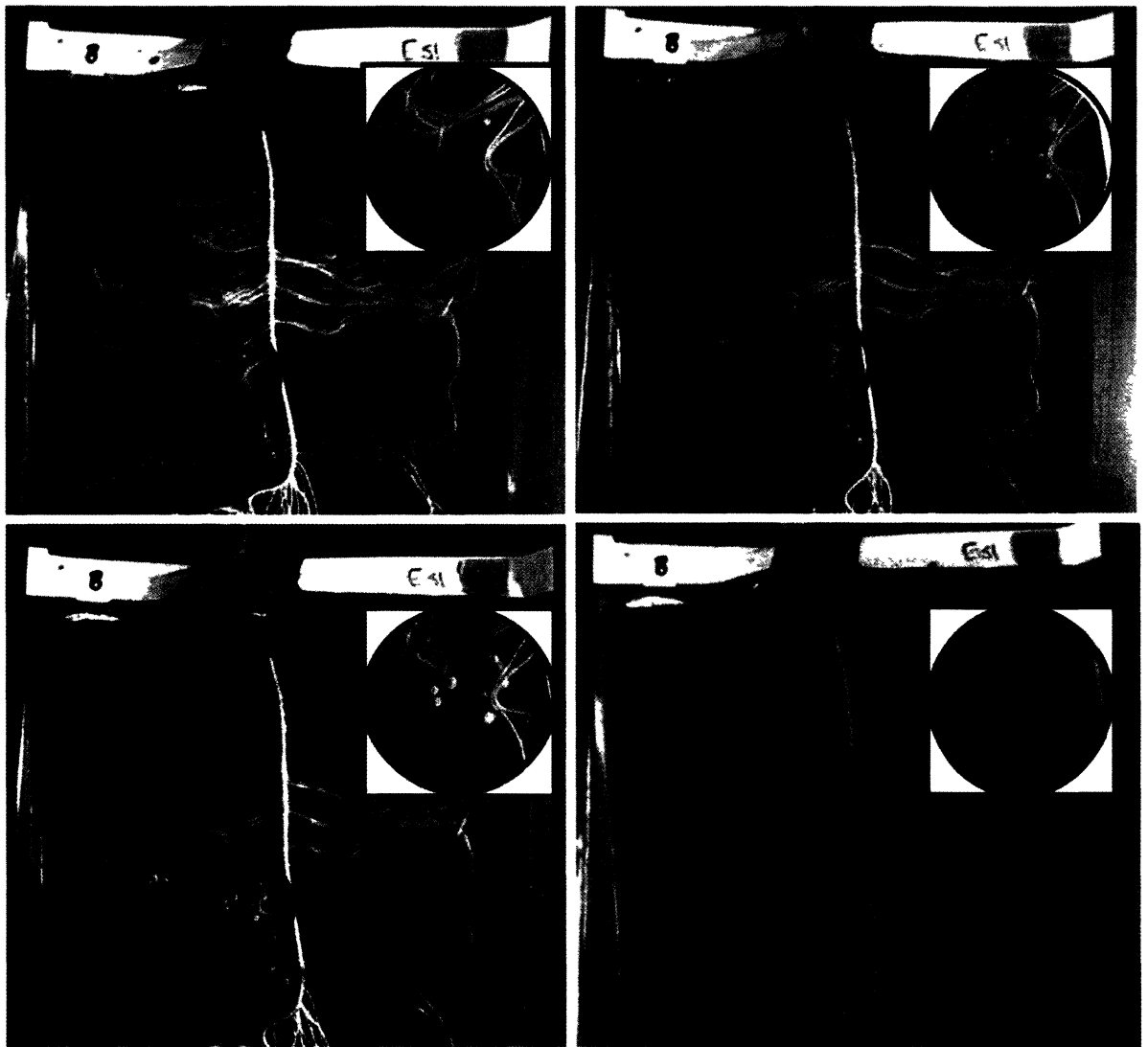


**Figure 4-6. Observations of the root system and nodules of E151.**

The plants were grown in pouches and flood-inoculated. Plants were tracked over time at 21 DAI (A), 28 DAI (B), 35 DAI (C), and 42 DAI (D). Insets display a zoomed-in view of the nodules in that region of the root.

Interestingly, nodules did not appear at the top of E151 root systems at any time; however, nodules did appear in the lower half.

Apparently the epidermal program which controls the IT in E151 was functional but there did not seem to be a simultaneous cortical program (Fig. 4-4). Compared to Sparkle, there were a higher number of events in stages A, B, and E for E151 and that at each harvest, as seen in the graphs based on DAI (Fig. 4-4). There were 29%, 38%, and 24% of the total infections, respectively, at these stages (Table 4-1). A large accumulation of events in stage A suggests that root hairs remained curled and do not later on straighten (Fig. 4-4A). Thus, it appeared as though a block in nodule organogenesis was present both in stage B and stage E. An accumulation of nodulation events at these two stages was noted at 21 DAI (Figs. 4-4B and 4-4E). When considering the first block, it was obvious that almost all E151 ITs in stage B (Fig. 4-4B) did not progress to the outer cortex. Indeed, once the IT had reached the wall forming the interface epidermis/cortex, either it stopped abruptly, or it grew parallel to this inner periclinal wall and entered a second (or third) epidermal cell. In hindsight, the stage that I labelled B should have been further dissected in two. I would now have a stage B1 where the IT remains in the epidermis and a stage B2 where it progresses through. However, from a cortical program point of view, there would still be no divisions in either B1 or B2. In Sparkle, there were few ITs arrested in B1; most ITs progressed to B2. As for E151, most ITs were arrested in B1. This may explain why the cortical program is not progressing. The second block in E151 involved directly the cortical program at stage E (Fig. 4-4E), which was represented by an IT in the inner cortex associated with cortical divisions. Contrary to what was seen in Sparkle, divisions did not progress to form a nodule primordium, indicating that in E151, the cortical program did not pass the key stage mentioned earlier and therefore only few events were seen in stages F (Fig. 4-4F) and G (Fig. 4-4G), with only one instance of an emerged nodule (H; Fig. 4-4H). Indeed, rarely do early-formed nodules emerge. This second block reinforces the coordination seen between the epidermal and the cortical programs.

In addition to the two blocks, the branched IT was the most peculiar thing of E151. The E151 IT branched abnormally and quite excessively compared to that of Sparkle, so that it covered a large area, and likely volume, of the inner cortical cells (Fig. 4-7A and 4-7B). The base of the E151 nodule (Fig. 4-7A) was much larger than that of Sparkle (Fig. 4-5C). As the IT branched in the inner cortex, it progressed in many directions, making bulges and knobs when it

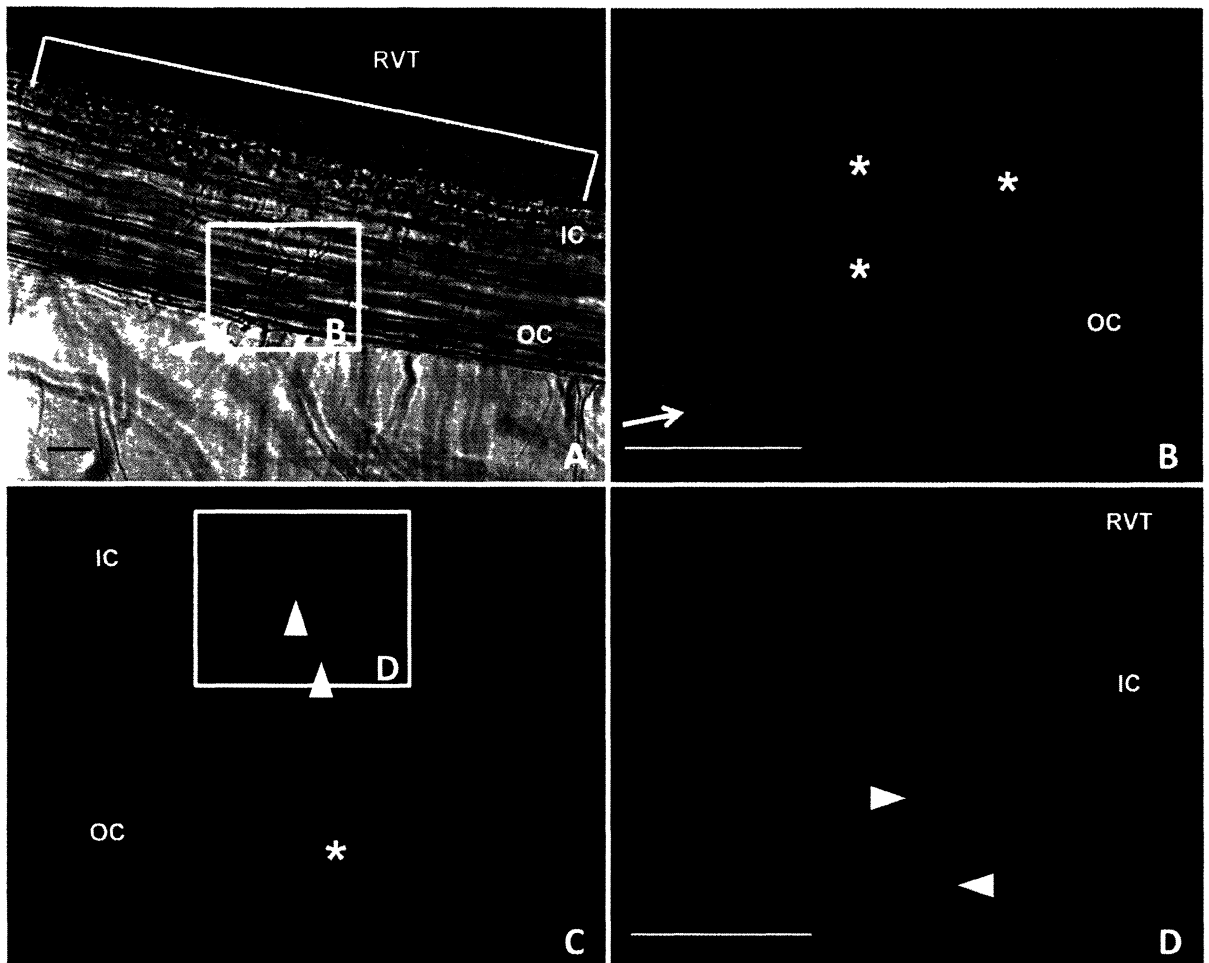


**Figure 4-7. E151 in stage E of nodule organogenesis, where the infection thread has penetrated the inner cortex and there are inner cortical cell divisions.**

In A an infection event is displayed. A root hair has curled (arrow), an IT has formed and progressed from the outer cortex (OC) to the inner cortex (IC). In IC, the IT branched and formed a wide infection area, delineated by the white line, covering 600  $\mu\text{m}$ . B is an inset of A to view the IT in more detail. The IT can be seen coming from the curled root hair (arrow) and progressing through OC. Note the branching (asterisk) which occurs as the IT passes through each cell layer. In C, a branched IT is progressing from OC to IC, but this time more knobs (arrowheads) and branching (asterisk) can be seen. D is an inset of C where the abnormalities of the IT can be viewed in more detail. Knobs (arrowheads) are seen when the IT changes direction, branches, enters a new cell or curls within it. Note that the IT is not uniform in its diameter. RVT = root vascular tissue. Bars represent 50  $\mu\text{m}$ . Samples were observed under a Nikon Eclipse 50i compound microscope (objective 10X; NA = 0.25 [A], objective 20X; NA = 0.40 [C], and objective 40X; NA = 0.65 [B,D]). The microscope was equipped with a PaxCam Arc digital camera. B and D are composite images where many photographs were taken at different depths of field, and then stacked using a Pax-it imaging software ([www.paximaging.net](http://www.paximaging.net)) to give a sense of three-dimensionality.

turned and curled (Figs. 4-7C and 4-7D). The IT at least doubled the number of its branches each time it entered a new cortical cell layer. When the IT was branching and entwined, some of the cells it entered became enlarged. At times the IT became thin in both the outer and inner cortex, and it was not uniform in diameter (Figs. 4-7B and 4-7C).

### **4.3.3 Nodule excision**

After all Sparkle nodules were excised at 21 DAI, it was seen when the root systems were observed two weeks later that new nodules had formed (Fig. 4-8). These were observed over the entire root system. However, they were mostly lower down and further away from the primary root than the early-formed nodules. In general, less and smaller nodules were seen at the 35 DAI observation time-point than at the 21 DAI excision time-point; 80% of the plants had less nodules at 35 DAI than before the excision at 21 DAI. On average, there were  $38 \pm 8$  less nodules after the excision. It makes sense that the nodules were found lower down on the root system because the first wave of nodules had already emerged (Fig. 4-5H) and been excised at 21 DAI, with the new nodules appearing slightly lower down. The plants of E151 produced few emerged nodules, as was seen earlier. Because of this and because of the temporal delay in its nodule emergence, plants were senescing before the new nodules could be counted. Therefore, the experiment could not be completed for E151.

## **4.4 Discussion**

### **4.4.1 Organogenesis – E151 phenotype**

The results found from this experiment support those found from the nodulation maps, that E151 is both a delayed and a low nodulator. As well, for the individual pea lines, the distribution of the nodules in pouches is similar to that of plants grown in Conetainers™, i.e. as seen in nodulation maps. On the root system of Sparkle, the nodules are located close to the primary root and close to the cotyledons, in a confined nodulation zone (Fig. 4-3). However, those of E151 appear more scattered on the root system and are located further down from the



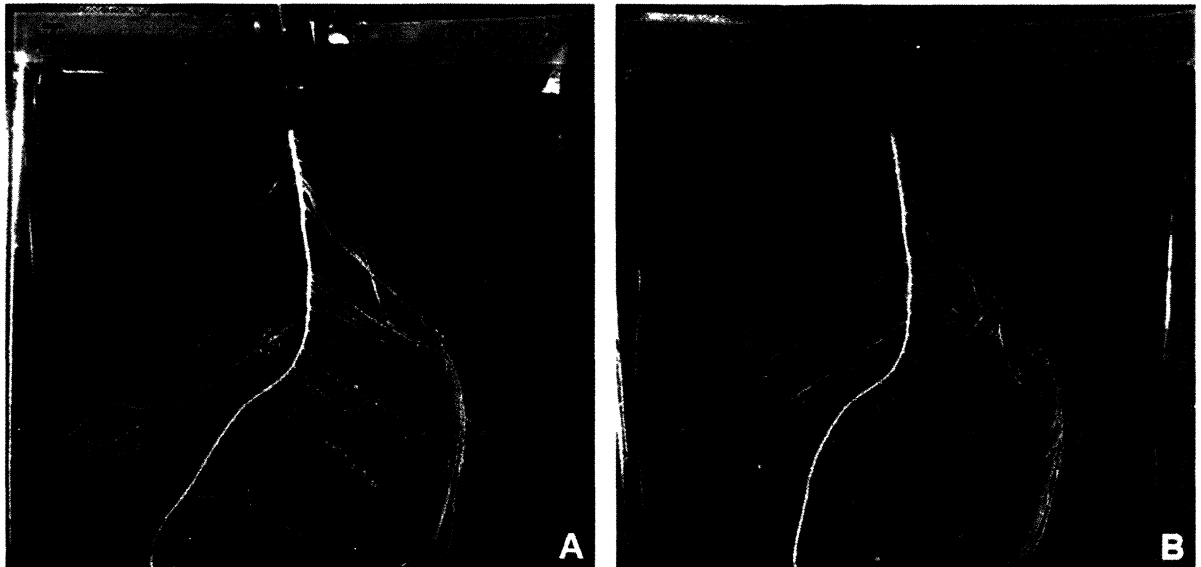


**Figure 4-8. Sparkle plant which had its nodules excised.**

Plants were photographed prior to nodule excision at 21 DAI (A). Nodules were excised using a razor blade and plants were re-potted until 35 DAI. Plants were removed at this time and new nodule emergence was observed (B).

cotyledons (Fig. 4-6). The nodules of E151 appeared delayed in space, i.e. further down on the root system. There are, however, less nodules overall but this is the case for both pea lines, likely because of the smaller volume that the roots occupied (Nutman, 1967). Francisco and Harper (1995) compared soybean plants grown in pots of vermiculite to plants grown in growth pouches and noticed also that the former had more nodules than the latter. Because of this different nodulation response, the authors emphasize that caution should be taken when interpreting nodulation results of plants grown in growth pouches (Francisco and Harper, 1995). The differing number of nodules must be put into perspective of the growth medium. Because in this study there are no discrepancies in nodule distribution between methods, the pouches can be considered useful for such studies.

The early-formed non-emerged nodules of E151 have been further analyzed here using the spot-inoculation technique. The technique allowed me to know exactly where a nodule would form and to track the timing of nodule organogenesis based on when the roots were inoculated; furthermore nodule development was followed for a long time. Chlup (2007) found that on E151 nodule primordia and emerged nodules rarely formed and mature nodules were never seen. The work by Chlup (2007) was based on the gross classification of infection events by Guinel and LaRue (1991). I decided to further subdivide nodule organogenesis by adding two more stages to that classification, which did not have enough stages to describe the growth of the IT. However, in hindsight, my classification should actually have had another stage with my stage B divided into two additional stages.

E151 seems affected in both programs, near the beginning of the cortical program (few divisions) and later in the epidermal program (interface epidermis-cortex). If the IT breaches this interface, the IT progresses and branches practically every time it advances by one cell layer. I propose that E151 has more than one blocked stage in its nodule organogenesis. One block is at stage B1, i.e. root hair curling with IT in the epidermal cell but with no inner cortex division, and the other at stage E, i.e. IT in the inner cortex with inner cortical cell divisions, according to my classification system. As mentioned earlier, Guinel and Geil (2002) suggested two developmental programs for nodulation, an epidermal and a cortical program; the authors differentiate that bacteria are required for the former but that Nod factors can trigger the latter. Because nodule organogenesis is a complex process involving the coordination of the two programs, it is possible for two blocked stages to occur, one in each program. If that were the

case, the problem with the overarching control would likely lie with the coordinator (Ding and Oldroyd, 2009), which has been proposed to be a hormone, yet researchers are still unsure which hormone it may be.

Murray *et al.* (2007) characterized a *L. japonicus* plant with a mutation in the *HYPERINFECTED 1 (HIT1)* locus, which exhibits abundant infection-thread formation and fails to initiate cortical cell divisions in response to rhizobial presence. The authors noticed an accumulation of ITs within the cortex where nodule primordia do not develop. Murray *et al.* (2007) describe the ITs as misguided and looping within the root cortex. The mutant had enlarged and flattened nodules and a low nodulation phenotype. E151 seems to be similar to this mutant, especially when one examines carefully the photographs shown in the supplementary data of the article (Murray *et al.*, 2007), in its nodulation phenotype and its nodule organogenesis. However, E151 does not appear to experience hyper-infection because there was no significant difference between the number of infections per cm segment in E151 and Sparkle. Murray *et al.* (2007) showed that the *LjHIT1* gene encodes a cytokinin receptor required for the activation of nodule organogenesis. Gonzalez-Rizzo *et al.* (2006) demonstrated that *MtCRE1*, encoding a cytokinin receptor orthologous to *LjHIT1*, is also required for barrel medic nodulation at an early stage of the epidermal program and/or cortical program. The authors explained that the cytokinin signalling mediated by *MtCRE1* is crucial to the early stages of the symbiotic interaction. Perhaps cytokinin is the culprit for the nodulation abnormality in E151 and is the coordinator of the epidermal and the cortical program. Murray *et al.* (2007) suggested that the *hit1* mutant's reduced nodule organogenesis likely restricts the feedback mechanism that limits root susceptibility to infection, resulting in hyperinfection events, with none leading to nodule primordia development. A lack of primordium formation has been suggested to induce premature termination of the IT by Gonzalez-Rizzo *et al.* (2006); this could well explain the E151 nodulation phenotype.

E151 early-formed nodules appear to be aborted because emerged nodules were never seen at the top of the root system even late in the life of the plant (Fig. 4-6). There were nodules which entered stage E by 7 DAI, therefore these nodules had the potential to emerge. By 10 DAI and 14 DAI, there were some events tallied for stage F and G, respectively but there are not many events in stage G or H by 35 DAI, indicating that they are not delayed but aborted. From the micro-observations, I confirmed that infection did occur, but did not lead to an emerged

nodule. Optical sectioning was beneficial in locating where the block in nodule organogenesis occurred. Because I observed plants past 21 DAI, I gained insight into whether the nodule was re-triggered to grow, which I discovered was not the case.

Perhaps the difference between the abortion I see in pea and the arrest Caetano-Anollés and Gresshoff (1991b) saw in soybean is due to the differences in nodule meristem activity of these two legumes. The former has indeterminate nodules with an apical meristem which continues to grow and the latter has determinate nodules with a peripheral meristem which stops growing at a predetermined time (Guinel, 2009). Caetano-Anollés and Gresshoff (1991b) removed emerged nodules also from alfalfa and found that new nodules formed around the location where previous infection was absent, while on soybean they had observed that the nodules emerged from infections already present on both primary and lateral roots. This difference in location of new nodule emergence could be again explained by a difference in nodule meristem formation since alfalfa has indeterminate nodules while soybean formed determinate nodules. The authors, however, explain the variation in location of new nodules for the two species as a result of two alternative mechanisms which control nodulation: one is the preference of the plant for multiple infections with just a few succeeding in nodule development and the other is a tight control of nodule initiation (Caetano-Anollés and Gresshoff, 1991a). The former is in fact AON and the latter would be a non-systemic control.

Nodules likely form lower down on E151 because there is no regulation to block nodule formation. Nodule primordia have been suggested to initiate the AON mechanism (Li *et al.*, 2009). Because E151 rarely forms primordia, the root-ascending signal is not sent, and the shoot-descending signal is not synthesized. This results in no inhibition of nodules further down on the root system.

#### **4.4.2 The placement of E151 according to other pea mutants**

The molecular investigation of nodule development in multiple mutants has allowed a very fine dissection of all the stages required for a proper organogenesis. These mutants were developed so that the symbiotic genes required for legume nodulation could be characterized (Kneen *et al.*, 1994), and researchers have been able to link a specific phenotype to a specific gene. With these mutants in mind, Guinel and Geil (2002) have proposed the two

aforementioned programs (Fig. 4-9). For example, E107 (*brz*) is affected in the epidermal program, with the IT blocked in the epidermis with few entering the inner cortex (Guinel and LaRue, 1992). More mutants seem, however, to be blocked in the cortical program. E2 (*sym5*) is blocked just before the inner cortical cells divide with the IT present in the inner cortex (Fig. 4-8; Guinel and LaRue, 1991). R50 (*sym16*) is blocked at the nodule primordium stage (Fig. 4-8; Guinel and Sloetjes, 2000). Guinel and Sloetjes (2000) indicate that the nodule primordia of R50 are abnormal and flat. The infection threads are also abnormal and are arrested in the inner cortex. The threads have lost their directional growth towards the vasculature and coil within enlarged outer cortical cells. Very few infection threads are associated with divisions in the inner cortical cells. Although E151 and R50 both have abnormal ITs, they are quite different in that E151 ITs are branched extensively while R50 IT loop back and forth. With E132 (*sym21*), a nodule meristem forms but it does not emerge (Fig. 4-8; Markwei and LaRue, 1997). E151 appears to be unique in our collection of mutants because it is affected in both programs and also has many unique features such as an usual IT, different from that of R50, and multiple meristems leading to a multi-lobed nodule.

It is difficult to place E151 on the model by Tsyganov *et al.* (2002) because of its two blocks found in the concurrent programs (Fig. 4-10). I have attempted to place E151 in both these locations (Fig. 4-10) but this is difficult as its two blocks do not correspond to linked events between the simultaneous programs. Tsyganov *et al.* (2002) outlined three checkpoints (labelled 1 to 3 in Fig. 4-10); for E151, one of the two blocks is that which is labelled 2 on the illustration by Tsyganov *et al.* (2002). A root hair curls and an infection thread forms and enters the epidermal cell, then a block can occur, with some infection threads able to enter the outer cortex. In E151, it seems as though if the IT can get past that first epidermal cell and into the outer cortex, then it will likely be able to enter the inner cortex and concurrently the inner cortical cells will divide. However, another block may occur here with few infections actually continuing on to produce a mature emerged nodule. Wipf and Cooper (1940) indicated that some ITs stimulate proliferation of cortical cells which result in the formation of nodules while others enter many cells without stimulation, addressing checkpoints 3 and 2 of Tsyganov *et al.* (2002), respectively. The two programs could be seen as two clocks (Guinel, personal communication). As the nodulation events progress, the epidermal clock and the cortical clock tick together. The IT grows towards the primordium with the first clock and the primordium

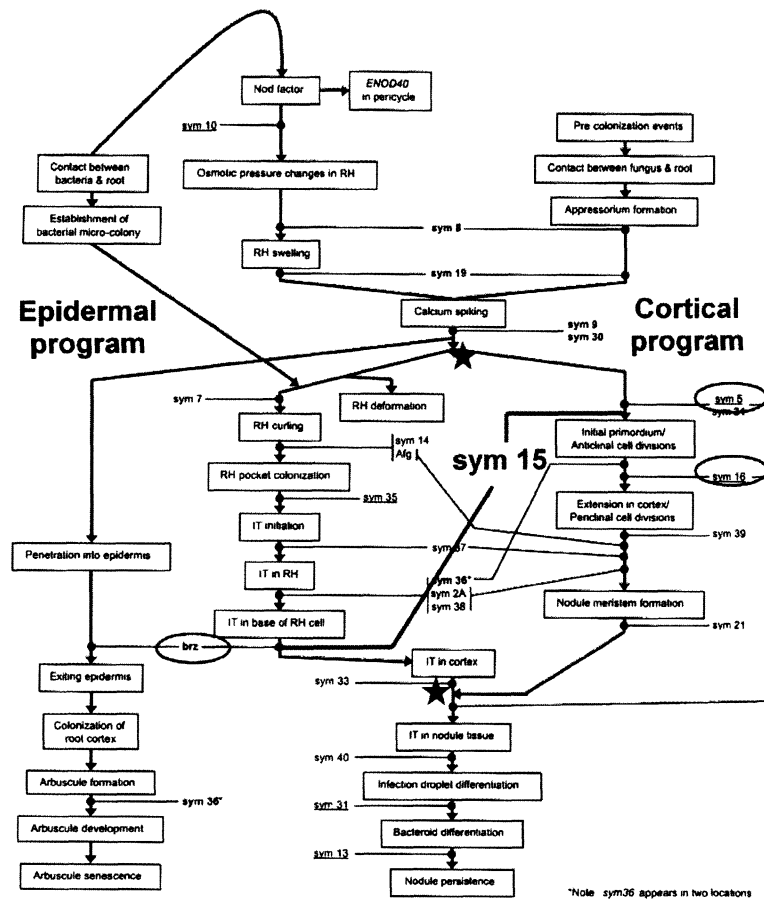


**Figure 4-9. The location of *sym15* on the modified schematic of Guinel and Geil (2002).** Stars indicate where the coordination of the epidermal and the cortical programs must occur. The mutants encircled in red are those which are referred to in the text.

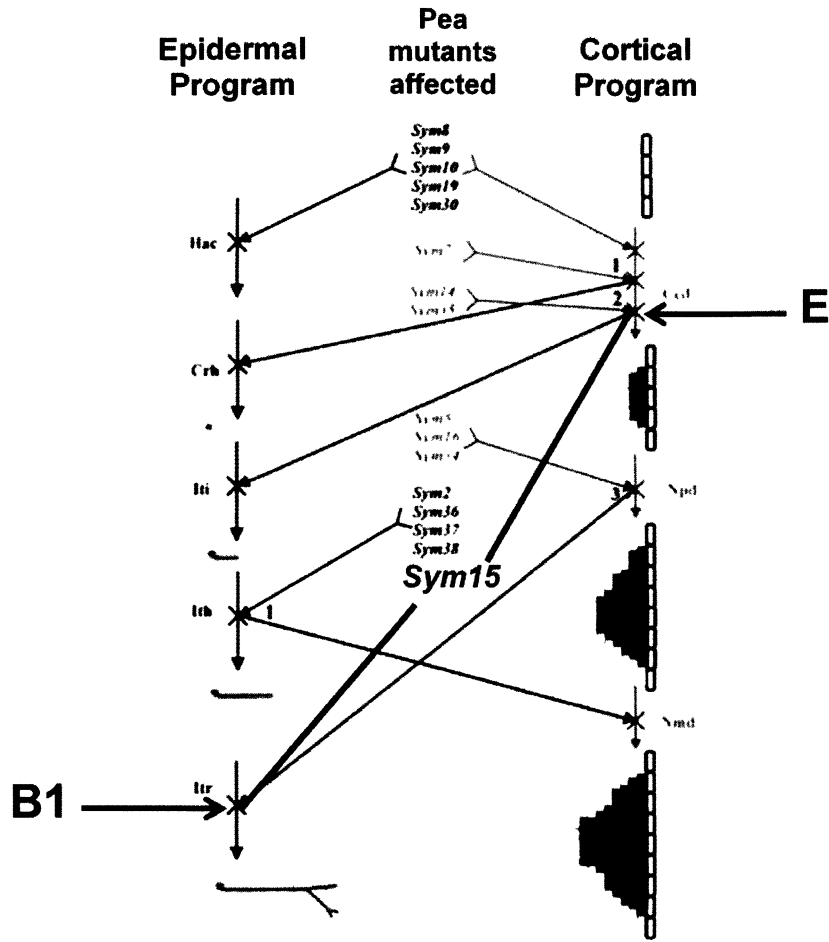


**Figure 4-10. Placement of sym15 on the modified schematic of Tsyganov et al. (2002).**

The epidermal program is depicted on the left-hand side and connected by blue arrows and the cortical program is on the right-hand side connected by red arrows. The former program involves Hac - root hair curling, Crh – curled root hair, Iti - infection thread growth initiation, Ith – infection thread growth in the root hair, and Itr – infection thread growth inside root cortex. The latter involves Ccd – cortical cell divisions, Npd – nodule primordium development, Nmd – nodule meristem development. Pea mutants and their placement on the schematic according to their block in nodule organogenesis are illustrated in the middle. The checkpoints (numbers) are control points of one program or the other. One checkpoint is outlined for the epidermal program and three checkpoints for the cortical program. IT growth in the epidermis is the checkpoint of the former program (blue 1). For the latter program, the first two check points are both at the stage of abortion of nodule tissue development with mutants differing in whether no or some divisions occur (red 1 and 2, respectively). The third checkpoint is nodule primordium development (red 3). I have placed E151 on the schematic, showing its block at the stage I named B1 in the epidermal program, i.e. IT entering the epidermis, and at the stage E in the cortical program, i.e. some divisions occurring.

grows towards the epidermis with the second clock. In E151, there would be two possible scenarios. In one, the epidermal clock would be arrested fast, when the IT is stopped in the epidermis. This would lead to a concurrent arrest of the cortical clock. In the other, the epidermal clock would tick properly with the IT progressing in the cortex but the cortical clock would be arrested. There is no primordium to guide the IT so it branches many times in an attempt to trigger a primordium to form. Therefore, in E151 the two clocks or programs are not in phase. Shtark *et al.* (2010) developed a recent model of pea mutants, to which E151 now may be added (Fig. 4-11). However, its placement will be more accurate once its mycorrhization phenotype is confirmed. From preliminary data, the mycorrhization formation is thought to be blocked at the Pen (root penetration) stage (Lindsey Clairmont, personal communication; Fig. 4-11) where many appressoria developed with little entry of hyphae into the cortical cells.



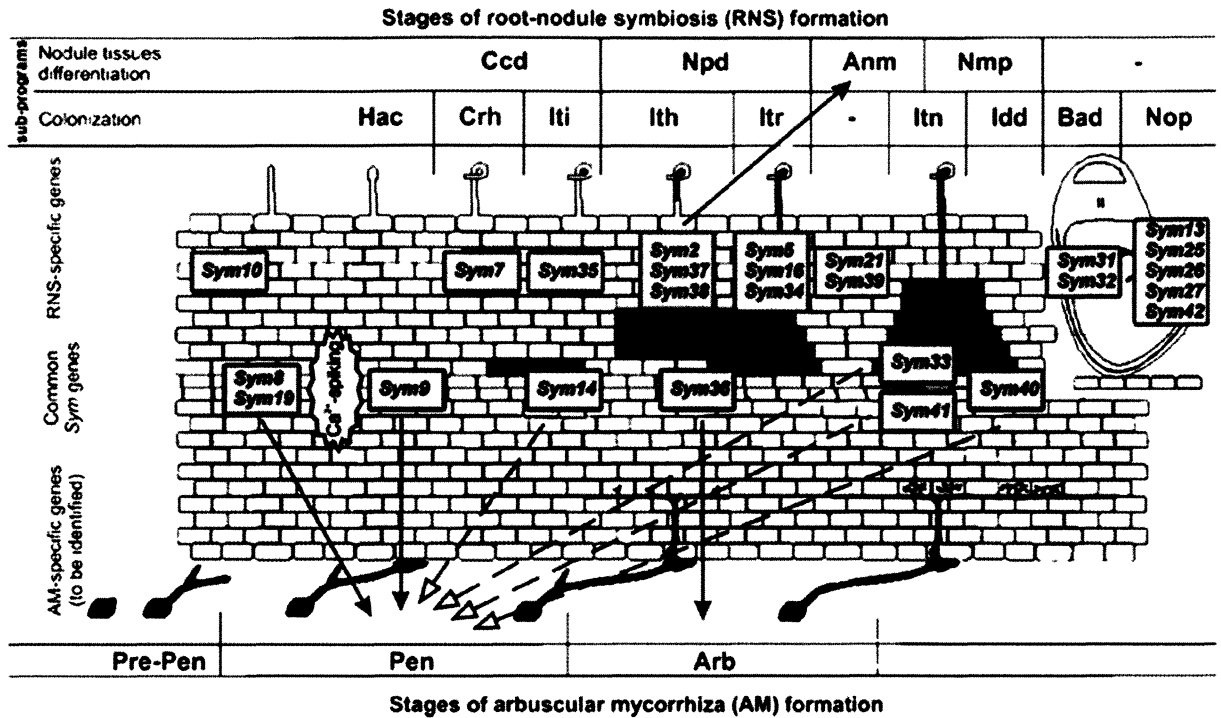


**Figure 4-11. The placement of E151 on the model by Shtark et al. (2010).**

Nodule organogenesis is broken down as nodule tissue differentiation and colonization. The former involves Ccd – cortical cell division, Npd – nodule primordium development, Anm – apical nodule meristem development, Nmp – nodule meristem persistence. The latter involves Hac – root hair curling, Crh – colonization of curled root hair, Iti – infection thread growth initiation, Ith – infection thread growth inside root hair cells, Itr – infection thread growth in root tissue, Itn – infection thread formation in nodule primordium, Idd – infection droplet differentiation, Bad – bacteroid differentiation, Nop – nodule persistence. Pea mutants and their placement on the schematic according to their block in nodule organogenesis are illustrated in grey boxes. On the bottom of the figure, the mycorrhization progression is outlined as Pre-Pen – pre-penetration, Pen – root penetration, and Arb – arbuscule development. I have placed E151 on the schematic, showing its block at Itr. It should be more to the left at the end of Ccd for the cortical program, however this is difficult as the blocked events do not correspond with how Shtark has linked the stages of the two programs. More information about its mycorrhization phenotype will allow for a more accurate placement.

## **Chapter V: Concluding Remarks**

### **5.1 The E151 nodulation phenotype and its efficiency**

In this thesis I took an integrative approach to study the E151 nodulation phenotype. I will outline what was found according to my objectives of Chapter I.

#### **5.1.1 Characterize E151 nodule distribution. (Chapter II)**

E151 can be classified as a low and delayed nodulator; these descriptions have been proven to be correct in multiple experiments throughout this thesis. The nodules of E151 were found to be spread across a larger root surface area than those of Sparkle. The nodules of E151 were also noted to be heavier than those of Sparkle. I suggest that the nodule distribution should be added as a trait to mutant phenotypes. I would then describe E151 as being affected in the first wave of nodulation.

#### **5.1.2 Determine if E151 has a differential response to rhizobial strains. (Chapter III)**

E151 did in fact have a differential response to the rhizobial strains compared to Sparkle; however, this was not a unique feature of E151, as it was also seen for R50. Using R50 as a control was beneficial, as I was able to determine whether the response of E151 was unique to this mutant or may be reflective of other mutants.

#### **5.1.3 Determine the efficiency of the E151-*Rhizobium* association. (Chapter III)**

I believe that I have added insights into both defining efficiency and measuring efficiency. With efficiency being such a complex parameter, it was determined that a cocktail of criteria should be analyzed for it to be clearly assessed. Efficiency should be measured according to parameters involving both species of the association rather than to reflect only one side of the symbiosis. Thus, I would suggest looking at the following: nodule number, nodule DW, morphology, nitrogen fixation rate, nodule construction cost, specific nodulation, and specific nodule DW. Understanding the efficiency of the symbiosis will allow us to optimize nitrogen fixation to achieve a more sustainable agriculture (Bhatia *et al.*, 2001). E151 is in fact not as efficient when in association as Sparkle, likely because of its mutated symbiosis gene.

#### **5.1.4 Confirm the location of the block in E151 nodule organogenesis. (Chapter IV)**

There were two blocks in E151 nodule organogenesis, disturbing in a unique manner both the epidermal and the cortical programs. The first block, in the former program was at the stage where the IT is present in the epidermis but cannot progress to the outer cortex. The second block, in the latter program, was at the stage where the IT has reached the inner cortex and the inner cortical cells have begun to divide. An explanation for the E151 multi-lobed nodule morphology still remains unknown; its vasculature must be studied, along with the organogenesis of later-formed nodules.

#### **5.1.5 Determine whether E151 early-formed nodules are aborted or arrested. (Chapter IV)**

E151 early-formed nodules are in fact aborted. This was seen from micro-observations of tallied infection events and confirmed with temporal macro-observations of plants grown in pouches. Abortion is suggested from the former as nodule organogenesis seemed to be blocked in the two aforementioned stages and never later in time resulted in the emergence of a nodule. Only one nodule was noted to emerge during this study. However, the mutant is capable of performing correctly organogenesis to its completion, as seen in the emerged nodules appearing further down on the root system. This emphasizes that the first wave of nodules is regulated differently from the second wave; this may be via AON or a hormone. With macro-observation, nodules were never seen to emerge at the top of the root system, indicating that early-formed nodules do not emerge while later-formed nodules are the only one to emerge. Future developmental studies should be performed to observe the organogenesis of later-formed nodules.

## **5.2 Classifying low nodulators**

I propose that low nodulators be divided into categories to better classify them, just like high nodulators have been placed into separate divisions (Table 5-1) of super- (Carroll *et al.*, 1985) and hyper- (Gremaud and Harper, 1989) nodulators, with the further refinement of enhanced nodulators (Nishimura *et al.*, 2002). Nishimura *et al.* (2002) introduced the idea of enhanced nodulators after investigating the *L. japonicus* mutant *astray*. The *astray* mutant had

**Table 5-1. Nodulation phenotypes of super-, hyper-, and enhanced nodulators compared to WT.**

	Supernodulator	Hypernodulator	Enhanced nodulator
Nodule number	- 5 to 20% more	- 5 to 20% more	- double
Nodule DW	?	- heavier	?
Nodule distribution	- outside typical zone	- same	- wide spread
Ethylene sensitivity	- sensitive	- insensitive	- responds as WT does
Nitrate sensitivity	- insensitive	- sensitive	- responds as WT does

twice the number of nodules which were spread over more of the root system than the wild-type. Interestingly, instead of being delayed as E151, *astray* is unique in initiating its nodule development earlier than the WT, this results with nodule primordia appearing earlier in *astray* (Nishimura *et al.*, 2002). Because of the larger extent of nodulation, the authors believe there may have been an impairment of AON. Previously, researchers had been mainly looking at nodule number to classify AON-deficient mutants. Clearly, timing of nodule development is also important; this is why developmental studies are important to see if nodule organogenesis occurs early or is delayed. Nishimura *et al.* (2002) hinted that maybe nodule organogenesis should be considered when characterizing a nodulation phenotype.

The low nodulation classification could be based on parameters similar to those used to divide the high nodulators, for example nodule number, nodule DW, nodule distribution or spread, ethylene sensitivity, and nitrate sensitivity. Although the nodulation phenotypes of E151 and R50 can be separated (Table 5-2), they cannot be easily linked with either super-, hyper-, or enhanced nodulators. Of interest is the nodule distribution, with hypernodulators having the same distribution as the WT and supernodulators having a more wide-spread distribution (Novák, 2010a). With E151 and R50 there was a difference in the degree of low nodulation; E151 produced about a quarter of the number of nodules and R50 about half compared to Sparkle (Table 5-2). E151 and R50 both have extended ratios with nodules appearing much lower down on the root system; however, that of R50 is larger than that of E151 (Table 5-2). As well, the distribution of R50 resembled that of Sparkle initially and later was much more spread while that of E151 was always different from that of Sparkle. The physiological responses must still be tested; however, it is known that R50 has differential sensitivity to ethylene (Ferguson *et al.*, 2005) with its nodulation phenotype sensitive to ethylene action (Guinel and Sloetjes, 2000). E151 was found to have the same nitrate sensitivity as Sparkle (Clairmont, 2011). Its ethylene sensitivity is more complex; the shoot is as sensitive to ethylene as the WT, while the root is insensitive to ethylene biosynthesis but sensitive to ethylene action (Clairmont, 2011). Both E151 and R50 have been classified as delayed nodulators, from this thesis. From my observations, R50 is more delayed than E151, in terms of germination and nodulation. Overall, these mutants belong in separate categories of low nodulating mutants. However, more investigations should be performed to add traits to the list so that the two mutants may be distinguished further.

**Table 5-2. Nodulation phenotype of the low nodulators E151 and R50 compared to WT Sparkle.**

	E151 ( <i>sym15</i> )	R50 ( <i>sym16</i> )
Nodule number	- quarter of WT	- half of WT
Nodule DW per plant	- 1/3 of WT	-2/3 of WT
Nodule individual DW	- almost double WT	- similar
Nodule distribution	- larger zone	- early on similar to WT - later on larger zone (almost double)
Ethylene sensitivity	- shoot responds as WT does - root insensitive to ethylene biosynthesis, sensitive to ethylene action	- shoot insensitive to C <sub>2</sub> H <sub>4</sub> -root responds to C <sub>2</sub> H <sub>4</sub> as WT does
Nitrate sensitivity	- sensitive	?

### 5.3 E151 in the context of AON

Because of the disparity in the coordination of the epidermal and cortical programs in E151, the problem likely lies in the coordinator (Ding and Oldroyd, 2009). The *L. japonicus* mutant *hit1* that Murray *et al.* (2007) investigated seems quite similar to E151 and its link to cytokinin indicates that perhaps this is the coordinator of the two programs, and therefore the culprit for the blocks in E151 nodule organogenesis. Likely, however, more than one hormone plays a role in the coordination of the two programs. Stougaard (2001) addressed the idea of delayed nodulation mutants. He proposes that these mutants are uncoupled in the parallel pathways that synchronize IT formation and cortical cell divisions; this appears to be true.

E151 is known to be root-controlled (Chlup, 2007). Therefore, if a deficit exists in AON, it must either be in the making of the root signal or in the perception of the shoot signal. I suggest that it is in the making of the root signal. It was suggested that either the nodule primordium (Li *et al.*, 2009) or the Nod factors (Lin *et al.*, 2010) trigger AON. E151 suggests that the answer to this question is the former. Indeed, since E151 does not form a primordium, there is no root signal made, and nodulation further down on the root is not inhibited, leading to a unique extensive nodulation zone. Approach-grafting experiments (modified from Li *et al.*, 2009) have been performed where preliminary results indicate that the AON signal takes 24 hours to be completed in the pea Sparkle (De Carvalho, 2011). Further grafting experiments involving E151 will add more information about its AON.

Gresshoff *et al.* (2005) identified five common characteristics of mutants with an absence of AON focussing only on the supernodulators. In our lab, we think that low and delayed nodulators should also be taken into account. Their qualifications of a mutant deficient in AON were: 1. A larger nodule number; 2. An increased nodulation interval; 3. An increased nodule mass per plant; 4. An increased nodule number in the presence of nitrate; 5. A less developed root system. This needs to be re-evaluated. I propose 1. An altered nodule number (higher or lower); 2. An altered nodule distribution or spread; 3. An altered nodule mass per plant or individual nodule DW, 4. An altered nodule number in the presence of nitrate; 5. An earlier or later initiation in nodule development. To categorize these different mutants, one should therefore study not only nodule distribution and nodule characteristics, but also nodule organogenesis.

## References

- Bhatia, C.R., Nichterlein, K., Maluszynski M. 2001. Mutations affecting nodulation in grain legumes and their potential in sustainable cropping systems. *Euphytica*, **120**: 415-432.
- Bhuvaneshwari, T.V., Turgeon, B.G., Bauer, W.D. 1980. Early events in the infection of soybean (*Glycine max* L. Merr) by *Rhizobium japonicum*. *Plant Physiology*, **66**: 1027-1031.
- Bhuvaneshwari, T.V., Bhagwat, A.A., Bauer, W.D. 1981. Transient susceptibility of root cells in four common legumes to nodulation by rhizobia. *Plant Physiology*, **68**: 114-1149.
- Bond, L. 1948. Origin and developmental morphology of root nodules of *Pisum sativum*. *Botanical Gazette*, **109**: 411-434.
- Borisov, A.Y., Barmicheva, E.M., Jacobi, L.M., Tsyganov, V.E., Voroshilova, V.A., Tikhonovich, I.A. 2000. Pea (*Pisum sativum* L.) mendelian genes controlling development of nitrogen-fixing nodules and arbuscular mycorrhiza. *Czech Journal of Genetics and Plant Breeding*. **36**: 106-110.
- Brelles-Mariño, G. & Ané, J. 2008. Nod factors and the molecular dialogue in the rhizobia. In: *Nitrogen Fixation Research Progress* (Couto, G.N., ed.). Nova Science Publishers Inc., NY, pp. 1-57.
- Burias, N., Planchon, C., Paul, M.H. 1990. Phenotypic and genotypic distribution of nodules on soybean root system inoculated with *Bradyrhizobium japonicum* strain G49. *Agronomie*, **10**: 57-62.
- Caetano-Anollés, G. 1997. Molecular dissection and improvement of the nodule symbiosis in legumes. *Field Crops Research*, **53**: 47-68.
- Caetano-Anollés, G. and Gresshoff, P.M. 1991a. Plant genetic control of nodulation. *Annual Review of Microbiology*, **45**: 345-482.
- Caetano-Anollés, G. and Gresshoff, P.M. 1991b. Excision of nodules induced by *Rhizobium-meliloti* exopolysaccharide mutants releases autoregulation in alfalfa. *Journal of Plant Physiology*, **138**: 765-767.
- Caetano-Anollés, G. and Gresshoff, P.M. 1993. Nodule distribution on the roots of soybean and a supernodulating mutant in sand-vermiculite. *Plant and Soil*, **148**: 265-270.
- Caetano-Anollés, G., Paparozzi, E.T., Gresshoff, P.M. 1991. Mature nodules and root-tips control nodulation in soybean. *Journal of Plant Physiology*, **137**: 389-396.
- Carroll, B.J., McNeil, D.L., Gresshoff, P.M. 1985. Isolation and properties of soybean [*Glycine max* (L.) Merr.] mutants that nodulate in the presence of high nitrate concentrations. *Proceedings of the National Academy of Sciences of the United States of America*, **82**: 4162-4166.



- Chen, N.K. and Thornton, H.G. 1940. The structure of 'ineffective' nodules and its influence on nitrogen fixation. *Proceedings of the Royal Society of London, Series B, Biological Sciences*, **129**: 208-229.
- Chlup, M. 2007. Characterization of the nodulation phenotype of E151, a pleiotropic pea (*Pisum sativum* L.) mutant. Waterloo, ON. University of Waterloo, MSc Thesis.
- Clairmont, L. 2011. Investigating the regulation of root symbioses using the low nodulating pea (*Pisum sativum* L.) mutant E151 (*sym15*). Waterloo, ON. Wilfrid Laurier University, BSc Thesis.
- Clemow, S. 2010. Insights into the world of pea nodulation using the low nodulator R50. Waterloo, ON. Wilfrid Laurier University, MSc Thesis.
- De Carvalho, P. 2011. Testing AON characteristics of *Pisum sativum* cv. Sparkle and mutant E151 (*sym15*) with a series of approach-graft experiments. Waterloo, ON. Wilfrid Laurier University, BSc. Thesis.
- Delanghe, S.G. 2007. Investigation of the nodule development in the low nodulating pea mutant E151 (*sym15*). Waterloo, ON. Wilfrid Laurier University, BSc Thesis.
- Delves, A.C., Mathews, A., Day, D.A., Carter, A.S., Carroll, B.J., Gresshoff, P.M. 1986. Regulation of the soybean-*Rhizobium* nodule symbiosis by shoot and root factors. *Plant Physiology*, **82**: 588-590.
- Denison, R.F. 2000. Legume sanctions and the evolution of symbiotic cooperation by rhizobia. *The American Naturalist*, **156**: 567-576.
- Ding, Y. and Oldroyd, G.E.D. 2009. Positioning the nodule, the hormone dictum. *Plant Signalling and Behavior*, **4**: 89-93.
- Downie, J.A. 2005. Legume haemoglobins: symbiotic nitrogen fixation needs bloody nodules. *Current Biology*, **15**: R196-R198.
- Downie, J.A., Knight, C.D., Johnston, A.W.B., Rossen, L. 1985. Identification of genes and gene products involved in the nodulation of peas by *Rhizobium leguminosarum*. *Molecular and General Genetics*, **198**: 255-262.
- Eddie, S.A. and Phillips, D.A. 1983. Effect of the host legume on acetylene reduction and hydrogen evolution by *Rhizobium* nitrogenase. *Plant Physiology*, **72**: 156-160.
- Estrada-Navarrete, G., Alvarado-Affantranger, X., Olivares, J., Guillén, G., Díaz-Camino, C., Campos, F., Quinto, C., Gresshoff, P.M., Sanchez, F. 2007. Fast, efficient and reproducible genetic transformation of *Phaseolus* spp. by *Agrobacterium rhizogenes*. *Nature Protocols*, **2**: 1819-1824.

FAO. 2006. Fertilizer and Plant Nutrition Bulletin: Fertilizer use by crop. Rome, Italy.

Fei, H. and Vessey, J.K. 2009. Stimulation of nodulation in *Medicago truncatula* by low concentrations of ammonium: quantitative reverse transcription PCR analysis of selected genes. *Physiologia Plantarum*, **135**: 317-330.

Ferguson, B.J., Indrasumunar, A., Hayashi, S., Lin, M., Lin, Y., Reid, D.E., Gresshoff, P.M. 2010. Molecular analysis of legume nodule development and autoregulation. *Journal of Integrative Plant Biology*, **52**: 61-76.

Ferguson, B.J., Ross, J.J., Reid, J.B. 2005a. Nodulation phenotypes of gibberellin and brassinosteroid mutants of pea. *Plant Physiology*, **138**: 2396-2405.

Ferguson, B.J., Wiebe, E.M., Emery, R.J.N., Guinel, F.C. 2005b. Cytokinin accumulation and an altered ethylene response mediate the pleiotropic phenotype of the pea nodulation mutant R50 (*sym16*). *Canadian Journal of Botany*, **83**: 989-1000.

Ferguson, B.J., Wiebe, E.M., Emery, R.J.N., Guinel, F.C. 2005. Cytokinin accumulation and an altered ethylene response mediate the pleiotropic phenotype of the pea nodulation mutant R50 (*sym16*). *Canadian Journal of Botany*, **83**: 989-1000.

Francisco, P.B. and Harper, J.E. 1995. Autoregulation of soybean nodulation – delayed inoculation increases nodule number. *Physiologia Plantarum*, **93**: 411-420.

Gage, D.J. & Margolin, W. 2000. Hanging by a thread: invasion of legume plants by rhizobia. *Current Opinion in Microbiology*, **3**: 613-617.

Galibert, F., Finan, T.M., Long, S.R., Puhler, A., Abola, P., Ampe, F., Barloy-Hubler, F., Barnett, M.J., Becker, A., Boistard, P., Bothe, G., Boutry, M., Bowser, L., Buhrmester, J., Cadieu, E., Capela, D., Chain, P., Cowie, A., Davis, R.W., Dréano, S., Federspiel, N.A., Fisher, R.F., Gloux, S., Godrie, T., Goffeau, A., Golding, B., Gouzy, J., Gurjal, M., Hernandez-Lucas, I., Hong, A., Huizar, L., Hyman, R.W., Jones, T., Kahn, D., Kahn, M.L., Kalman, S., Keating, D.H., Kiss, E., Komp, C., Lelaure, V., Masuy, D., Palm, C., Peck, M.C., Pohl, T.M., Portetelle, D., Purnelle, B., Ramsperger, U., Surzycki, R., Thébault, P., Vandenbol, M., Vorhölter, F.J., Weidner, S., Wells, D.H., Wong, K., Yeh, K., Batut, J. 2001. The composite genome of the legume symbiont *Sinorhizobium meliloti*. *Science*, **293**: 668-672.

Golding, A. and Dong, Z. 2010. Hydrogen production by nitrogenase as a potential crop rotation benefit. *Environmental Chemistry Letters*, **8**: 101-121.

Gonzalez-Rizzo, S., Crespi, M., Frugier, F. 2006. The *Medicago truncatula* CRE1 cytokinin receptor regulates lateral root development and early symbiotic interaction with *Sinorhizobium meliloti*. *Plant Cell*, **18**: 2680-2693.

- Graham, P.H. and Vance, C.P. 2003. Legumes: importance and constraints to greater use. *Plant Physiology*, **131**: 872-877.
- Gremaud, M.F. and Harper, J.E. 1989. Selection and initial characterization of partially nitrate tolerant nodulation mutants of soybean. *Plant Physiology*, **89**: 169-173.
- Gresshoff, P.M., Gualtieri, G., Laniya, T., Indrasumunar, A., Miyahara, A., Nontachaiyapoom, S., Wells, T., Biswas, B., Chan, P.K., Scott, P., Kinkema, M., Djordjevic, M., Hoffman, D., Pregelj, L., Buzas, D.M., Li, D.X., Men, A., Jiang, Q., Hwang, C., Carroll, B.J. 2005. Functional genomics of the regulation of nodule number in legumes. In: *Biological Nitrogen Fixation*, Springer, Netherlands.
- Gubry-Rangin, C., Garcia, M., Béna, G. 2010. Partner choice in *Medicago truncatula*-*Sinorhizobium* symbiosis. *Proceedings of the Royal Society of London, Series B, Biological Sciences*, **277**:1947-1951.
- Guinel, F.C. 2009. Getting around the legume nodule: I. The structure of the peripheral zone in four nodule types. *Botany*, **87**: 1117-1138.
- Guinel, F.C. and Geil, R.D. 2002. A model for the development of the rhizobial and arbuscular mycorrhizal symbioses in legumes and its use to understand the roles of ethylene in the establishment of these two symbioses. *Canadian Journal of Botany*, **80**: 695-720.
- Guinel, F.C. and LaRue, T.A. 1991. Light microscopy study of nodule initiation in *Pisum sativum* L. cv Sparkle and in its low-nodulating mutant E2 (*sym 5*). *Plant Physiology*, **87**: 1206-1211.
- Guinel, F.C. and LaRue, T.A. 1992. Ethylene inhibitors partly restore nodulation to pea mutant E107 (*brz*). *Plant Physiology*, **99**: 515-518.
- Guinel, F.C. and Sloetjes, L.L. 2000. Ethylene is involved in the nodulation phenotype of *Pisum sativum* R50 (*sym16*), a pleiotropic mutant that nodulates poorly and has pale green leaves. *Journal of Experimental Botany*, **51**: 885-894.
- Gulden, R.H. and Vessey, J.K. 1998. Low concentrations of ammonium inhibit specific nodulation (nodule number g<sup>-1</sup> root DW) in soybean (*Glycine max* [L.] Merr). *Plant and Soil*, **198**: 127-136.
- Hardy, R.W.F., Holsten, R.D., Jackson, E.K., Burns, R.C. 1968. The acetylene-ethylene assay for N<sub>2</sub> fixation: laboratory and field evaluation. *Plant Physiology*, **43**: 1185-1207.
- Heidstra, R., Yang, W.C., Yalcin, Y., Peck, S., Emons, A., van Kammen, A., Bisseling, T. 1997. Ethylene provides positional information on cortical cell division but is not involved in Nod factor-induced root hair tip growth in *Rhizobium*-legume interaction. *Development*, **124**: 1781-1787.

- Held, M., Pepper, A.N., Bozdarov, J., Smith, M.D., Emery, R.J.N., Guinel, F.C. 2008. The pea nodulation mutant R50 (*sym16*) displays altered activity and expression profiles for cytokinin dehydrogenase. *Journal of Plant Growth and Regulation*, **27**: 170-180.
- Hirsch, A.M. 1992. Developmental biology of legume nodulation. *New Phytologist*, **122**: 211-237.
- Hunt, S. and Layzell, D.B. 1993. Gas exchange of legume nodules and the regulation of nitrogenase activity. *Annual Review of Plant Physiology and Plant Molecular Biology*, **44**: 483-511.
- Jiang, Q. and Gresshoff, P.M. 2002. Shoot control of hypernodulation and aberrant root formation in the *har1-1* mutant of *Lotus japonicus*. *Functional Plant Biology*, **29**: 1371-1376.
- Kereszt, A., Li, D., Indrasumunar, A., Nguyen, C., Nontachaiyapoom, S., Kinkema, M., Gresshoff, P.M. 2007. *Agrobacterium rhizogenes*-mediated transformation of soybean to study root biology. *Nature Protocols*, **2**: 948-952.
- Kiers, E.T., Rousseau, R.A., West, S.A., Denison, R.F. 2003. Host sanctions and the legume-rhizobium mutualism. *Nature*, **425**: 78-81.
- Kinkema, M., Scott, P.T., Gresshoff, P.M. 2006. Legume nodulation: successful symbiosis through short- and long-distance signalling. *Functional Plant Biology*, **33**: 707-721.
- Kneen, B.E., Weeden, N.F., LaRue, T.A. 1994. Non-nodulating mutants of *Pisum sativum* (L.) cv. Sparkle. *Journal of Heredity*, **85**: 129-133.
- Koch, M., Delmotte, N., Rehrauer, H., Vorholt, J.A., Pessi, G., Hennecke, H. 2010. Rhizobial adaptation to hosts, a new facet in the legume root-nodule symbiosis. *Molecular Plant-Microbe Interactions*, **23**: 784-790.
- Krusell, L., Madsen, L.H., Sato, S., Aubert, G., Genua, A., Szczyglowski, K., Duc, G., Kaneko, T., Tabata, S., de Bruijn, F., Pajuelo, E., Sandal, N., Stougaard, J. 2002. Shoot control of root development and nodulation is mediated by a receptor-like kinase. *Nature*. **420**: 422-426.
- Krusell, L., Sato, N., Fukuhara, I., Koch, B.E.V., Grossmann, C., Okamoto, S., Oka-Kira, E., Otsubo, Y., Aubert, G., Nakagawa, T., Sato, S., Tabata, S., Duc, G., Parniske, M., Wang, T.L., Kawaguchi, M., Stougaard, J. 2011. The *Clavata2* genes of pea and *Lotus japonicus* affect autoregulation of nodulation. *The Plant Journal*, **65**: 861-871.
- Laguerre, G., Depret, G., Bourion, V., Duc, G. 2007. *Rhizobium leguminosarum* bv. *viciae* genotypes interact with pea plants in developmental responses of nodules, roots and shoots. *New Phytologist*, **176**: 680-690.

- Lavin, M., Herendeen, P.S., Wojciechowski, M.F. 2005. Evolutionary rates analysis of Leguminosae implicates a rapid diversification of lineages during the tertiary. *Systematic Biology* **54**: 575-594.
- Layzell, D.B. and Atkins, C.A. 1997. The physiology and biochemistry of legume N<sub>2</sub> fixation. *in*: Dennis, D.T., Turpin, D.H., Lefebvre, D.D., Layzell, D.B., editors. Plant Metabolism 2<sup>nd</sup> ed. Addison Wesley Longman. Edinburgh Gate, Harlow, Essex, England: pp. 631
- Layzell, D.B., Weagle, G.E., Canvin, D.T. 1984. A highly sensitive, flow through H<sub>2</sub> gas analyzer for use in nitrogen fixation studies. *Plant Physiology*, **75**: 582-585.
- Lee, K.H. and LaRue, T.A. 1992. Pleiotropic effects of *sym17*: a mutation in *Pisum sativum* L. cv Sparkle causes decreased nodulation, altered root and shoot growth, and increased ethylene production. *Plant Physiology*, **100**: 1326-1333.
- Leong, S.A., Williams, P.H., Ditta, G.S. 1985. Analysis of the 5' regulatory region of the gene for  $\delta$ -aminolevulinic acid synthetase of *Rhizobium meliloti*. *Nucleic Acids Research*, **13**: 5965-5976.
- Li, D., Kinkema, M., Gresshoff, P.M. 2009. Autoregulation of nodulation (AON) in *Pisum sativum* (pea) involves signalling events associated with both nodule primordial development and nitrogen fixation. *Journal of Plant Physiology*, **166**: 955-967.
- Lin, Y., Ferguson, B.J., Kereszt, A., Gresshoff, P.M. 2010. Suppression of hypernodulation in soybean by a leaf-extracted, NARK- and Nod factor-dependent, low molecular mass fraction. *New Phytologist*, **185**: 1074-1086.
- Lira Jr., M. de A. and Smith, D.L. 2000. Use of standard TWAIN scanner and software for nodule number determination on different legume species. *Soil Biology and Biochemistry*, **32**: 1463-1467.
- Long, C. 2010. The pleiotropic mutant R50 (*sym16*): a link between cytokinin and starch metabolism may explain its seed phenotype. Waterloo, ON. Wilfrid Laurier University, MSc Thesis.
- Lorteau, M., Ferguson, B.J., Guinel, F.C. 2001. Effects of cytokinin on ethylene production and nodulation in pea (*Pisum sativum*) cv. Sparkle. *Physiologia Plantarum*, **112**: 421-428.
- Macdonald, E.S. 2009. Developmental study of E151 (*sym15*), a nodulation mutant of the pea (*Pisum sativum*) cv. Sparkle. Waterloo, ON. Wilfrid Laurier University, BSc. Thesis.
- Magori, S., Oka-Kira, E., Shibata, S., Umehara, Y., Kouchi, H., Hase, Y., Tanaka, A., Sato, S., Tabata, S., Kawaguchi, M. 2009. *TOO MUCH LOVE*, a root regulator associated with the long-distance control of nodulation in *Lotus japonicus*. *Molecular Plant-Microbe Interactions*, **22**: 259-268.

- Malik, N., Calvert, H.E., Bauer, W.D. 1987. Nitrate induced regulation of nodule formation in soybean. *Plant Physiology*, **84**: 266-271.
- Markwei, C.M. and LaRue, T.A. 1997. Phenotypic characterization of *sym21*, a gene conditioning shoot-controlled inhibition of nodulation in *Pisum sativum* cv. Sparkle. *Physiologia Plantarum*, **100**: 927-932.
- McPhee, K. 2005. Variation for seedling root architecture in the core collection of pea germplasm. *Crop Science*, **45**: 1758-1763.
- Murray, J.D., Karas, B.J., Sato, S., Tabata, S., Amyot, L., Szczyglowski, K. 2007. A cytokinin perception mutant colonized by *Rhizobium* in the absence of nodule organogenesis. *Science*, **315**: 101-104.
- Nelson, L.M. and Salminen, S.O. 1982. Uptake hydrogenase activity and ATP formation in *Rhizobium leguminosarum* bacteroids. *Journal of Bacteriology*, **151**: 989-995.
- Nishimura, R., Ohmori, M., Kawaguchi, M. 2002. The novel symbiotic phenotype of enhanced-nodulating mutant of *Lotus japonicus*: *astray* mutant is an early nodulating mutant with wider nodulation zone. *Plant and Cell Physiology*, **43**: 853-859.
- Novák, K. 2010a. On the efficiency of legume supernodulating mutants. *Annals of Applied Biology*, **157**: 321-342.
- Novák, K. 2010b. Early action of pea symbiotic gene NOD3 is confirmed by adventitious root phenotype. *Plant Science*, **179**: 472-478.
- Nutman, P.S. 1967. Varietal differences in nodulation of subterranean clover. *Australian Journal of Agricultural Research*, **18**: 381-425.
- Ofek, M., Ruppel, S., Waisel, Y. 2007. Differences between bacterial associations with two root types of *Vicia faba* L. *Plant Biosystems*, **141**: 352-362.
- Okamoto, S., Ohnishi, E., Sato, S., Takahashi, H., Nakazono, M., Tabata, S., Kawaguchi, M. 2009. Nod factor/nitrate-induced *CLE* genes that drive HAR1-mediated systemic regulation of nodulation. *Plant & Cell Physiology*, **50**: 67-77.
- Oke, V. and Long, S.R. 1999. Bacteroid formation in the *Rhizobium*-legume symbiosis. *Current Opinion in Microbiology*, **2**: 641-646.
- Oldroyd, G.E.D. and Downie, J.A. 2008. Coordinating nodule morphogenesis with rhizobial infection in legumes. *Annual Review of Plant Biology*, **59**: 519-546.
- Oono, R. and Denison, R.F. 2010. Comparing symbiotic efficiency between swollen versus nonswollen rhizobial bacteroids. *Plant Physiology*, **154**: 1541-1548.

- Oono, R., Anderson, C.G., Denison, R.F. 2011. Failure to fix nitrogen by non-reproductive symbiotic rhizobia triggers host sanctions that reduce fitness of their reproductive clonemates. *Proceedings of Royal Society of London, Series B, Biological Sciences*, doi:10.1098/rspb.2010.2193.
- Penmetsa, R.V., Frugoli, J.A., Smith, L.S., Long, S.R., Cook, D.R. 2003. Dual genetic pathways controlling nodule number in *Medicago truncatula*. *Plant Physiology*, **131**: 998-1008.
- Pepper, A.N., Morse, A.P., Guinel, F.C. 2007. Abnormal root and nodule vasculature in R50 (*sym16*), a pea nodulation mutant which accumulates cytokinins. *Annals of Botany*, **99**: 765-776.
- Peters, N.K. and Crist-Estes, D.K. 1989. Nodule formation is stimulated by the ethylene inhibitor aminoethoxyvinylglycine. *Plant Physiology*, **91**: 690-693.
- Pueppke, S.G. 1986. Nodule distribution on legume roots specificity and response to the presence of soil. *Soil Biology and Biochemistry*, **18**: 601-606.
- Qubit Systems Manual, 2005. Open flow gas exchange system for measuring nitrogenase activity, instructors manual. Published in Canada.
- Sagan, M. and Duc, G. 1996. *Sym28* and *sym29*, two new genes involved in regulation of nodulation in pea (*Pisum sativum* L.). *Symbiosis*, **3**: 229-245.
- Schnabel, E., Mukherjee, A., Smith, L., Kassaw, T., Long, S., Frugoli, J. 2010. The *Iss* supernodulation mutant of *Medicago truncatula* reduces expression of the *SUNN* gene. *Plant Physiology*, **154**: 1390-1402.
- Schneider, A., Walker, S.A., Poyser, S., Sagan, M., Ellis, T.H.N., Downie, J.A. 1999. Genetic mapping and functional analysis of a nodulation-defective mutant (*sym19*) of pea (*Pisum sativum* L.). *Molecular and General Genetics*, **262**: 1-11.
- Schubert, K.R. and Evans, H.J. 1976. Hydrogen evolution: a major factor affecting the efficiency of nitrogen fixation in nodulated symbionts. *Proceedings of the National Academy of Sciences of the United States of America*, **73**: 1207-1211.
- Schulze, J. 2004. How are nitrogen fixation rates regulated in legumes? *Journal of Plant Nutrition and Soil Science*, **167**: 125-137.
- Shtark, O.Y., Borisov, A.Y., Zhukov, V.A., Provorov, N.A., Tikhonovich, I.A. 2010. Chapter 5: intimate associations of beneficial soil microbes with host plants. In: *Soil Microbiology and Sustainable Crop Production* (Dixon, G.R. and Tilston, E.L., eds.) Springer Science and Business Media, New York.
- Simms, E.L., Taylor, D.L., Povich, J., Shefferson, R.P., Sachs, J.L., Urbina, M., Tausczik, Y. 2006. An empirical test of partner choice mechanisms in a wild legume-rhizobium interaction. *Proceedings of the Royal Society of London, Series B, Biological Sciences*, **273**: 77-81.

- Skøt, L. 1983. Cultivar and *Rhizobium* strain effects on the symbiotic performance of pea (*Pisum sativum*). *Physiologia Plantarum*, **59**: 585-589.
- Sprent, J. 2001. Nodulation in legumes. London: Royal Botanic Gardens, Kew. pp. 1, 15, 16, 26.
- Sprent, J.I. 2007. Evolving ideas of legume evolution and diversity: a taxonomic perspective on the occurrence of nodulation. *New Phytologist*, **174**: 11-25.
- Sprent, J.I. 2008. 60Ma of legume nodulation. What's new? What's changing? *Journal of Experimental Botany*, **59**: 1081-1084.
- Sprent, J.I. 2009. *Legume nodulation: a global perspective*. Wiley-Blackwell, Chichester, UK.
- Stein, S., Selesi, D., Schilling, R., Pattis, I., Schmid, M., Hartmann, A. 2005. Microbial activity and bacterial composition of H<sub>2</sub>-treated soils with net CO<sub>2</sub> fixation. *Soil Biology and Biochemistry*, **37**: 1938-1945.
- Stougaard, J. 2001. Genetics and genomics of root symbiosis. *Current Opinions in Plant Biology*, **4**: 328-335.
- Suzuki, A., Hara, H., Kinoue, T., Abe, M., Uchiumi, T., Kucho, K., Higashi, S., Hirsch, A., Arima, S. 2008. Split-root study of autoregulation of nodulation in the model legume *Lotus japonicus*. *Journal of Plant Research*. **121**: 245-249.
- Terpolilli, J.J., O'Hara, G.W., Tiwari, R.P., Dilworth, M.J., Howieson, J.G. 2008. The model legume *Medicago truncatula* A17 is poorly matched for N<sub>2</sub> fixation with the sequenced microsymbiont *Sinorhizobium meliloti* 1021. *New Phytologist*, **179**: 62-66.
- Tsyganov, V.E., Morzhina, E.V., Stefanov, S.Y., Borisov, A.Y., Lebsky, V.K., Tikhonovich, I.A. 1998. The pea (*Pisum sativum* L.) genes *sym33* and *sym40* control infection thread formation and root nodule function. *Molecular and General Genetics* **259**: 491-503.
- Tsyganov, V.E., Voroshilova, V.A., Priefer, U.B., Borisov, A.Y., Tikhonovich, I.A. 2002. Genetic dissection of the initiation of the infection process and nodule tissue development in the *Rhizobium*-Pea (*Pisum sativum* L.) symbiosis. *Annals of Botany*, **89**: 357-366.
- Tsyganov, V.E., Voroshilova, V.A., Herrerra-Cervera, J.A., Sanjuan-Pinilla, J.M., Borisov, A.Y., Tikhonovich, I.A., Priefer, U.B., Olivares, J., Sanjuan, J. 2003. Developmental downregulation of rhizobial genes as a function of symbiosome differentiation in symbiotic root nodules of *Pisum sativum*. *New Phytologist* **159**: 521-530.
- Turgeon, B.G. and Bauer, W.D. 1983. Spot inoculation of soybean roots with *Rhizobium japonicum*. *Protoplasma*, **115**: 122-128.



- Voroshilova, V.A., Demchenko, K.N., Brewin, N.J., Borisov, A.Y., Tikhonovich, I.A. 2009. Initiation of a legume nodule with an indeterminate meristem involves proliferating host cells that harbour infection threads. *New Phytologist*, **181**: 913-923.
- Wadisirisuk, P., Danso, S.K.A., Hardarson, G., Bowen, G.D. 1989. Influence of *Bradyrhizobium japonicum* location and movement on nodulation and nitrogen fixation in soybeans. *Applied and Environmental Microbiology*, **55**: 1711-1716.
- Weaver, R.W. and Frederick, L.R. 1972. A new technique for most-probable-number counts of Rhizobia. *Plant and Soil*, **36**: 219-222.
- Wielbo, J., Kuske, J., Marek-Kozaczuk, M., Skorupska, A. 2010. The competition between *Rhizobium leguminosarum* bv. *viciae* strains progresses until late stages of symbiosis. *Plant and Soil*, **337**: 125-135.
- Wipf, L. and Cooper, D.C. 1940. Somatic doubling of chromosomes and nodular infection in certain Leguminosae. *American Journal of Botany*, **27**: 821-824.
- Young, J.P.W., Crossman, L.C., Johnston, A.W.B, Thomson, N.R., Ghazoui, Z.F., Hull, K.H., Wexler, M., Curson, A.R.J., Todd, J.D., Poole, P.S., Mauchline, T.H., East, A.K., Quail, M.A., Churcher, C., Arrowsmith, C., Cherevach, I., Chillingworth, T., Clarke, K., Cronin, A., Davis, P., Fraser, A., Hance, Z., Hauser, H., Jagels, K., Moule, S., Mungall, K., Norbertczak, H., Rabinowitsch, E., Sanders, M., Simmonds, M., Whitehead, S., Parkhill, J. 2006. The genome of *Rhizobium leguminosarum* has recognizable core and accessory components. *Genome Biology*, **7**: R34.
- Zhu, H., Choi, H., Cook, D.R., Shoemaker, R.C. 2005. Bridging model and crop legumes through comparative genomics. *Plant Physiology*. **137**: 1189-1196.
- Zupancic, J., Macdonald, E., Guinel, F., Znotinas, N. 2010. The construction of nodulation maps to study nodule distribution in legumes. *Proceedings of the Canadian Botanical Association Annual Meeting*. Ottawa, ON, Canada.

## Appendices

### Appendix A

#### Low- nitrogen Nutrient Solution Recipe

<b>Stock</b>	<b>Weight (g/L)</b>	<b>Molarity (M)</b>	<b>mL stock per 20L</b>	<b>Final Concentration (mM)</b>
KH <sub>2</sub> PO <sub>4</sub>	27.2	0.2	200	2
Ca(NO <sub>3</sub> ) <sub>2</sub>	236.16	1.0	10	0.5
K <sub>2</sub> SO <sub>4</sub>	34.9	0.2	200	2
MgSO <sub>4</sub> (7H <sub>2</sub> O)	98.6	0.4	50	1
Fe III EDTA	16.4	0.04	100	0.2
Micronutrient			20	
KCl	3.727	0.05		0.05
H <sub>3</sub> BO <sub>3</sub>	1.546	0.025		0.025
ZnSO <sub>4</sub> (7H <sub>2</sub> O)	0.575	0.002		0.002
MnSO <sub>4</sub> (H <sub>2</sub> O)	0.338	0.002		0.002
CuSO <sub>4</sub> (5H <sub>2</sub> O)	0.125	0.0005		0.0005
Na <sub>2</sub> MoO <sub>4</sub> (2H <sub>2</sub> O)	0.121	0.0005		0.0005

## Appendix B

Yeast Mannitol Agar Recipe – To be used to prepare 5ml slants.

	Amount added in 200ml
Mannitol	2g
K <sub>2</sub> HPO <sub>4</sub>	0.10 g
MgSO <sub>4</sub> (7H <sub>2</sub> O)	0.04 g
NaCl	0.02 g
Yeast extract	0.08 g
Agar	3 g

## Appendix C

### Yeast Mannitol Broth Recipe

	Amount added in 1L, pH 6.8
Mannitol	10 g
K <sub>2</sub> HPO <sub>4</sub>	0.5 g
MgSO <sub>4</sub> (7H <sub>2</sub> O)	0.2 g
NaCl	0.1 g
Yeast extract	0.4 g

Medium was aliquoted 20 mL into Erlenmeyer flasks and then autoclaved using the prevacuum 60 cycle (15 psig for 60 minutes).